KTH Industrial Engineering
and Management

Techno-Economic Analysis of Hybrid PV-CSP Power Plants

Advantages and disadvantages of intermediate and peak load operation

Federico Dominio

Abstract

The present master thesis work deals with the techno-economic analysis of a combined PV-CSP utility scale power plant that operates to meet intermediate and peak load demand under the well-defined REIPPP price scheme in South Africa. For such analysis, a multi-objective optimization was carried out in order to find optimal plant designs for the selected market. Subsequently, the same optimization was performed for CSP alone and PV alone plants and its results used in a comparative analysis that allowed the economic feasibility of the PV-CSP combined plant to be assessed.

The study is based on a utility scale Solar Tower Power Plant (STPPP) with thermal energy storage and a PV plant models previously developed, validated and implemented in an in-house tool developed in KTH for techno-economic modelling of power plants. Such models were coupled together for combined operation and a specific dispatch strategy for intermediate and peak load operation was developed. The resulting combined model was further verified by using data gathered from real PV-CSP projects currently under development and the dispatch strategy was tested by using newly implemented indicators. Additionally, a methodology for calculating the average tariff that must be granted to ensure a desired level of profitability (fixed IRR) under a Power Purchase Agreement (PPA) contract was implemented. The resulting indicator was used in the techno-economic analysis of the plant, together with other performance indicators such as CAPEX and capacity factor.

The results of the multi-objective optimization show that, for the same dispatch strategy and tariff scheme, both the CSP alone and PV alone plants yielded lower average PPA prices and CAPEX than the PV-CSP hybrid. This was further confirmed by the fact that the PV capacity was minimized in all PV-CSP optimums, thus converging to a CSP only power plant. Furthermore, the CSP alone plant proved to be more flexible in varying its hourly and seasonal output levels on demand. PV alone optimum configurations all featured tracking systems to maximize power production during daytime and did not follow a peaking dispatch strategy due to the lack of a storage system. The PV-CSP hybrid solution scored higher values of capacity factor and performed better in meeting the dispatch strategy compared to the CSP alone and PV alone solutions, thus suggesting that the value of a combined plant can be increased when an operational strategy that maximizes capacity factors is sought (baseload), or when constraints are applied in terms of matching peak hours or meeting a fixed number operational hours per day.

Acknowledgment

I would like to thank my supervisor Rafael Guédez for the constant guidance and precious advice provided throughout the whole development of this master thesis. Special thanks also to Dr. Björn Laumert, head of the solar group in KTH, for allowing me to be part of this research team. The same gratitude goes also to César Valderrama and Prof. Ivette Rodriguez, for giving me the opportunity to come to Stockholm and supervising me from UPC.

To all the friends I met around Europe in these past two years of studying abroad and especially to my fellow master students in the solar research group: thanks for the fun moments and support we provided each other every day, without you this master thesis would have borne a much heavier weight.

Last but not least, I must express my deepest gratitude to my family, for always supporting my choices and showing their support throughout these two years spent abroad away from home.

Table of Contents

Abstract 3

1 Introduction 12

1.1 Previous work on peaking CSP and PV-CSP 12

1.2 Objectives 13

1.3 Methodology 14

2 Theoretical Framework 14

2.1 Structure of electricity demand 14

2.2 Solar Photovoltaic 16

2.2.1 Fundamentals 17

2.2.2 PV Types 17

2.2.3 PV Characteristics 17

2.2.4 PV Systems 18

2.2.5 Electrical Storage 19

2.2.6 Fossil Fuel Hybridisation 21

2.3 Concentrating Solar Power 21

2.3.1 Fundamentals 22

2.3.2 CSP Types 22

2.3.3 Solar Tower Power Plants 23

2.3.4 Solar Field 23

2.3.5 Thermal Energy Storage 24

2.3.6 Power Block 26

2.3.7 Hybridisation 26

2.4 PV-CSP Hybrid 26

2.5 Multi objective optimization 28

2.5.1 Performance Modelling 29

2.6 Suitable Markets for Hybrid PV-CSP 29

2.6.1 Chile 29

2.6.2 South Africa 30

2.6.3 The United States of America 30

2.6.4 Saudi Arabia 31

2.6.5 Morocco 31

3 Model Description 33

3.1 Introduction 33

3.2 Case study – South African market 34

3.3 Solar Tower Plant model 36

3.4 Photovoltaic plant model 37

3.5 Combined model 38
3.6 Pre-defined dispatch strategy 40
3.7 Dynamic model 44
3.7.1 TRNSYS inputs 45
3.7.2 Control system 45
3.7.3 TRNSYS output 47
3.8 Techno-economic calculations 48
3.8.1 PDS indicators 49
3.8.2 Performance indicators 50
3.9 Model Verification 55
3.10 Multi-Objective Optimization 58
4 Results and discussion 60
4.1 Installed capacity 60
4.2 Load factors 61
4.3 Storage, solar multiple, PV penetration 63
4.4 Capacity factor 64
4.5 Dynamic operation 65
5 Conclusions 69
6 Model limitations and future work 71
Bibliography 72
7 Appendix 77

List of Figures

Figure 1 – Typical demand curve in a day (13) 15
Figure 2 – Typical load duration curve (14) 15
Figure 3 - Global PV capacity growth (3) 16
Figure 4 - I-V curve example (11) 18
Figure 5 - I-V curve with varying solar irradiance and ambient temperature (15) 18
Figure 6 - Simplified PV plant configuration (11) 19
Figure 7 - PV strings and arrays I-V curves when strings and curves are added (15) 19
Figure 8 - Utilisation of fossil generators before and after hybridisation (24) 21
Figure 9 - Simplified CSP plant configuration (11) 23
Figure 10 – Solar receiver types (26) 24
Figure 11 - LCOE as a function of SM (34) 25
Figure 12 - PV-CSP schematic (4) 27
Figure 13 – Generic Pareto optimal front (12) 28
Figure 14 - DYESOPT flow chart (50) 33
Figure 15 – REIPPP price scheme for CSP 35
Figure 16 – STPPP layout (10) 36
Figure 17 – Example of pre-defined PV-CSP daily operation in summer (a) and winter (b) 40
Figure 18 – Simplified algorithm for the selection of operational hours 41
Figure 19 –Pre-Defined Dispatch Strategy (PDS) of the combined plant 42
Figure 20 – Relation between thermal and electric power in the power block 44
Figure 21 – TRNSYS output for high (a), low (b) and adopted (c) proportional gain of the PID controller. 46
Figure 22 – Example of weekly dynamic operation of the PV-CSP plant. 47
Figure 23 – Example of weekly dynamic operation of the CSP alone plant 48
Figure 24 – PPA-CAPEX trade-off with respect to the net power output for all considered cases 60
Figure 25 – PV-CSP trade-off for summer and winter load factors 62
Figure 26 – CSP alone trade-offs for summer and winter load factors 62
Figure 27 – Pareto fronts for various parameters of the PV-CSP plant 63
Figure 28 – PPA-CAPEX tradeoff with respect to the capacity factor for all considered cases 64
Figure 29 – Weekly operation of the selected PV-CSP optimum (A) 65
Figure 30 – Weekly operation of the selected CSP alone optimum (B) 65
Figure 31 - Weekly operation of the selected CSP alone optimum (C) 66
Figure 32 - Maltab functions for the STPP plant 80
Figure 33 – Matlab functions for the PV plant. 81

List of Tables

Table 1 - Main types of CSP plants (4) 22
Table 2 – CSP tariff scheme on the third bid window of the REIPPP (51) 35
Table 3 – Design-related parameters for the chosen location 36
Table 4 – Economic input parameters for the chosen location (26) 36
Table 5 – Operating modes of the combined PV-CSP plant 42
Table 6 – Input parameters values used for the PID controller 46
Table 7 – Reference technical data for the planned PV-CSP plant in Copiapó (36) 56
Table 8 – Design parameters for the Copiapó project and the DYESOPT model 56
Table 9 – Results of the dynamic simulation run using two different PV modules 57
Table 10 – Input variables for the multi-objective optimization. 58
Table 11 – Objective functions for the multi-objective optimization 59
Table 12 – PPA and CAPEX results for the selected optimums 61
Table 13 – Summer and winter load factors results of the selected optimums 62
Table 14 – Capacity factor values for the selected optimums 64
Table 15 – Dispatch indicators for the selected optimums 67
Table 16 – Discussed results for the optimums selected in each case 68
Table 17 – Selected PV-CSP optimum plant configuration (A). 77
Table 18 – Selected optimum CSP-only plant configuration (B). 78
Table 19 – Selected optimum PV-only plant configuration (C). 79
Table 20 – Technical reference values used in the direct CSP CAPEX cost functions 83
Table 21 – Technical reference values used in the indirect CSP CAPEX cost functions 84
Table 22 – Technical reference values used in the CSP OPEX cost functions 86
Table 23 – Technical reference values used in the direct PV CAPEX cost functions 87
Table 24 – Technical reference values used in the indirect PV CAPEX cost functions 88
Table 25 – Technical reference values used in the PV OPEX cost functions 88
Table 26 – Technical specifications for the PV modules implemented in the model 89
Table 27 – Technical specifications for the inverters implemented in the model 89

Nomenclature

Abbreviations

AC	*Alternating Current*
ACC	*Air-Cooled Condenser*
a-Si	*Amorphous Silicon*
CAPEX	*Capital Expenditure*, *Capital Expenditure*
CdTe	*Cadium Telluride*
CIGS	*Copper Indium Gallium Selenide*
CPV	*Concentrating Solar PV*
c-Si	*Crystalline Silicon*
CSP	*Concentrating Solar Power*
CT	*Cold Tank*
DC	*Direct Current*
DE	*Deareator*
DHI	*Diffuse Horizontal Irradiance*
DNI	*Direct Normal Irradiance*
DOD	*Depth of Discharge*
DYESOPT	*Dynamic Energy System Optimizer*
EC	*Economiser*
EPFL	*École Polytechnique Fédérale de Lausanne*
EV	*Evaporator*
FiT	*Feed-In Tariff*
GHI	*Global Horizontal Irradiance*
HP-ST	*High-Pressure Steam Turbine*
HT	*Hot Tank*
HTF	*Heat Transfer Fluid*
IPP	*Independent Power Producer*
IRR	*Internal Rate of Return*, *Internal Rate of Return*
ISCC	*Integrated Solar Combined Cycle*
KTH	*Kungliga Tekniska högskolan*
LCOE	*Levelised Cost of Electricity*
LPOE	*Levelised Profit of Energy*
LP-ST	*Low-Pressure Steam Turbine*
MASEN	*Moroccan Agency for Solar Energy*
MPP	*Maximum Power Point*
MPPT	*Maximum Power Point Tracker*
m-Si	*Monocrystalline Silicon*
NOCT	*Normal Operating Cell Temperature*
NPV	*Net Present Value*
O&M	*Operation and Maintenance*
OCGT	*Open Cycle Gas Turbine*
OPEX	*Operational Expenditure*
PB	*Power Block*
PDS	*Pre-Defined Dispatch Strategy*
PID	*Proportional-Integral-Derivative*
PPA	*Power Purchase Agreement*
p-Si	*Polycrystalline Silicon*
PV	*Solar Photovoltaic*
QMOO	*Queueing Multi-Objective Optimiser*
REIPPP	*Renewable Energy Independent Power Producers Program*
RH	*Reheater*
SF	*Solar Field*
SH	*Superheater*
SING	*Sistema Interconectado del Norte Grande*
SM	*Solar Multiple*
STC	*Standard Testing Conditions*
STPP	*Solar Tower Power Plant*
TES	*Thermal Energy Storage*
TF	*Thin Film*
THD	*Total Opertaing Hours per Day*
TMY	*Typical Meteorological Year*

Symbols

Symbol	*Description*	*Units*
A	*Area*	*[m²]*
C	*Cost*	*[USD]*
E_{gen}	*Generated electricity*	*[MWh]*
f_{av}	*Plant availability factor*	*[%]*
f_{CAP}	*Capacity factor*	*[%]*
f_{load}	*Load factor*	*[%]*
FYE	*First Year Energy production*	*[MWh]*
i	*Real debt interest rate*	*[-]*
IC	*Installed Capacity*	*[MW]*
k_{ins}	*Annual insurance rate*	*[-]*
k	*PDS indicator*	*[%]*
n	*Plant lifetime*	*[yr]*
N_{PH}	*Number of pre-heaters*	*[-]*
p	*Pressure*	*[bar]*
Q_{th}	*Thermal power*	*[MWth]*
REV	*Annual revenues*	*[milUSD/yr]*
SDR	*PV annual degradation factor*	*[-]*
T_h	*Tower height*	*[m]*
$\mathrm{W_{el}}$	*Net electrical output*	*[MWel]*
$X_{tax,\%}$	*Corporate sales tax (VAT)*	*[%]*
y	*Cost scaling coefficient*	*[-]*

Subscripts

Symbol	*Description*	*Symbol*	*Description*
adm	*Administration*	nom	*Nominal*
av	*Availability*	op	*Operation*
base	*Base tariff*	p	*Constant pressure*
BOP	*Balance of Plant*	PB	*Power block*
BOS	*Balance of System*	PDS	*Pre-Defined Dispatch Strategy*
Cap	*Capacity*	PH	*Pre-Heater*
con	*Construction*	peak	*Peak tariff*
Cont	*Contingency*	Ponds	*Evaporation ponds*
CT	*Cold Tank*	price	*Tariff hours*
dec	*Decomissioning*	rec	*Receiver*
ECO	*Economizer*	ref	*Reference*
E&D	*Engineering and Design*	RH	*Re-Heater*
el	*Electrical*	SA	*Field aperture*
EPC	*Engineering, procurement and construction*	Salts	*Molten salts*
EV	*Evaporator*	Serv	*Services*
gen	*Generated*	Set	*Set parameter*
gross	*Gross power*	SF	*Solar Field*
HPT	*High-Pressure Turbine*	SH	*Super-heater*
HT	*Hot Tank*	SM	*Solar Multiple*
in	*Inlet*	site	*Site adaption*
ins	*Insurance*	t	*Transversal*
inv	*Inverter*	TAX	*Taxation*
labor	*Labour*	TES	*TES*
land	*Land purchase*	th	*Thermal*
load	*Electrical load*	Tower	*Tower*
Maint	*Maintenance*	Tracking	*Tracking system*
mech	*Mechanical*	utility	*Utilities*
Misc	*Miscellaneous*		

1 Introduction

The steady growth of energy demand, coupled with increasing concern about energy security and climate change is posing a challenging scenario for the future energy supply. In this context, renewable energy technologies, including solar power, are increasingly gaining interest. Fossil fuels continue to dominate the power sector, although their share of generation is projected to decline from 68% in 2012 to 55% in 2040 (1). On the other hand, in 2014, global renewable electricity generation rose by an estimated 7% (350 TWh) and accounted for more than 22% of the overall generation. Within this framework, solar energy accounts for 18% of the share of renewables, being overcome only by hydropower (34%) and wind power (34%) (2).

The conversion of solar energy into electricity is achieved by means of two drastically different technologies, which today have reached different levels of growth and penetration: Solar Photovoltaic (PV) and Concentrating Solar Power (CSP). Solar PV is currently the most widespread solar technology thanks to the rapid pace at which it has developed and it is anticipated to reach 16% of global overall consumption by 2050 (3). The cost of PV modules has dropped by a factor of five in the last six years and the cost of full PV systems has been divided by almost three. This allowed PV to significantly drop its Levelised Cost of Electricity (LCOE) and reach grid parity without incentives is some markets (3).Despite this, important barriers, such as the lack of an economically feasible system of electricity storage, still make large scale grid integration of electricity from PV troublesome due to intermittency and unpredictability of the solar resource.

The deployment of CSP has also experience robust growth in the latter years, reaching nearly 4 GW of cumulative capacity at the end of 2013, but not enough to compete with PV, which featured 150 GW of cumulative capacity in the same year (4). The main reason behind this difference lies in the added complexity of CSP systems, together with high capital intensity, where almost all expenditures for new plants are made upfront. Furthermore, drops in costs have been experienced but at a slower pace than PV (4). Nevertheless, the strength of CSP over PV lies in the possibility of integrating thermal energy storage, thus allowing CSP plants to supply electricity at the request of power grid operators and become dispatchable during times of peak demand after sunset, when electricity prices are generally high.

Within this context, while being initially perceived as competitors, PV and CSP proved to be ultimately complementary. Rising attention is being posed in the idea of implementing the two technologies in a single system, where abundant and cheap daytime generation from PV could be supported by CSP with storage and integrated with production of power during evening peak hours, thus resulting in a potentially more cost-effective system compared to the two technologies alone. As a result solar energy companies have begun marketing hybrid projects associating PV and CSP to offer fully dispatchable power at lower costs to some customers (4).

1.1 Previous work on peaking CSP and PV-CSP

As it was just mentioned, PV-CSP hybridization represents a new and unexplored field of utility scale electricity generation and as such, little literature is available for hybrid PV-CSP systems, especially for a specific operational strategy such as intermediate and peak demand operation. A review on the most recent studies performed in this field is reported here.

Hybridization of conventional power technologies with solar energy was investigated by (5), who perform a techno-economic study of different hybridization options of combined cycle power plants with solar energy technologies, encompassing both PV and CSP, with the goal of finding the best hybrid option in terms of emission reduction and profitability. However the analysis is only focused on combined cycle power plants with fixed dispatch strategy, therefore lacking a study on operation strategies under different market conditions and pure PV-CSP hybridization.

The effect of PV hybridization to achieve high plant capacity factors was studied by (6). A multi-tier output dispatch strategy was successfully implemented, in which the plant is dispatched at different levels

of output during the day without compromising a minimum firm output during the whole year, resulting in an increase of the hybrid plant capacity factor. However, such analysis does not take into account any economics neither of the plant nor of the location and is limited to baseload operation, for which the dispatch strategy is significantly different compared to a peak or intermediate load power plant.

More specifically about peaking operation, (7) investigate the feasibility of operating CSP plants with storage as peak load power plants in the South African market as a replacement of the currently used diesel open cycle gas turbines. A distributed hybrid system with diesel open cycle gas turbines as a backup was found to be a viable solution, capable of dropping the LCOE of 45% with respect to diesel peaking power plants alone. The study is followed by a recent work in which the effect of the South African two tier CSP tariff scheme on a fleet of CSP plants operating to meet peak load demand was investigated in more detail (8). In the study, an optimization of the CSP system is performed to enhance its performance under the double tariff scheme. The optimized system was found to be profitable both under the two tier tariff scheme and under a fixed price scheme. However, the optimization only takes into account storage sizes, while other relevant parameters such as turbine and solar field sizes are kept constant. Furthermore, the Levelised Profit of Energy (LPOE) is the only parameter used to assess the feasibility of the plant configurations, therefore lacking a more comprehensive set of performance indicators.

An optimization method for storage sizes in peaking CSP power plants located in Seville is proposed by (9). Results showed that for small power blocks and storage units a peaking strategy would yield more revenues. However, the study considered only solar multiple and storage sizes as the only parameters to be optimized, with respect to a fixed capacity. In the follow up of the previously mentioned work (10) a techno-economic study to find optimum CSP configurations for peaking and baseload in South Africa under different tariff and incentives scheme is performed. The analysis was performed using the same tool on which this thesis work will be based, yielding optimum CSP plants configurations able to meet predefined objectives such as maximizing Internal Rate of Return (IRR)and minimizing the Capital Expenditure (CAPEX). Nevertheless, the study does not consider PV hybridization. Furthermore, the plant is dispatched at fixed nominal output in all cases, therefore an analysis on how different hourly and seasonal output levels affect the capability of the plant to save storage and meet peak hours more effectively is missing.

Lastly, a master thesis from (11) deals with techno-economic analysis of a hybrid PV-CSP power plant in South Africa. The study deals with similar objectives as this thesis research, focusing on peak and intermediate load operation under the different South African tariff schemes. However, due to computational limitations of the model, no optimization studies were performed on the combined plant, both on the technical and economical sides. In this regard, this thesis work is proposed as a direct continuation and refinement of that study.

1.2 Objectives

The objective of this thesis work is to assess the techno-economic feasibility of a combined PV and CSP power plant that operates as an intermediate and peak load plant, under a well-defined price scheme. Such feasibility study will be performed by comparing optimum PV-CSP plant configurations with similar CSP alone and PV alone optimum systems under the same market conditions, by using the same performance indicators to measure both economic profitability and technical performance.

Specific objectives:

- Select a suitable market for PV and CSP utility scale projects.
- Develop a dispatch strategy for combined PV-CSP intermediate and peak load operation in such market.
- Verify the model and dispatch strategy with newly implemented indicators.

- Determine the suitable Power Purchase Agreement (PPA) average price that can guarantee a desired level of profitability for the plant.
- Perform multi-objective optimizations of the PV-CSP, CSP alone and PV alone models and carry out a comparative analysis of the resulting optimums.

1.3 Methodology

A literature review has been carried out as first step in chapter 2. This theoretical framework covers the basics of both technologies under investigation, namely PV and CSP. Further analysis is provided about existing/planned PV-CSP combined power plants, the basics of base, peak and intermediate load operation and a review about suitable markets for PV and CSP utility scale projects. Performance modelling is also introduced together with the theory of multi-objective optimization, which represents the main tool used to perform the techno-economic analysis of this thesis work.

After the theoretical framework has been defined, an acquaintance to the existing tool developed in KTH (12) for techno economic analysis of thermal power plants was needed. This included the study of both the CSP and PV models that were previously developed within the tool and which constitute the starting point of this thesis work.

As next step, the separate CSP and PV models were linked together and a dispatch strategy was developed in chapter 3 for the combined plant to make the operation suitable for intermediate and peak load, based on market electricity prices. Specific validation indicators and a methodology for determining a suitable PPA for the plant have been developed as well. The plants are then sized in a steady state model and their performance is dynamically simulated over the course of a year.

Once the model is completed, the final stage consists of running multi-objective optimizations both for the PV-CSP hybrid plant and for the PV and CSP alone cases. The optimum plant configurations and PPAs will then be used for comparison purposes to assess the techno-economic feasibility of the PV-CSP hybrid concept under the selected market conditions. Such analysis will represent the final outcome of the thesis and is presented in chapter 4.

2 Theoretical Framework

2.1 Structure of electricity demand

The operational strategy of power plants is generally strongly dependent on the structure of electricity demand, therefore it is important to define the various existing types of electrical loads and how they affect the design and operation of power plants.

Figure 1 shows a typical daily load curve of a country. It can be seen that electricity demand does not follow a flat curve but is strongly variable and dependent on the hour of the day. The magnitude of these variations depends on the location and on the type of electrical load that is taken into account; industrial loads tend to assume a flat profile over the day while domestic and commercial loads tend to be more variable, generally featuring peaks during daytime while being relatively low during nighttime. In addition to daily variations, electricity demand experiences seasonal variations as well, generally linked with environmental conditions. Cold countries generally experience maximum demand in winter due to high heating loads, while hot countries experience higher demand in summer due to cooling loads.

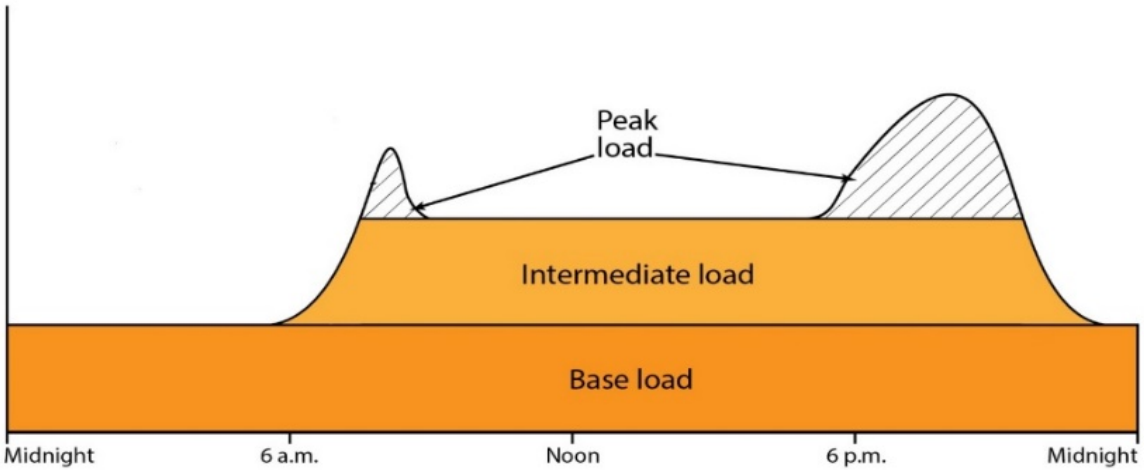

Figure 1 – Typical demand curve in a day (13)

If information about daily load curves is collected over a year, a cumulative frequency distribution of loads can be determined, showing the frequency of occurrence of different loads, defined as the load duration curve (Figure 2). From the load duration curves it is possible to distinguish three types of electrical loads, corresponding to three different segments of the curve: the minimum demand occurring for 100% of the time (right side of Figure 2) is defined as *base load***.** On the other hand, the system experiences high demand for relatively brief periods (left side of Figure 2**)**; the load associated to this period is defined as *peak load*. Peak load is generally defined as such when it occurs for less than 20% of the time in the year (14)**.** The variable demand occurring for the rest of the time in between peak and base load is then defined as *intermediate load*. From the load duration curve, the concepts of peak, intermediate and base load can then be applied to a daily load demand curve as well, as shown in Figure 1**.**

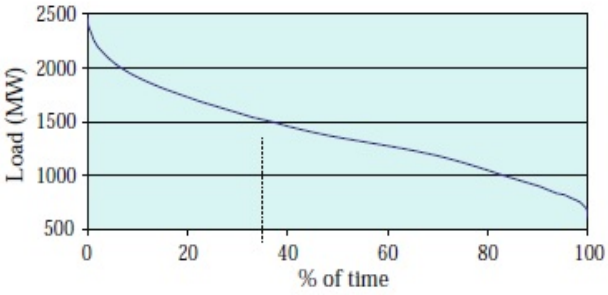

Figure 2 – Typical load duration curve (14)

Following this definition, the system operator needs different types of power plant to meet the daily and seasonal variations in demand. Base load power plants generally feature high investment costs but low operating cost, such as nuclear power plants; such plants normally have very limited capability of varying their output in response to demand changes, therefore are operated at constant nominal output for most of the time. On the other hand peak load plants feature high operating costs and fast startup and ramp up/down times in order to quickly meet the short-lasting peak loads, such as diesel or hydro power plants. Lastly, intermediate load power plants are required to be able to adjust their output throughout the day/year to follow the variations in electricity demand. For this reason, they are also identified ad "load

following power plants". Gas turbine power plants are usually employed for this purpose, being able to operate at part load without significantly compromising efficiency (14). As a consequence, power plant types can be defined based on their capacity utilization rate, also called *capacity factor,* defined as the ration between the energy actually produced in a year by the plant, to the energy produced if the plant would operate at full capacity for the whole time:

$$f_{CAP} = \frac{Energy\ produced\ in\ a\ year}{Capacity * 8760} \quad (1)$$

Base load power plant tend to maximize their capacity factor to close to 100%, while peaking plants feature capacity factors usually below 20% (14). The hybrid PV-CSP plant that will be modelled in this thesis will have characteristics close to a load following power plant, being able to adapt its output, within certain constraints, according to the time of the day or season.

2.2 Solar Photovoltaic

Solar photovoltaic is currently the most cost-effective solar technology available in the market. Due to the technology's technical simplicity and decreasing costs it has been able to penetrate several markets, including utility scale generation (11). Since 2010, global solar PV capacity has increased more than it has in the previous four decades. This perfectly encapsulates how fast this technology is growing with global capacity exceeding 150 GW in early 2014. China has been leading the global PV market, followed by Japan and the U.S. The IEA foresees PV's global share of electricity to reach 16% by 2050. For this vision to be achieved, approximately 4,600 GW of installed PV capacity must exist, leading to an emission avoidance of up 4 Gt of CO_2 annually (3).

Grid connected PV systems can be built at all scales, from a few kW to hundreds of MW. Currently, in the world, there are about 20 utility scale PV projects of over 100 MW capacity, most of which exist in the United States and China. It is important to know the fundamentals behind the technology and particularly the parameters that affect performance.

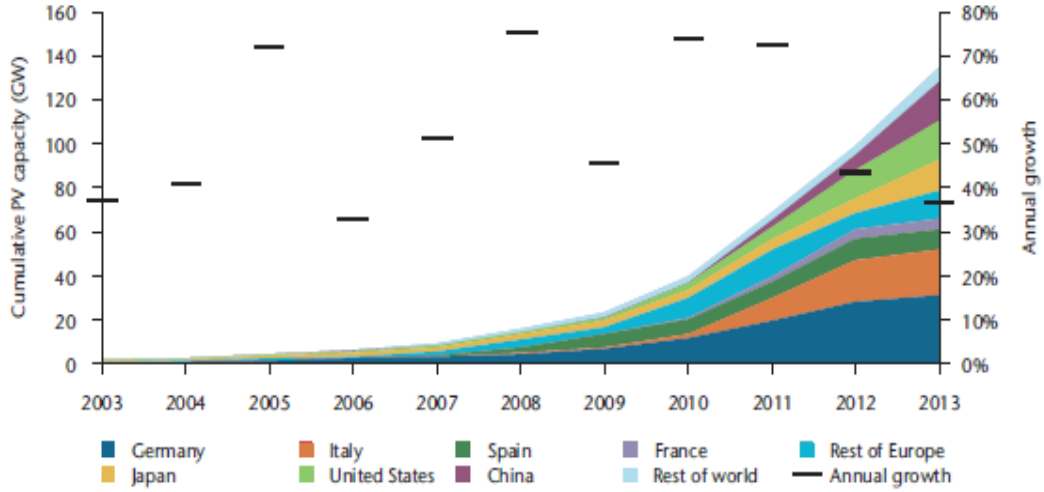

Figure 3 - Global PV capacity growth (3)

2.2.1 Fundamentals

Solar PV absorbs direct normal irradiance (DNI), diffuse horizontal irradiance (DHI) and reflected components, all of which sum up making global horizontal irradiance (GHI). PV cells directly convert this solar energy into electricity through the photovoltaic effect. When photovoltaic material receives a photon, it can be absorbed, reflected or transmitted. In the case where it is absorbed, and if the energy of photon is greater than the band gap of the semiconductor, an electron can be released and removed through the help of the p-n junction of the material. The electron is free to flow as current through the creation of an electric field between the n-type and p-type semiconductors (15).

2.2.2 PV Types

While there are many types of PV cells available today, the main two are:

- Crystalline silicon (c-Si)
- Thin film (TF)

Crystalline silicon cells currently dominates the market with a share of approximately 90%, while thin film is represented by approximately a 10% share, a decrease from 2009. Concentrating solar PV (CPV) has less than 1% (3). C-Si PV cells can be separated in monocrystalline (m-Si) and polycrystalline cells (p-Si). In m-Si cells, the silicon comes in the form of a single crystal, without impurities. The main advantage of this single crystal structure is that it can produce high efficiencies, typically about 14%-15% (15). However, these cells have a complicated manufacturing process resulting in higher costs. P-Si cells consist of numerous grains of single crystal silicon. These cells are less expensive to manufacture but have efficiencies slightly lower than m-Si, typically 13%-15%. One disadvantage of c-Si cells, in general, is that their performance decreases with an increase in cell temperature. As such c-Si modules perform better in winter than summer whilst the opposite can be said for amorphous silicon (a-Si) PV cells (16). A-Si cells, unlike c-Si cells, are arranged in a thin homogeneous layer because a-Si absorbs light more effectively. These PV cells have lower manufacturing costs and are less affected by cell temperature but have a lower efficiencies, of approximately 6%-7% (15). Other TF technologies include Cadium Telluride (CdTe) cells and Copper Indium Gallium Selenide (CIGS) cells which are both relatively tolerate to cell temperature and offer efficiencies of 10%-11% and 10%-13% respectively.

2.2.3 PV Characteristics

The performance of a PV cell, module or array can be visualised with an I-V curve, as shown in Figure 4. The curve describes the maximum power point (MPP) for given weather conditions, i.e. the PV panel's rated power under specified condition, usually standard testing conditions (STC) or normal operating cell temperature (NOCT). STC means that the solar panels are tested with an irradiance of 1000 W/m^2 under cell temperature conditions of 25 °C and assuming an airmass of 1.5. Airmass is the optical path length through the Earth's atmosphere for light where the airmass at the equator is 1. NOCT is a test that more closely resembles real world conditions. In this case, the irradiance is assumed to be 800 W/m^2, an ambient temperature is assumed to be 20 °C, an average wind speed of 1 m/s with the back of the solar panel open to a breeze (17). The performance of a PV module outside of rated conditions can be calculated using temperature correction coefficients and provided by the manufacturer (11).

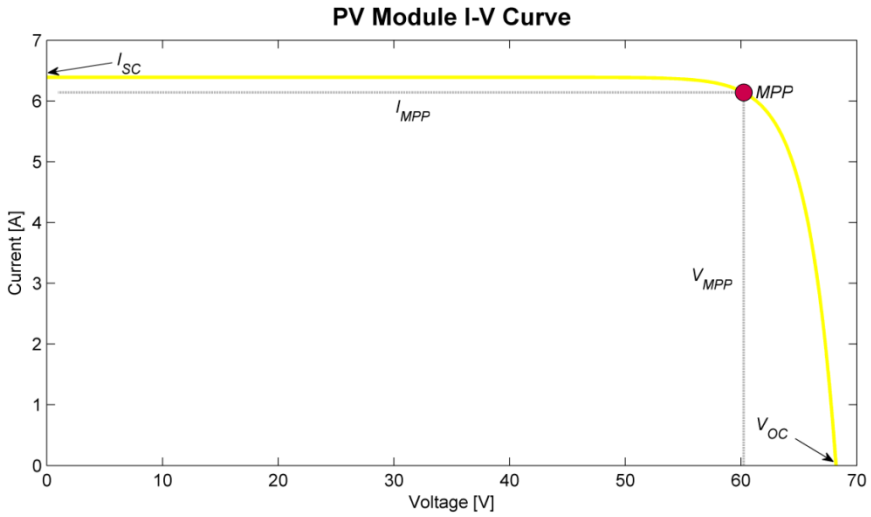

Figure 4 - I-V curve example (11)

There are two main parameters that significantly affect the performance of a PV panel.

- Solar irradiance
- Ambient temperature

It is very important that these two parameters are taken into consideration when designing a PV array. As can be seen in Figure 5, for a fixed temperature, the output current of the PV cell increases proportionally to the irradiance. Also, for a fixed irradiance, the output voltage shows a decreasing trend with an increase of temperature while the output current roughly stays constant.

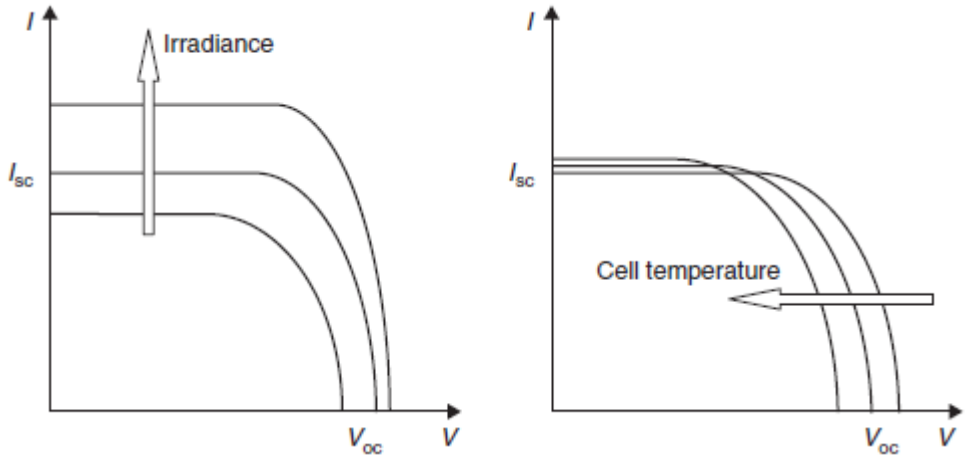

Figure 5 - I-V curve with varying solar irradiance and ambient temperature (15)

2.2.4 PV Systems

Figure 6 shows a simplified PV farm configuration consisting of four PV strings connected in parallel to a centralised inverter. The inverter is necessary because the power output is direct current (DC) and must be converted to alternating current (AC). Each PV string consists of three PV modules connected in series each with a bypass diode. The bypass diode is included to protect the system from irregular irradiation or partial shading (11).

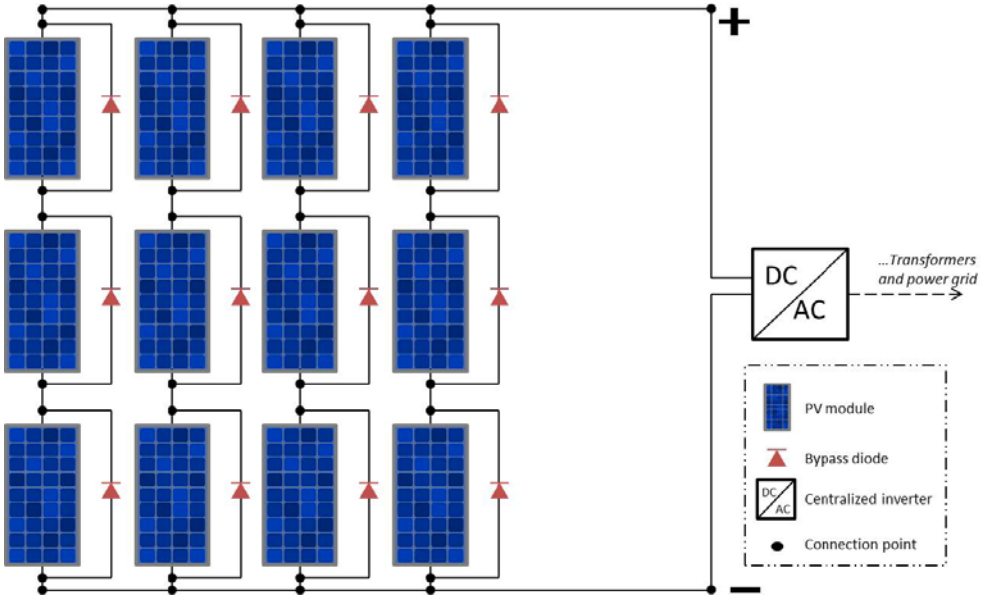

Figure 6 - Simplified PV plant configuration (11)

Connecting PV modules in series increases the voltage of the system and connecting the PV strings in parallel increases the current of the system. This can be seen in Figure 7. As is the case with a PV module, a PV plant has a single MPP, the product of the array voltage and current. In order to reach this MPP, for particular weather conditions, the voltage of the system must be regulated using a maximum power point tracker (MPPT) (11). The MPPT is usually located within the inverter for utility scale PV farms. DC to AC inverters have an input voltage range for which can be regulated to obtain a MPP and therefore, for this particular configuration, all the strings must operate at the same voltage. This is a disadvantage as the power output of the system can be reduced if the system is exposed to shadows. However to avoid this, alternate configurations may be employed; for example where smaller inverters are attached to every string. In this case the MPP is more flexible because the voltage and power output of each string can be change independently from the others (11).

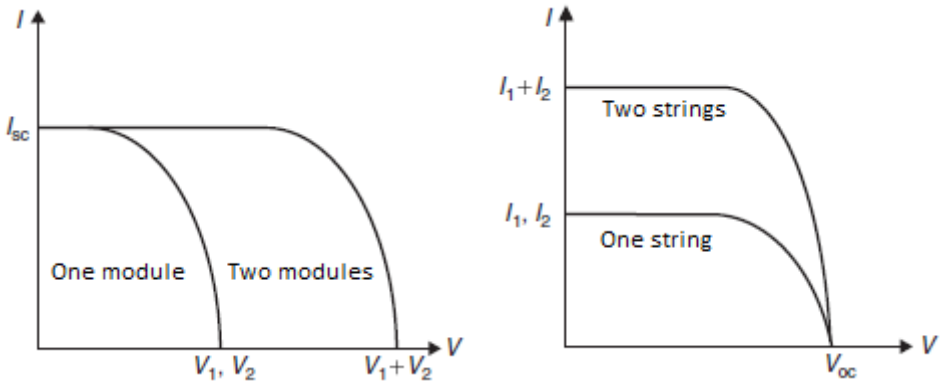

Figure 7 - PV strings and arrays I-V curves when strings and curves are added (15)

2.2.5 Electrical Storage

The successful implementation of energy storage technologies with PV might represent a potential breakthrough for the future large scale diffusion of solar electricity generation. Storage can compensate

for the fluctuations of the solar resource and extend the operating hours of the system, resulting in improved capacity factor and flexibility.

PV storage is carried out by means of batteries. Due to high capital and maintenance cost and current technical limitations, such as lifetime, capacity, self-discharge rates etc., battery systems have not been used yet in utility scale PV farms, but only in off grid standalone applications. The main types of batteries available today are the following: lead-acid, nickel cadmium, nickel metal hydride, lithium ion, sodium sulphur and flow batteries. Among these, lead-acid represents the most mature technology and is currently being used in PV applications (15). Batteries in general come in two forms: shallow cycle and deep cycle. Shallow cycle batteries are designed to produce a high amount of current over a short time, such as in cars ignition. On the other hand, deep cycle batteries feature thicker lead plates, resulting in deeper depth of discharge (DOD). Thicker lead plates reduce the surface available for the reactions; therefore less current is produced but over longer periods of time. Deep cycle batteries are the technology of choice, for PV applications, as shallow cycle batteries would not be able to stand repeated charge-discharge cycles typical of PV use (18). A large scale application of these batteries can be found in Puerto Rico, where a 20 MWe and 14 MWh lead acid battery storage system for grid ancillary services of frequency control and spinning reserve (19).

Other battery technologies are not mature enough yet to support renewable integration, but they show promising potential for large scale implementation. Nickel cadmium is a mature technology at the appliance level, but its use for high capacity applications is also being explored (20). Compared to lead acid, nickel cadmium offers longer life cycles, higher energy densities and lower maintenance requirements but its main drawbacks include the use of toxic heavy metals, its large dimensions and high self-discharge rates. A utility scale application of this technology is represented by the battery park deployed in Alaska, which is able to provide 27 MW for 15 min or 46 MW for 5 min for grid support services such as spinning reserve, frequency regulation, VAR support etc. (20). Nickel metal hydride can be seen as an advancement of the nickel cadmium by being more environmentally friendly and presenting 25-30% higher energy densities (21). Its main drawbacks are high self-discharge rates and scarce availability of the battery materials. Their implementation remains associated to the kW scale in consumer electronic and electric vehicles (20).

Lithium ion batteries are currently confined to the portable electronics market, but their characteristic make them extremely attractive for renewable energy application in the medium term. In fact, their storage efficiency reaches 100% and they feature the highest energy density amongst all. The main factor hindering the scaling up of this technology is the high investment cost and complicated charge management system (21). To give an idea of the potential of the technology, a 100 MW lithium ion facility was announced to be developed in Southern California to provide peak load support in replacement of gas fired power plants. Such project however, is not expected to be launched before 2021 (22).

Sodium sulphur batteries are high temperature devices which operate in the 300-350 °C range. They are characterised by the use of inexpensive materials, high energy densities, high charge/discharge efficiency (75-86%) and long cycle life. Conversely, their high temperatures lead to high self-discharge rates and corrosion issues (19). For this reason, they are mainly employed for stationary applications. The largest system up to date is the newly built 350 MWe battery park in the United Arab Emirates by the Amplex Group, used for grid stabilization and support purposes (19).

Flow batteries are a modern concept currently under study. Unlike conventional batteries, flow batteries use electrolyte solutions stored in external tanks, making these batteries highly scalable according to the chosen dimensions of the tanks. They feature high efficiency, short response times, symmetrical charge and discharge and quick cycle inversion. On the other hand low energy densities, toxicity of the materials and early stage of development make these batteries more likely to play a role in small scale applications in the near future (20).

An important factor to be taken into consideration about batteries is also the operating environment in which they work. High ambient temperatures must be avoided and proper ventilation has to be provided (15). This might reveal a hassle for CSP-PV integration, since the climatic conditions of the geographic areas in which CSP can operates are not favourable in this regard.

2.2.6 Fossil Fuel Hybridisation

The hybridisation of solar PV with fossil fuels has been mainly utilised to decrease fuel costs of existing fossil fuel plants. This allows plants to reduce output or be completely shut down during periods of sunshine (23). A typical hybridisation currently under study is PV with diesel generators, as described by (24), and (25).

This hybrid configuration consists of a PV array coupled with a MPPT, a battery bank for short-term storage, a bidirectional inverter and the diesel generator. Under normal operation, the PV array supplies the load and any excess of energy is stored in the battery until maximum capacity is reached. The battery can thus provide power during cloudy periods or in the evening. When the power produced by the PV generator is insufficient to meet demand, the diesel generators will start supplying power to satisfy load requirements and recharge the batteries. The presence of a bidirectional inverter is of key importance to convert the power in both modes of operation.

The most important parameter to consider for assessing the profitability of these projects is fuel consumption. The plant is designed to maximise the energy output from PV, thus minimising the generator's utilisation and fuel consumption. The typical influence of hybridisation can be seen in Figure 8, derived from the case study performed by (24) for a plant in Algeria.

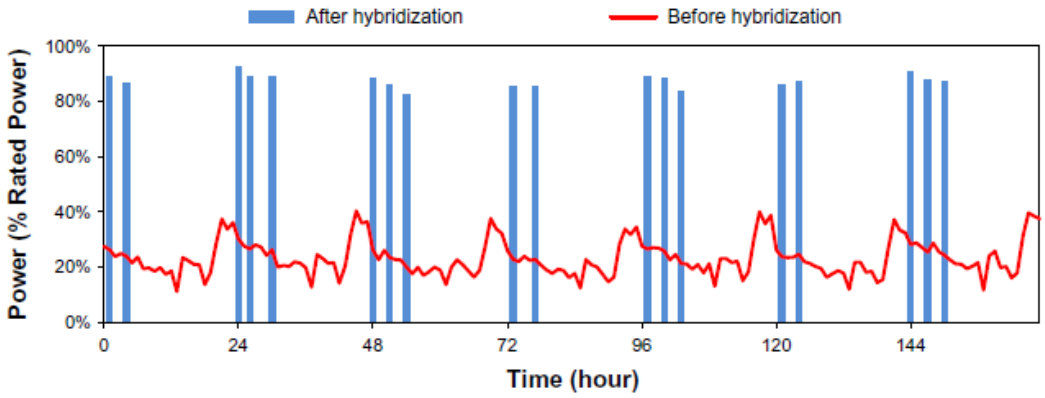

Figure 8 - Utilisation of fossil generators before and after hybridisation (24)

In hybrid mode, the diesel generators will be in operation for a significantly lower amount of time. Furthermore the generators will run at 82% to 92% of full-load operation thus increasing efficiency. 90.4% of the total fuel consumption in full fossil mode can be saved over one year and the annual operation duration of the diesel generators can decrease from 8760 h (365 days) to approximately 302 h (13 days), thus significantly reducing operating expenditure (OPEX) (24).

2.3 Concentrating Solar Power

Concentrating solar power is the second most popular solar harvesting technology available on the market. What is unique about this technology is that it can be combined with thermal energy storage (TES) or possibly hybridised with another fuel, so that not only can it generate clean energy but also energy that is dispatchable, along with other operational capabilities that support the electricity grid. This

will be discusses more in the greater detail later in the chapter. The main reason CSP is behind PV is because of the high cost attached to the electricity production. However, CSP is a well proven technology, and with the addition of cost effective TES, it is set to increase its share of the solar market (10). That being said, incentives are currently needed for this technology to be cost competitive with other traditional forms of energy generation (11).

2.3.1 Fundamentals

CSP, contrary to PV, does not directly convert solar radiation into electricity but rather uses secondary energy carrier/carriers, e.g. molten salts or steam. Furthermore, CSP is only capable of harvesting DNI. CSP is a very simple solar to mechanical to electrical energy concept where sunlight is concentrated to produce heat, using mirrors. This heat is then used in steam generation for a traditional Rankine cycle. The area needed for these plants is quite large so they are normally built in non-fertile locations, e.g. deserts (15).

2.3.2 CSP Types

There are four main types of CSP plants shown in Table 1:

Table 1 - Main types of CSP plants (4)

	Line Focus	**Point Focus**
Fixed Receiver	Linear Fresnel Reflectors	Solar Towers
Mobile Receiver	Parabolic Troughs	Parabolic Dishes

Due to the scope of the project, only solar tower is considered. The advantages of solar tower plants are its ability to reach high temperatures, the options of multiple storage types, and the great potential for efficiency improvement and cost reduction (26). Figure 9 shows a typical layout of a solar tower power plant (STPP) with TES. In the solar field, solar radiation is reflected by the field of heliostats and focused onto a single point at the top of the solar tower. The energy reflected is proportional to the distance between the heliostat and the tower. The further away the heliostat, the lower the energy reaching the receiver due to diffusion, i.e. scattering because of the presence of dust, etc. The energy reaching the receiver is transferred to the heat transfer fluid (HTF) travelling from the cold tank. Once heated, the HTF is stored in the hot tank for later use or directly discharged at a specified flow rate to generate steam for the steam cycle. The power block consists of a Rankine steam cycle similar to ones used in conventional fossil fuel plants (27).

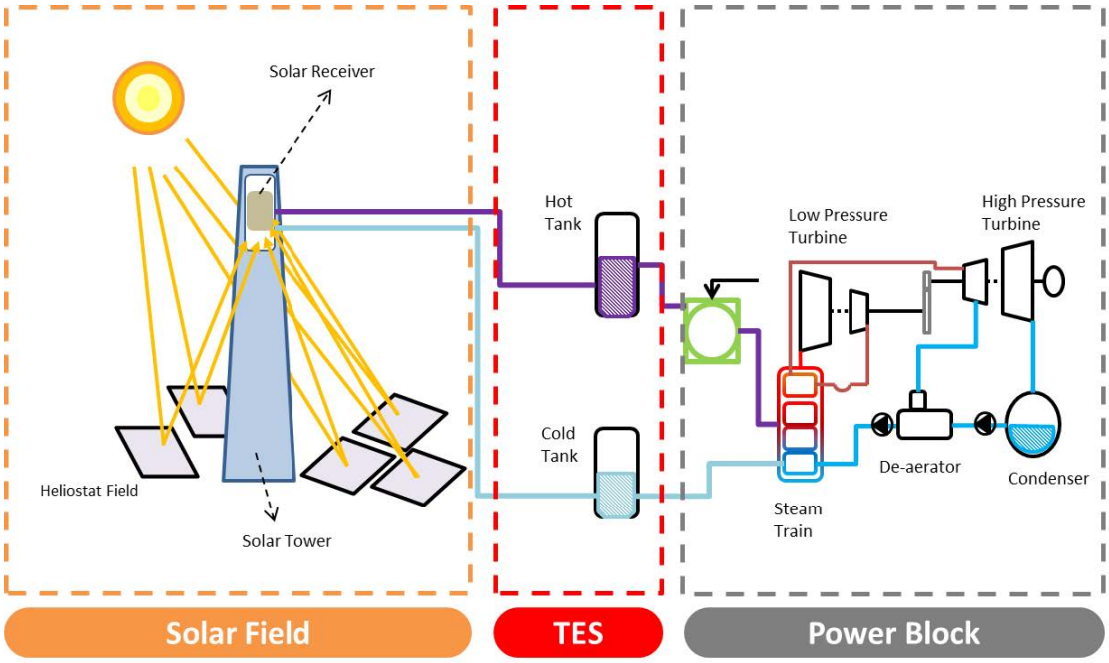

Figure 9 - Simplified CSP plant configuration (11)

2.3.3 Solar Tower Power Plants

STPP vary in configuration including the option of various HTFs and the inclusion of TES. HTFs include air, molten salts or water/steam. Water as a HTF is currently used in a number of operating STPPs. The maximum operating temperature is approximately 540 °C but high pressures are required. Water is the cheapest HTF available but it has a major disadvantage in the fact there is difficulty adding TES. If molten salts are used, it can also be used as the storage medium, therefore reducing the number of components and TES costs. However, it has a high freezing point of around 140-220 °C and so the HTF must be heated even when the plant is shutdown (26).

2.3.4 Solar Field

2.3.4.1 Heliostats

The Solar Field (SF) is the largest single capital investment of a STPP and the largest cost components are the heliostats (28) (29). The heliostats are important elements that consist of mounted mirrors that track the sun on two axes and reflect accurately. They must concentrate the irradiance onto the tower located between 100 m and 1000 m away (26). There are a number of factors that affect the arrangement of CSP heliostats. The first is in relation to the size and number of heliostats. There is no standard form of heliostat so they vary wildly in shape and size, ranging from approximately 1 m^2 to 160 m^2. Experts have divided views on what is the optimal design as both big and small designs have their advantages and disadvantages. One important factor is that they must have a sufficient distance from each other to avoid shading and blocking.

In lower latitudes the heliostats tend to be in a surround field configuration around the tower, while in high latitudes they tend be concentrated on the polar side of the tower, or north field configuration. North field configurations tend to perform more efficiently at solar noon and during winter seasons. Surround field configurations tend to perform better in non-solar noon hours and summer seasons and have a better annual performance (26). In large MW size plants solar fields must be surround, due to the fact that in North fields the high number of heliostats significantly increases the distance between the heliostats and the receiver, thus increasing attenuation losses to a point where the optical efficiency drops compared

to surround fields (26). The solar field at Crescent Dunes is 1,000,000 m^2 and is perhaps close to the maximum efficient size (4).

2.3.4.2 Solar Receiver

The solar receiver is located on top of the tower and represents the device to which the incoming radiation from the solar field is directed and concentrated. Here, heat is transferred from the concentrated heat flux to the HTF.

There are two main types of solar receiver: external and cavity. External receivers consist of vertical piping that is exposed to solar flux, in which the HTF flows. The surface areas of these receivers must be kept to a minimum in order to reduce heating losses (26). In the case of the cavity design, the solar flux enters a cavity in the form of, for example, a window. The cavity design is thought to be more efficient with a reduction of heat losses, even though the angle of incoming flux is limited. Also, if the heliostat field is circular in nature, multiple cavity receivers are required. A correct aiming strategy must be implemented to maximise the solar input while ensuring that the receivers do not get overheated (26) (4).

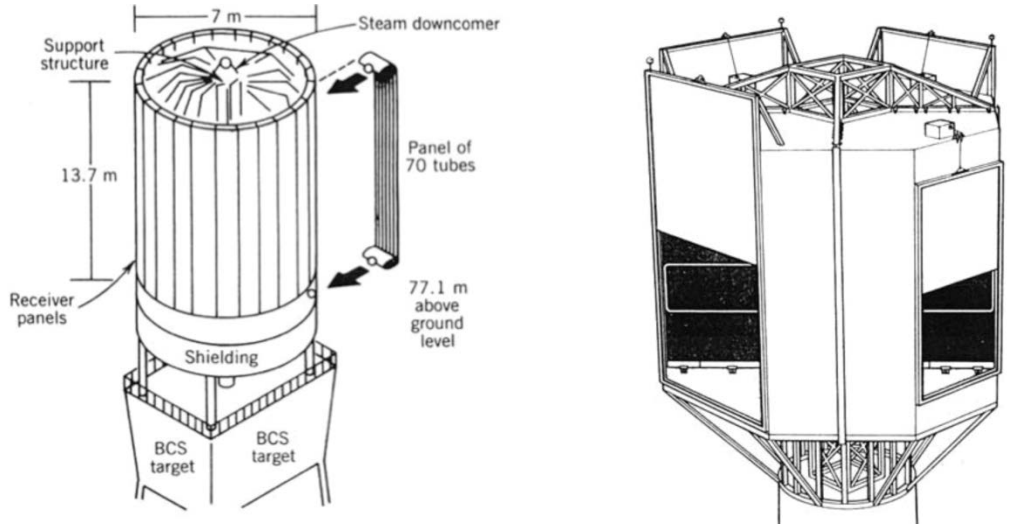

Figure 10 – Solar receiver types (26)

Solar Multiple

The solar multiple (SM) is an important factor in the design of a CSP plant. It is a design parameter used for estimating how oversized a solar field is in comparison to the rest of the system. In other words it is the real size of the solar field in comparison to a field size required to run the plant at design capacity under solar reference conditions. The SM is, therefore, dependent on the reference conditions used as the design point, e.g. solar noon at summer solstice or equinox (30). Higher multiples allow power plants to operate at full output even when the solar input is less than rated. This allows for an increased capacity factor value, increased annual solar share and a better overall utilisation of the power block. The SM size also depends on the specific plant configuration; solar plants without storage tend to have an optimal SM of 1.1 to 1.5, while storage integrated systems can have a SM up to 3 to 5 (30) (31).

2.3.5 Thermal Energy Storage

There are a significant advantages brought by the implementation of TES, the most striking one being the possibility of making CSP dispatchable, thus removing one of the principal drawbacks associated with other renewable technologies such as PV. Dispatchability offers power generation that is less reliant on weather conditions, allowing plants to increase their flexibility and operational range resembling traditional

fossil fuels power plants. Furthermore it also enables the plant to provide ancillary services. The most important benefits of TES with CSP include the following:

Capacity factor: The capacity factor can be increased from 20-25% of plants without storage to values up to 40-45%, associated with integrated storage capacity of 6-7 hours (32). Recent projects such as the Gemasolar plant reached even higher capacities of 15 hours of storage, allowing for continuous operation. In fact, Gemasolar was the first CSP plant to repeatedly reach 24 hours of uninterrupted operation (33). Such features make CSP a suitable technology for baseload operation.

Shifting generation: Besides baseload operation, flexibility brought by storage makes possible to consider shifting from periods of low demand, when the energy price is lower, to peak demand periods associated with high prices of electricity, thus maximizing the economic performance of the plant (9).

Avoidance of intermittency: Thermal storage can compensate for the fluctuating behaviour of the solar resource, thus reducing transient operation in the power generating units and improving stability/performance.

Frequency response: Frequency response is an ancillary service provided by conventional generators consisting of varying their power output in order to maintain the frequency of the grid. Frequency variations can occur for instance when there is a sudden loss of generation due to a fault in the network or when an error in the forecast of the energy demand occurs, resulting in a deficit or surplus of generation. Integration of storage allows CSP to be able to provide frequency response services, making the technology more competitive with conventional generation.

Lower LCOE: Since the adoption of TES in CSP plants leads to increased capital costs, it might be expected that the levelised cost of electricity (LCOE) would also increase. However, as Figure 11 shows, for increasing sizes of the solar multiple, the resulting LCOE is significantly higher in systems with no storage, making the implementation of TES convenient from an economic point of view as well.

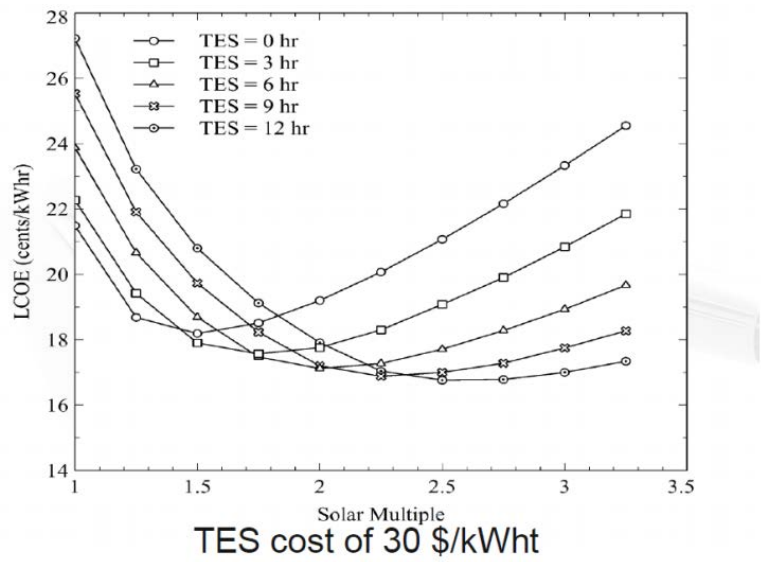

Figure 11 - LCOE as a function of SM (34)

2.3.5.1 Solar Tower TES Configurations

Storage in solar tower systems generally consists of direct double tank configurations employing molten salts as the storage medium, as seen in Figure 9. In contrast to the relatively older and more established indirect systems, direct storage systems are characterized by the use of the same fluid as both the HTF and the storage medium. The main reason for the shift from an indirect to a direct system (both with molten salts) lies in the fact that higher maximum process temperatures can be achieved with the latter option.

Consequently, with the increased operating temperature of STPP, the required tank volumes become smaller reducing the power required for pumping the storage medium (35). Due to the fact that almost half of the cost of indirect storage systems is covered by the salts, the direct storage concept is estimated to lead to a 50% capacity-cost saving (32)

2.3.6 Power Block

The Power Block (PB) consists of a Rankine cycle usually found in conventional thermal power plants. One issue with using Rankine cycles for STPP is that conventional power cycles are designed to run nonstop at rated power, which is usually not the case with STPPs. Therefore the power block must be optimised to meet daily transient cycles and improve efficiencies during part-load operation. Furthermore, minimising start-up times are an important issue in the CSP field today (26). Frequent start-up and shutdown processes also can reduce the life time of the turbine through propagation of thermal stresses (11).

2.3.7 Hybridisation

CSP technologies can be hybridised with fossil fuels for greater capacity factors, even as far as baseload applications. In reality, almost all existing CSP plant uses fossil fuels for a variety of reasons, e.g. for backup, to remain dispatchable, etc. Some can also be considered full hybrids where fossil fuels, or other sources of energy, are used routinely with solar energy (4). This can be seen in the solar generating systems built in California. During the summer natural gas was used as back up and during the winter the gas was used to boost the capacity rate.

The hybridisation of solar and fossil fuel can also consist of adding a small solar field to a conventional fossil fuel thermal plant. The addition of a solar field to either a combined cycle or coal fired plant reduces OPEX and CO_2 emissions. Integrated solar combined cycles (ISCC) use solar fields to provide steam generation. The high temperatures achieved with solar towers could also be used to heat pressurised air, up to 1000 °C, that is fed directly into a Brayton cycle turbine. Excess heat can be fed into steam cycle to run a second generator. This type of setup could produce a solar to electricity efficiency of higher than 30% (4) (26). Solar boosters can be used to on coal based thermal plants to boost the cycle efficiency, by preheating the feedwater into the boiler.

It is also possible to combine a solar field to other renewable sources, such as biomass. This has been demonstrated by the 22 MW Termosolar Borges plant in Spain. Two biomass burners heat the HTF when sunshine is insufficient (4). The hybridisation of CSP and geothermal power has also be put forward by Enel Green Power who plans on coupling a solar field to a 33 MWe geothermal plant in the U.S. The idea is that the HTF from the solar field, which is pressurised demineralised water, will provide extra heat to the geothermal fluid during the day increasing the efficiency of the system (4).

2.4 PV-CSP Hybrid

In recent times, the concept of hybrid PV-CSP power plants has been gaining interest. PV-CSP hybrids may offer a more economical way of producing intermediate, peaking or baseload power generation for specific markets than CSP or PV alone. A simplified PV-CSP plant configuration is shown in Figure 12. The basic concept is that PV, with option of storage, operates during the day at low cost, since PV generally has a lower LCOE than CSP. CSP with TES operates supplementing the PV during the day, i.e. is dispatched in response to PV output, and also operates at night. There is also an option for PV further fossil fuel hybridisation for backup or for capacity factor increase.

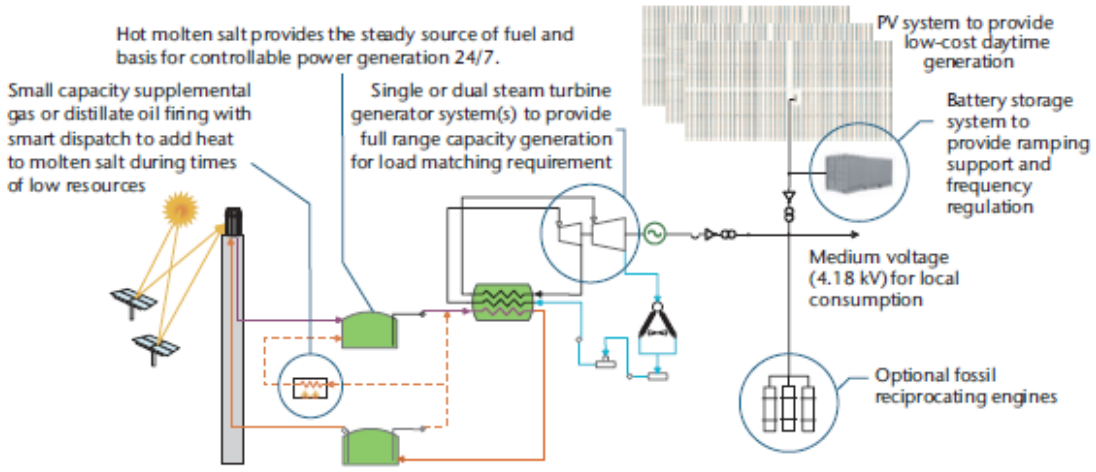

Figure 12 - PV-CSP schematic (4)

Several PV-CSP projects, both hybrid and co-located, are currently being developed worldwide, particularly in Chile, South Africa and Israel.

In Chile, the Copiapó PV-CSP hybrid project, developed by SolarReserve, incorporates two 130 MW molten salt CSP towers with a 150 MW PV plant and is designed to meet the baseload demand of the Copiapó mine in the Atacama region. Using PV supplemented by CSP during the day and CSP during the night, the plant can operate at below spot market prices (36). Molten salt TES will be used as it offers the most cost effective and efficient method of energy storage for this application and also because the molten salts can be sourced locally in Chile.

Atacama 1 consists of a CSP tower plant co-located with a PV farm in Cerro Dominador. With a CSP capacity of 110 MW and a PV capacity of 100 MW, the plant will be capable of supplying clean electricity 24 hours a day for a region where the electricity consumption is heavily tied with an active mining industry (37). The proposed Atacama 2 plant is a 210 MW CSP and PV solar project, very similar in configuration to the Atacama 1 project. It is located in the Sierra Gorda municipality in the Antofagasta region where it will also provide clean electricity to the northern electricity system SING (38).

In South Africa, the Redstone CSP project is currently under development. SolarReserve were awarded a 100MW CSP project in conjunction with ACWA Power, a Saudi water and power developer. The project was developed in response to the REIPPP is planned to start operations in 2018. The 100MW project will have 12 hours of full load energy storage and will deliver stable electricity to approximately 20,000 homes in South Africa. The interesting thing about this project is that it will be located beside the Lesedi and Jasper PV solar fields and so the combination of the three will be become the world's first combined PV-CSP solar park with a combined power capacity of 271MW (39).

The Bokpoort 2 plant is a proposed 500 MW solar project consisting of four 75 MW PV arrays and two 100 MW CSP plants. The project is planned to be located beside the Bokpoort 1 facility. The facility is proposed by the developer ACWA and plans to make a bid in the next bidding window of the REIPPP (40).

One major combined PV-CSP project has also been reported in Israel, namely the Ashalim Solar Power Plant in the Negev desert, consisting of two CSP power plants under construction (120 + 110 MW) by Abengoa and BrightsourceEnergy and one smaller (30 MW) PV power plant for a total of 280 MW. The two CSP project are currently at the construction stage (41).

2.5 Multi objective optimization

Energy systems analysis often requires multiple objectives of different nature (performance, economic, environmental etc.) to be taken into account. These objectives are likely to be conflicting to each other and a single design that is optimal in meeting all objectives cannot usually be found. This fact is especially true in the case of solar energy, where a multitude of performance indicators exists and optimizing with respect to only one objective (e.g. maximizing conversion efficiency) can result in the degradation of the others (e.g. costs). As such, the approach based multi-objective optimization considers the whole range of optimal solutions by determining trade-off curves that exist between the different objectives. Such trade-off is called "Pareto optimal front". Based on this, the decision maker can choose the desired compromise between the objectives (12).

As just mentioned, a Pareto optimal curve represents the whole range of feasible solutions within the conflicting objectives and constraints posed by the user. Each point of the curve represents a "Pareto-optimal design", which is defined as the plant configuration that performs best in each objective. In other words, there exists no other design that is simultaneously better in all objectives, so moving from an optimal design to any other results in a degradation of at least one of the objectives. An example of such trade-off can be seen in Figure 13:

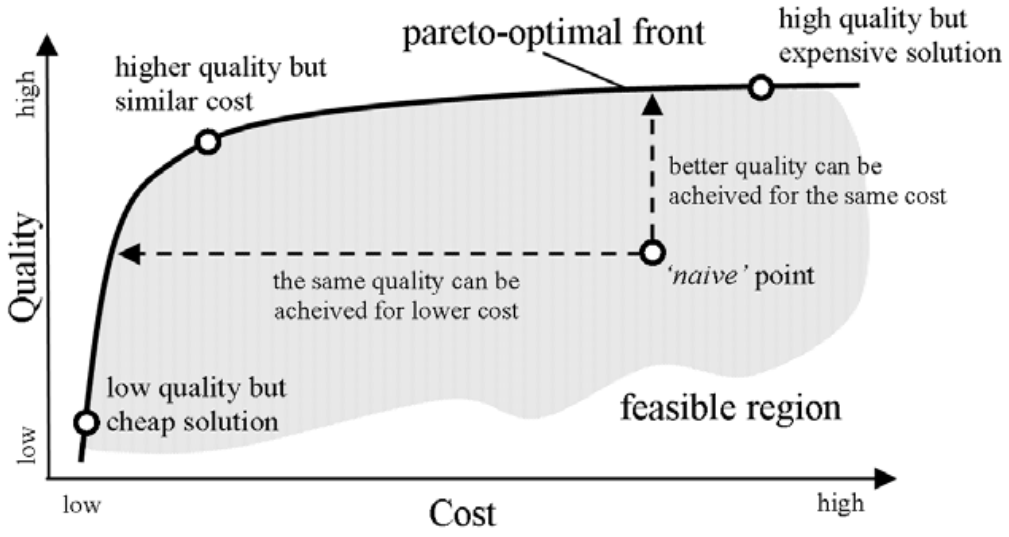

Figure 13 – Generic Pareto optimal front (12)

It can be seen that the points that do not belong to the Pareto front, i.e. "naïve points", do not represent optimum designs, since an improvement in one objective could be achieved without compromising the other (better quality for the same cost or lower cost for the same quality).

Due to the vast number and nature of the variables and objectives involved at the same time in energy system analysis, such optimization is a mixed-integer non-linear problem that cannot be solved using standard gradient-based techniques but requires the use of evolutionary algorithms.

An evolutionary algorithm uses a population based approach, in which multiple resolutions of the models take part in the creation of an initial population, which then moves towards a set of optimal designs by means of "evolution". Such algorithms are characterized by four main steps: selection, cross-over, mutation and elite-preservation. After the creation of the initial population of solutions, a stochastic "selection" criterion is implemented. For instance in the tournament selection method, two or more solutions of the evaluated pool are randomly picked and the best one "survives" for the next iteration. Subsequently a variation operator is called. One of its functions is the "cross-over" operator in which, two solutions (parents) are picked to create one or more "child" solutions by exchanging information among the parents. The decision variables for the child are derived by blending the values from the parents. Only

a percentage of the population is subjected to cross-over (probability of cross-over). Thereafter a "mutation" operator perturbs each child solution, meaning that every variable is mutated with a probability such as at least one parameter is varied (42). Such step allows diversity to be added in the range of designs within the population, avoiding that the current population stagnates close to local optima given by the initial population. Lastly, the "elite-preservation" operator combines the newly created population with the old one and keeps the better solutions for the next iterations. This step is necessary to ensure a convergence to the optimal trade-offs curves (42).

The main advantage of evolutionary algorithms is that the model and the optimizer itself can be treated as two separate entities, allowing a "black box" approach to be employed. In such approach the optimizer and model only exchange information in the form of the values and ranges of the decision variables and the corresponding values of the objective functions, resulting in considerable flexibility and easiness in applying the same optimizer to different kinds of models. On the other hand, one of the major inconveniences associated to such algorithms is that a well-defined criterion for knowing when to stop the iterations does not exist. However, a qualitative criterion can be adopted for stopping the algorithm when the current set of solutions does not vary substantially over a large number of iterations. In the context of the model used in this thesis, based on previous work with the same optimizer it was found that an acceptable degree of convergence can be reached when 2000 iterations are exceeded (10).

2.5.1 Performance Modelling

An application of multi-objective optimization for solar technologies can be seen in the method of performance modelling developed for a CSP power plant, which can be extended to PV-CSP hybrid, that is taken from "*A Methodology for Determining Optimum Solar Tower Plant Configurations and Operating Strategies to Maximise Profits Based on Hourly Electricity Market Prices, 2015*" (10). In this study a STPP plant with 2 tank molten salt TES is examined in a location in South Africa. A multi-objective optimisation modelling approach was carried out with two conflicting objective functions; to minimise the capital investment (CAPEX) and to maximise the internal rate of return (IRR). The performance modelling of a PV-CSP plant will also involve conflicting design objectives and trade-offs in the final results. The design objectives and performance indicators may include minimising LCOE for baseload operation. However it may be more relevant, for peaking operation, to maximise IRR as LCOE does not take into account the actual hour of generation or dispatchability. This method is an effective way of identifying the true trade off, through Pareto optimality, between the chosen design objectives for a given location while simultaneously considering a complete plant design.

2.6 Suitable Markets for Hybrid PV-CSP

The following section is a description of suitable markets for a hybrid PV-CSP plant. The information resulting from this analysis will then be used to select an market on which this study will be based For a PV-CSP plant to be technically and economically viable, the location must first of all have good solar resources, both DNI and GHI. For peaking it is also important for the electricity market to have clear peaking periods during the day. Specific frameworks and financial incentives such as power purchasing agreements (PPA) and feed-in tariffs (FiT) are also desirable and so would be a factor for the choice in potential market.

2.6.1 Chile

Chile has very good solar resource and according to different sources, Chile's Atacama Desert is the best solar irradiated place in the world with an accumulated annual DNI and GHI of approximately 3,300 kW/m^2 and 2,400 kW/m^2 respectively (26) (43). In 2012, the Chilean government initiated a National Energy Strategy for the promotion of a stronger, more diverse electricity structure. In this energy strategy, the share of renewable sources is to be 10% by 2024 with the introduction of incentives such as soft loans,

tax incentives and subsidies. Also a 12 year PPA scheme for renewable projects is also under consideration at this time (44).

Currently, Chile experiences the second highest electricity prices in the South American region, second only to Uruguay. The Chilean power market is based on the concept of marginal cost pricing, where the last unit to be dispatched is the one which determines the final electricity price. The use of costly diesel plants for meeting the peak load therefore causes the prices to climb, with a 400% increase experienced between 1998 and 2011, reaching $ 256.4/MWh, way above the average price in the other OECD countries ($ 159.4/MWh). This fact poses a window of opportunity for solar energy, which could make the Chilean power market the first one to reach grid parity without need of incentives (44).

The Atacama Desert is dominated by a large mining industry with stable baseload energy demand that accounts for about 80% of the demand in the northern region (26). The region also has no domestic fossil fuels, a powerful community of environmental stakeholders, no nearby hydropower and an abundance of land, all of which makes it ideal for high capacity baseload solar projects (6). The electricity demand from the central part of the country also experiences a relatively flat profile and is more associated with bulk residential and commercial loads. Chile's growing economy could cause this profile to change in the next years, presenting daily demand peaks typical of more developed nations. However, little information is available in this regard, since the daily Chilean market prices are currently not public (45). Current market assessments report that spot price varies between EUR 70 and EUR 80 per MWh (44) . All of these factors considered PV-CSP for baseload can be very interesting in this case.

2.6.2 South Africa

South Africa is regarded as one of the most promising CSP markets ranking number one in the CSP Today markets scorecard; a scorecard that identifies which markets hold the best opportunities for CSP (44). The country boasts a DNI of approximately 2,760 kW/m^2 annually with northern regions of the countries reaching as high as 2,900 kW/m^2 (26). It also has an annual GHI of up to 2,300 kW/m^2 (43). Not only is the solar resource excellent but the government shown some real support in the development of renewables. State support comes in the form of the Renewable Energy Independent Power Producers Program (REIPPP). This program promotes foreign investment by setting an amount of renewable energy capacity and offering the projects to independent power producers (IPP). The commissioned plants will operate under PPA to ensure economic feasibility (46).

The current demand curve in South Africa shows peak periods from 7 AM to 10 AM and from 6 PM to 9 PM both in summer and winter (7). At the current state, the South African Integrated Resource Plan states that peak load demand is expected to be satisfied in the near future mostly with diesel powered open cycle gas turbines (OCGT), while CSP is not seen as a potential solution for meeting peak demand (47). However, recent studies showed that at the current fuel prices, OCGT generate peak electricity at a cost of ~0.63 US$/kWh (7), way above current CSP generating costs. Therefore, PV-CSP for either baseload or peaking operation can be an interesting idea for this market.

2.6.3 The United States of America

With an annual accumulated DNI and GHI of approximately 2,636 kW/m^2 and 2,200 kW/m^2 respectively, mostly located in the south western part of the country, the U.S is also a prime candidate for solar technologies (26) (43).

The daily trend of the electricity demand in the south-western states represents an interesting opportunity for PV-CSP implementation. In fact, the grid currently experiences sharp demand peaks during mornings and during the evening due to household and lightning loads (44). The daytime peak matches the peak in PV solar generation, while the early-evening peak can be covered by the implementation of storage in CSP. It must be noted though that California, due to the high rates of implementation of renewable energy in the grid, is experiencing the so called "*duck curve*" in which the daily demand profiles flattens due

to risk of future over generation of solar energy. Nevertheless, the sharp evening peak remains unchanged, still making this market interesting for peaking.

The U.S is very active in the field of CSP with about 1.7 GW capacity currently operational with about 800 MW under development (48). A number of incentives have been put in place for the promotion of CSP technologies and also a lot of high level research has be carried out to achieve grid parity for CSP. These incentives come at both a federal and a state level and include both financial incentives, such as loan guarantees, grants and tax incentives, but also green power purchasing goals (44). Enhanced oil recovery can also be another market for PV/CSP besides electricity generation to increase oil production and reduce emissions. Although low cost unconventional gas and reducing PV prices have made the future market for CSP challenging (26).

2.6.4 Saudi Arabia

Saudi Arabia, according to CSP Today, is the second most promising CSP market behind South Africa. With a DNI and GHI of approximately 2,566 kW/m^2 and 2,450 kW/m^2 per year Saudi Arabia also makes a good location for PV-CSP (26) (43). In 2012, the state announced a set capacity of 25 GW of CSP by the end of 2032 which means it must deploy at least 1.35 GW of capacity per year (44). The ambitious renewable energy program is led by the King Abdullah City of Atomic and Renewable Energy (K.A.CARE) and comes at a time when less than 1% of the energy produced in the country is from renewable sources and with the country being the largest consumer of oil per capita in the world. Other reasons why Saudi Arabia wants to expand their energy mix are to meet the demand of an increased domestic consumption and also to increase profits from exporting oil rather than consuming it (44). A plan of a competitive procurement process was announced in 2013, with plans to develop projects with IPPs through long-term PPAs. While there is no CSP specific framework established at the moment, it is said that a decision will be made after the second bidding round to set up a FiT (44).

The electricity demand in Saudi Arabia is mainly characterized by the residential sector covering 82% of the overall demand. This is due to high to cooling loads, that represent 85% of the total residential electricity consumption (44). This reflects in large seasonal variations, with peaks occurring during summer months. The daily load profile is characterized by peaks during daytime and evenings, therefore CSP with storage has already been identified by K.A.CARE as an optimal technology to meet both the daytime and evening demands (44).

Other markets that could be interesting for CSP and PV-CSP are water desalination and enhance oil recovery. Saudi Arabia's location makes water a scarce commodity, with most it coming from underground reservoirs and energy dependent desalination processes. Therefore solar power desalination is an interesting prospect for meeting water needs and also reducing fossil fuel consumption. While using CSP enhanced oil recovery can boost oil production and reduce natural gas consumption by up to 80% (44).

2.6.5 Morocco

Morocco is another highly promising PV-CSP market. Morocco has an annual accumulated DNI of approximately 2,515 kW/m^2 with regions in the interior reaching a maximum of about 2,800 kW/m^2 (26) (4). Morocco also has GHI levels of up to 2,300 kW/m^2 (43).

Morocco is a very energy deprived nation with almost no fossil fuel production and imports for approximately 98% of its energy needs (44). Furthermore, according to IEA, (2014), operating PV during the day and CSP during the night would be less costly for the government than the fossil fuel alternatives, e.g. natural gas during the day and diesel during the night. In 2010 a renewable bill was passed to promote the implementation of renewable technologies. With this the state has launched the Moroccan Solar Plan to encourage the development of solar energy production in the country, with their first parabolic trough system currently under construction (26). Furthermore, an ambitious target of 2 GW capacity of solar

power by 2020 was announced. The Moroccan Agency for Solar Energy (MASEN), who oversees project procurements, will also act as the single electricity buyer of CSP energy through PPAs. The tariffs of the PPA will vary with time of generation including a peak tariff of a 15% increase occurring between 5 PM and midnight. This aspect might reveal interesting for CSP with storage given the fact that the country experiences a late-evening peak due to lighting loads and the demand profile does experiences variations during the year (44).

Another interesting market for CSP and PV-CSP hybrid is water desalination. As was with Saudi Arabia, Morocco's geographical location and increasing population, combined with a reduced precipitation means that water availability is limited (44).

3 Model Description

3.1 Introduction

In the framework of solar energy technologies, simulation is an essential tool to support decisions related to investment and design in such technologies. In performance modeling, the prediction of economic, energetic and operational characteristics of installations is of fundamental importance.

A simulation tool usually takes into account many factors such as the performance of the components, natural resources (i.e. solar radiation), economic constraints and operational behaviors to establish the optimum design of technical systems. Currently, in the market there is software available to establish the performances of both CSP and PV plants. With regards to CSP, there are two approaches that have been carried out so far. In the first typology, an in-depth simulation of the SF (Solar Field) and TES (Thermal Energy Storage) block is performed, while the PB (Power Block) is described with characteristic curves illustrating the trend of conversion of heat energy to electricity (49). In the second category, several programs that are used to model conventional power plant are expanding to include CSP plants. However, even though these programs offer detailed power plant block models, the solution they produce are often quite complex equations and rather slow.

DYESOPT, a tool developed by the energy department at KTH, is the model on which this thesis work will be based. As with other counterparts, the modelling tool calculates the performance of power plants, taking into account both transient operation and techno-economic performance. This is all in respect with constraints such as operational strategies, economics of a location and electricity prices. The software uses the integration of both MATLAB and TRNSYS, for the technical design and dynamic performance respectively.

Figure 14 shows an illustrative flow of information of the main blocks of the software. These include both thermodynamic and economic aspects. This is coupled with a multi-objective optimizer which allows trade-offs of conflicting designs to be observed and analyzed. The different input values required are characterized by different colors depending on the nature of the data: cost functions (in green), location related (in blue) and design configuration (in yellow).

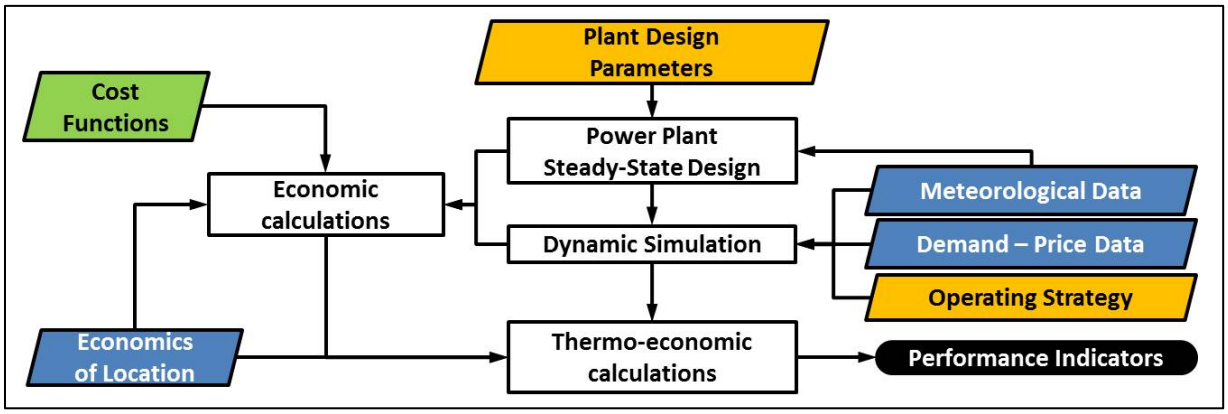

Figure 14 - DYESOPT flow chart (50)

As can be seen from the picture, the flow of information from the input data is processed in the model through three main stages, namely the steady state deign, the dynamic simulation and the thermo-economic calculations, to yield a set of desired performance indicators. Every block of the flowchart is handled by different routines in the MATLAB and TRNSYS environments. The conceptual flowchart of functions is presented in APPENDIX B.

In the case of the CSP plant, the input parameters for the model are introduced along with a description of the steady state analysis. This analysis is carried out in MATLAB and involves a number of different algorithms, which are utilized for the sizing of important plant components, i.e. the sizing of the solar field, the thermal energy storage and the power block; the calculation of the plant nominal operating point and also the determination of the pre-defined dispatch strategy (PDS). The PV farm model is introduced in the same fashion, giving a general overview of the model, the input parameters and the plant steady state design.

Thereafter the method of simulating the models dynamically is introduced. In the case of the PV model, the transient simulations over the lifetime of the farm are carried out in MATLAB. However due to the added complexity of the CSP model, the transient simulations are done on TRNSYS. In this case the plant layout of STPP in TRNSYS will be explained, how the software utilizes the steady state results carried out with MATLAB and what the outputs of the dynamic simulation are.

Thereafter post-simulation thermo-economic calculations are performed. These calculations include the chosen performance indicators and are the output of the whole tool itself. The method of calculating these indicators and also what they represent are explained in full.

The tool is not only capable of standard simulations but it is also capable of single and multi-objective optimization. The theory behind the optimization method adopted in the DYESOPT tool is discussed in section 2.5, while the inputs and outputs of such optimization that are entailed in this case are reported in section 3.10.

3.2 Case study – South African market

After a general overview of the most promising markets for PV-CSP implementation was carried out in section 2.6**,** South Africa was chosen as a representative case study for this thesis work. The choice is based both on availability of information about the market itself and on the favorability of the market with respect to both solar resource availability and structure of the energy demand.

As explained in 2.6.2**,** the structure of 2.3.4.1electricity demand in South Africa remains similar all year round, with peaks during morning and evening time. To promote the penetration of renewable energy technologies, the REIPPP program, currently at its fourth bid window (46) offers a well-defined tariff scheme for CSP under the form of a PPA, with three price tiers: a peak tariff during evenings from 4PM to 9PM, a base tariff from 5AM to 16PM and from 9PM to 10PM, and no tariff during night-time. Figure 15 and Table 2 show the structure of this tariff scheme for the CSP technology.

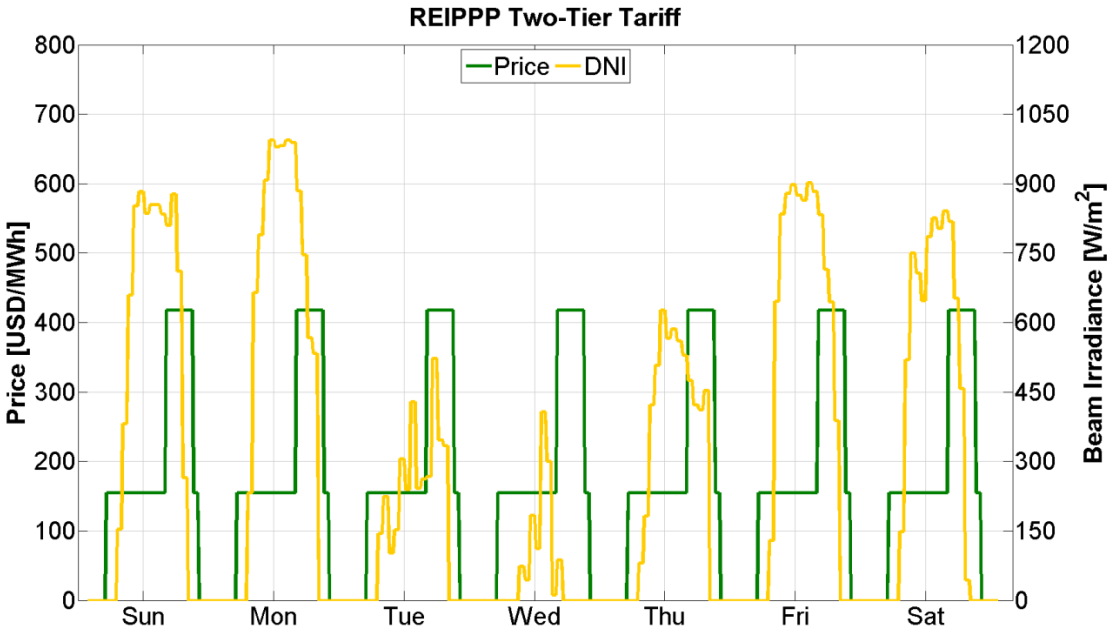

Figure 15 – REIPPP price scheme for CSP

Table 2 – CSP tariff scheme on the third bid window of the REIPPP (51)

Base hours [USD/MWh]	Peak hours [USD/MWh]
Base tariff	2.7*Base tariff

The most striking feature of this price mechanism is represented by the substantial difference between base and peak prices, being the peak tariff 2.7 times higher than the daytime price. Therefore, it might be interesting to investigate the feasibility of a hybrid PV-CSP solar power plant that is able to operate within this price scheme and is able to prioritize the evening peak hours in order to maximize revenues without significantly compromising operation during daytime.

For this thesis work, the price scheme explained above will be adopted. However, the values of the base and peak tariffs will be varied by the model according to the desired amount of revenues that the plant is expected to generate (IRR), and a new PPA value will be subsequently derived. Furthermore, even though in reality a different tariff applies for the PV technology with no peak prices, in this work the same price mechanism of the CSP will be applied when running the PV alone case, thus showing in the comparative analysis the real value of each technology when operating under the same tariff scheme.

Further input data about the design conditions of the location and the most relevant economic parameters is presented in Table 3 and Table 4**.**

Table 3 – Design-related parameters for the chosen location

RSC	Units	Data
Date (Gregorian day)	-	173
Time	-	Solar noon
DNI	W/m²	850
Ambient air temperature	°C	30
Ambient air pressure	kPa	92.6
Wind velocity	m/s	1.0

Table 4 – Economic input parameters for the chosen location (26)

Economic parameter		Values	Units
i	Real debt interest rate	12.5	[%]
IRR	Internal rate of return	15	[%]
k_{ins}	Annual insurance rate	1	[%]
$X_{tax,\%}$	Corporate sales tax (VAT)	28	[%]
n	Plant lifetime	30	[yr]

3.3 Solar Tower Plant model

The Solar Tower Power Plant (STPP) technology that has been utilized is based on a solar tower configuration with central receiver and direct double tank storage system, based on the Gemasolar plant layout (10), an established configuration that is already proven to be technically feasible. Figure 16 shows the schematic plant layout adopted in this study.

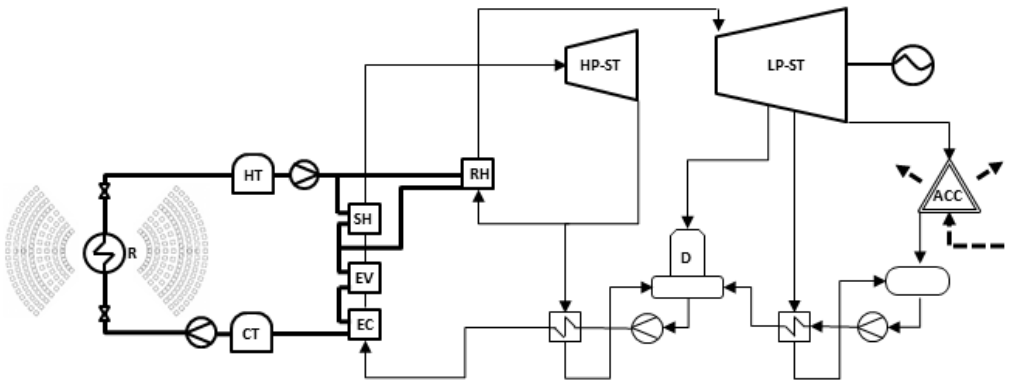

Figure 16 – STPPP layout (10)

The schematic is split into two clear thermodynamic cycles. The dark line represents the molten salts cycle (HTF cycle) while the thin represents the steam cycle. At nominal conditions, the salts initially stored in the cold tank (CT) are pumped up to the tower where they are heated by the incoming concentrated power coming from the heliostats field. Subsequently, the heated salts are stored in the hot tank (HT). When power production is requested the HT is discharged and the desired mass flow of salts is sent to the steam generator train, heating up water and generating steam. The steam generation train consists of an economiser (EC), evaporator (EV), superheater (SH) and a reheater (RH). The power block is a common reheat Rankine cycle that includes low and high pressure turbines (LP-ST and HP-ST), a deaerator (DE) and an air cooled condenser (ACC).

The sizing of the STPP plant represents the first step of the steady state sage shown in the flow chart of Figure 14. Based on the provided inputs, each component of the STPPP is individually sized by means of individual steady state models. The steady state design related functions in the model are presented in green in APPENDIX B. Through means of an iterative process the PB is designed first, then the SF and lastly, through direct calculations, the variable volume of TES is sized. The specific equations that are governing each model have been implemented by the developers of DYESOPT (52) which extracted the equations from (53), (54) and (29) for the SF, (55) for the HTF cycle and (56) (57) for the PB designs. The model has also been successfully validated by its authors (10) using the commercially available software Thermoflex (58).

In the dynamic model and its related functions the integration with TRNSYS (59) is implemented (in red in the graph in APPENDIX). Each of the previously mentioned blocks is then modelled in the TRNSYS environment for the dynamic simulation. Components from the standard STEC library (60) have been used, together with others developed by the authors themselves such as the receiver, the air cooled condenser and the logical controllers of the storage system. Each of these components has been previously validated in previous studies about transients in Rankine cycles of CSP plants (61).

Lastly in the techno-economic parameters of the STPP are calculated by combining the outputs from the steady state and dynamic simulations (in blue in the graph) and by applying specific cost functions. These will be explained in detail for the combined plant in section 3.8.2.

3.4 Photovoltaic plant model

The model of the PV power plant implemented in DYESOPT has been developed by (11) and it follows a similar structure of the previously described CSP model. In contrast to the CSP, the PV model is solely MATLAB based; steady state calculations are performed in order to size all the components of the plants, based on the capacity requirement that has been set as input. After that, the energy output at each hour of the year is calculated based on the hourly irradiation data provided in an external weather file. With this information, the model then derives economic parameters based on specific cost functions of PV power plants in a similar manner as it is performed in the CSP model. Even though a dynamic simulation with TRNSYS is not used in this case, specific text files are created in the MATLAB simulation, containing the hourly output of the plant throughout the whole year. These files can then be used by TRNSYS in order to set the control strategy in case the PV and CSP models are coupled; in this way it will possible to perform a dynamic simulation of a hybrid PV-CSP plant.

The sizing process consists of establishing the maximum number of modules that can be put in series in one string, the maximum number of strings per inverter and finally the total number of inverters, which leads to the complete sizing of the PV arrays. Afterwards, the model calculates the energy output of the plant at each hour of the year, based on the hourly irradiance information provided in the external weather file. The sizing was based on the methodology developed by (62).

The sizing and estimation of the annual energy yield of the plant are performed by taking into account several sub-steps:

- Estimation of the temperature and irradiance effect on the PV modules.

Both the current and voltage levels of a single PV cell are affected by the operating temperature of the cell itself, as shown in Figure 5. Therefore, the maximum and minimum values of cell voltage and current reached during the year need to be estimated based on the available ambient temperature and pressure data, before the sizing of the PV arrays can be performed. This was done based on the models of (63) and (64).

- Determination of the solar geometry.

The position of the sun in the sky at each hour of the year is derived by calculating typical astronomical parameters such as the declination angle, the hour angle, the solar zenith, the solar azimuth, the elevation and incidence angles. With this information, a model for estimating the hourly solar irradiation on the tilted surface of the PV modules (65) can be applied.

- Maximum Power Point.

As shown in Figure 4 there exist a specific combination of cell voltage V_{mp} and current I_{mp} that yield the maximum power output of the cell, for a given irradiance and cell temperature. Therefore, in order to evaluate the hourly energy yield of the plant, the values of V_{mp} and I_{mp} are calculated at each instant basing on a single diode circuit model for solar cells (66).

- Solar tracking

In addition to the fixed tilt option, the model implements three tracking modes, namely, single axis North-South, single axis East-West and double axis tracking. Specific equations and costs for each option have been implemented from (67).

- DC and AC outputs

Each string of modules produces a power output in DC form, which is then converted to AC by means of central inverters. A model to simulate the inverters behavior was extracted from (68). Furthermore, to preserve the lifetime of the inverters, whenever the available DC output of the array exceeds the inverter's input rated power the exceeding DC power is curtailed and the resulting AC power is set to the nominal power of the inverter. An example of DC curtailment can be seen in Figure 17 in the green dashed lines.

3.5 Combined model

After both the CSP and PV plants have been individually sized based on the provided inputs and the methodologies described above**,** the next step consists of their mutual coupling. This results in the two systems working together as a single power plant, providing a single combined output. Firstly, the nominal electrical output of the combined plant needs to be defined; as power production coming from the PV side is intermittent and unavailable during non-sun hours, the design nominal output needs to be always referred to the CSP plant:

$$W_{el_{PV\_CSP_{nom}}} = W_{el_{CSP_{nom}}} \quad (2)$$

Due to the fact that the PV hourly output is variable depending on weather conditions, the only way to ensure the planned output of the plant at all times is to vary the load of the CSP system by following the

PV generation. By knowing the hourly values of irradiation, the hourly PV output can be estimated and so the expected CSP output setpoint:

$$W_{el_{CSP\,i}} = W_{el_{PV\_CSP,desired,i}} - W_{el_{PV\,i}} \quad (3)$$

The instantaneous electrical output of the PV-CSP plant then can be simply defined as the sum of the instantaneous PV and CSP contributions:

$$W_{el_{PV\_CSP_i}} = W_{el_{PV\,i}} + W_{el_{CSP\,i}} \quad (4)$$

It must be noted that, due to the fact that the nominal output of the plant is referred to the CSP nominal output, high levels of PV production in sunny days might bring the working point of the CSP plant to load factors that are too low for the steam turbine to be operated both due to efficiency drops and increase in thermal stresses between the rotor and thick-walled components, that in the long term can result in permanent damage of the turbine (69). The lower limit of the turbine working point has been assumed to be 30% of the rated power based on typical ranges provided by suppliers found in literature (70). Consequently, when the CSP load reaches this lower limit, the extra AC output coming from the PV plant must be curtailed, as shown in Figure 17 (black line).

Another feature of the combined model is the capability of working at different levels of output according to the time of production, thus simulating in a more realistic way the behavior of real load-following power plants. The different output tiers that have been employed are the following:

- Hourly variation: The plant varies its output during the day following the hourly demand; this is measured based on the hourly values of electricity prices. During peak hours, the plant is always dispatched at nominal output, while in hours of lower demand, thus featuring lower prices, the output is reduced to save storage for peak times.
- Seasonal variation: The output tiers of the combined plant also vary seasonally, reflecting the different levels of demand and solar resource during the year. Nevertheless, the peak hours are dispatched at nominal output regardless of the season.

The concepts that have been explained above are illustrated in Figure 17, where one day of operation of the combined plant is shown both for the summer (a) and for the winter (b) case. The plots qualitatively represent the planned non-optimized operation that is performed in MATLAB prior of the dynamic simulation using the tariff scheme of REIPPP 4 that was explained in section 3.2**,** in which two tariff tiers, base for daytime and peak for evenings, are present during the day for the whole year.

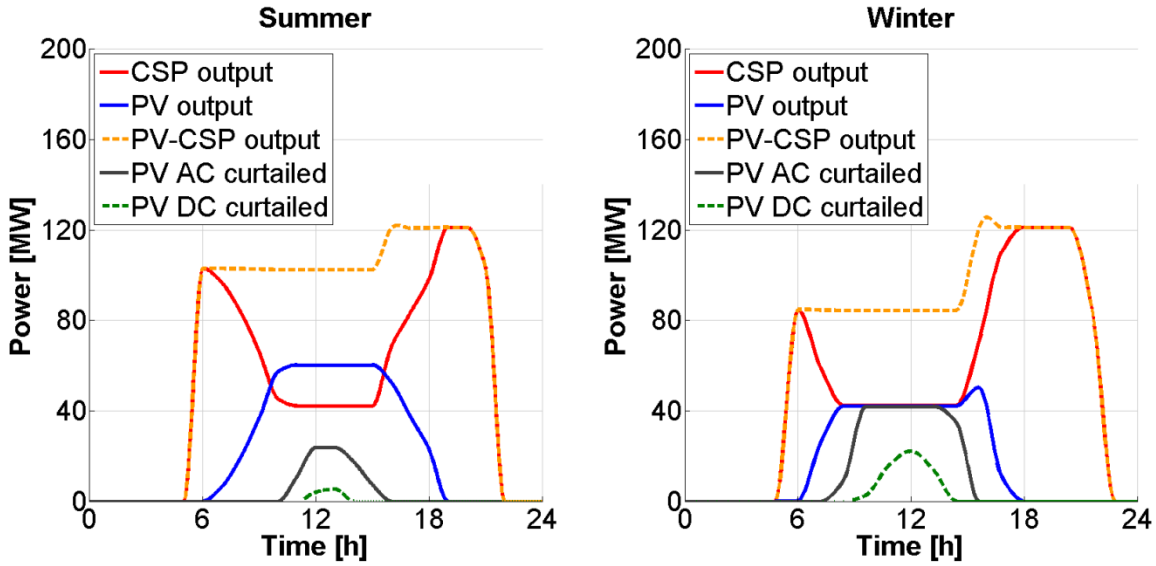

Figure 17 – Example of pre-defined PV-CSP daily operation in summer (a) and winter (b)

It can be seen how the CSP output (blue line) adapts to the PV production (red line) to provide a stable combined output (dashed line), decreasing its load while PV is ramping up. In the case shown in Figure 17, the PV capacity is high enough to make the CSP reach the lowest point of operation of the turbine, therefore its output must be curtailed to avoid that the CSP operates below 30% of the nominal output, as shown in the black line. The figure is also illustrative of the different output levels at which the plant is able to operate, both daily and seasonally. During daytime hours, associated with lower electricity prices, the combined output can be reduced to a percentage of the nominal, which is in turn dispatched during the evening hours corresponding to the peak electricity tariffs. It can be seen that in this case the difference between the output tiers during daytime and peak time is more pronounced in winter than in summer, reflecting the fact that in winter the solar resource is lower and the CSP plant might need to be operated at lower outputs during daytime to save storage for the evening peak hours. Again, the graphs show a non-optimized plant configuration, therefore the output tiers levels of optimized plants might differ from what is shown, as they will be set as open variables to be changed by the optimizer. The amount of AC power curtailed from the PV is also strongly dependent on the combined plant's output level that is dispatched during daytime; it can be seen in the illustrated case that in winter the amount of PV curtailment is much higher than in summer, due to the fact that the combined output during daytime is reduced and the CSP cannot work below its minimum working point. This fact implies the importance of finding an optimum configuration of the various parameters of the plant such as output levels, PV and CSP capacities etc. in order to maximize the combined performance. This represents the task that will be carried out in the multi-objective optimization, explained in section 3.10.

3.6 Pre-defined dispatch strategy

The pre-defined dispatch strategy (PDS) represents the core of the model for the specific analysis carried out in this thesis work. It is in fact in the PDS where the dispatch of the plant is set, in which it is established how much power the plant can produce and at what times it will do so. A thorough selection of the plant operating hours is of key importance particularly for the case studies that will be analyzed, in which a peaking/load-following power plant is being modelled. The fundamental objectives on which the PDS must be based are the following:

- Maximize plant revenues
- Optimize storage utilization

The amount of revenues a plant can generate strongly depends not only on the amount of energy that is able to produce, which is reflected in its capacity factor, but also on the time of energy production. In fact, electricity production during peak hours is generally rewarded a substantially higher price than hours of lower demand, as demonstrated by the REIPPP tariff scheme. Accordingly, for a peaking and intermediate load power plant it is of crucial importance to be able to match hours of high prices for as many times as possible during the year. As a consequence, the PDS that must be developed will prioritize time of production rather than the amount of energy produced.

As shown in Figure 1, peak hours usually occur at times when the solar resource is low i.e. early morning and evenings. This is also the case for the market subject to this case study (Figure 15). In absence of large scale battery storage, which is not considered in this work, PV generation can give little contribution to meeting demand at peak times. Consequently, the output of the hybrid plant must be ensured by the thermal energy storage system of the CSP side, making its optimization and correct usage an essential objective of the PDS as well. Therefore, the PDS is mostly focused on the CSP side of the combined plant.

The starting algorithm for the PDS used in this work is based on the one previously developed for a CSP alone plant by *Guedez et al* in *"A Methodology for Determining Optimum Solar Tower Plant Configurations and Operating Strategies to Maximise Profits Based on Hourly Electricity Market Prices"* (10). Firstly, the hourly price file of the chosen location is read and the hours in the day are rearranged in order of decreasing tariff to ensure that the hours with the highest tariffs are considered first as peak hours. A simplified explanatory flow chart of the algorithm is presented in Figure 18. After reading the price data, the hours Op_hr,j in which a tariff is present are marked with 1, representing the potential operational hours of the plant. Within these hours, peak ($Peak,j$) and base ($Base,j$) hours are distinguished on the basis of price. Due to the fact that in the REIPPP tariff scheme only two tariff tiers are present, the peak hours can be simply identified as the ones featuring the maximum price, as shown in the flow chart, while the base hours all belong to the other price level. These identification values are then summed at the end of the day giving the respective number of total peak ($N_{hrs,peak,i}$) and base ($N_{hrs,base,i}$) hours for that day. These vectors are then printed in a file to be used in the subsequent step of the PDS and then in the dispatch control during the transient simulations conducted by TRNSYS.

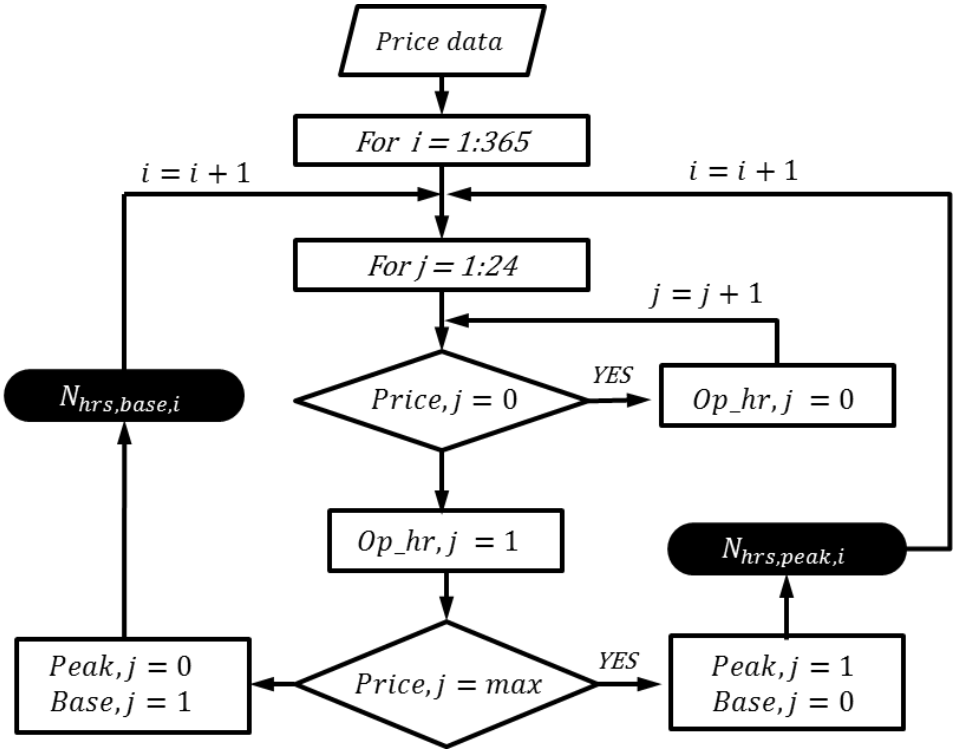

Figure 18 – Simplified algorithm for the selection of operational hours

After the hours of operation have been classified, the resulting behavior of the plant for the combined PV-CSP operation can be resumed in the following table, to be referred when further proceeding in the report:

Table 5 – Operating modes of the combined PV-CSP plant

Operation mode	Description	Time frame
Mode 1	Combined operation at nominal output	- Peak hours (mandatory) - Base hours (optional)
Mode 2	Combined operation at variable output	- Base hours
Mode 3	Dispatch of PV during base hours and CSP during peak hours.	- Day

As can be seen, three modes of operation are possible, according to the type of tariff hour in which the plant is currently operating. The algorithm developed for determining whether the plant should operate or not and with which operation mode in each hour is presented in Figure 19.

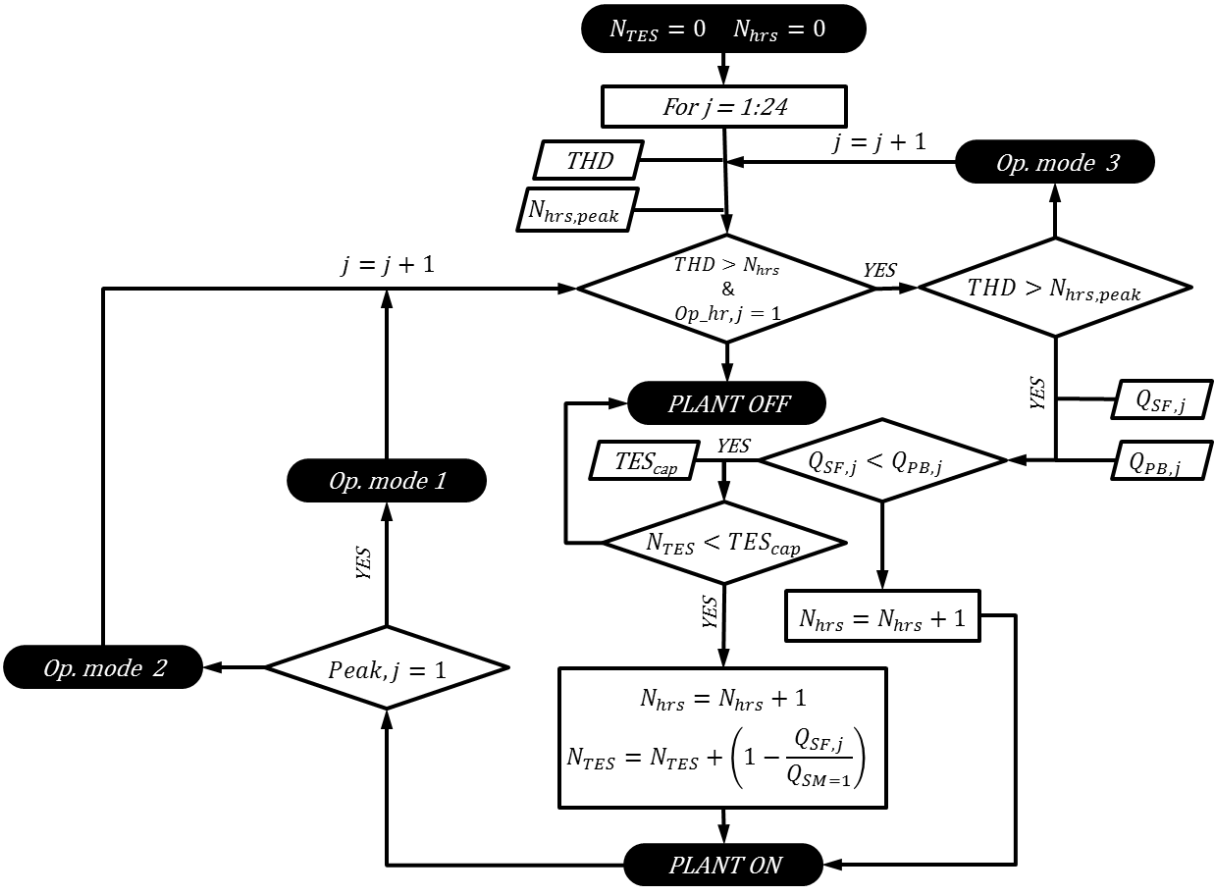

Figure 19 – Pre-Defined Dispatch Strategy (PDS) of the combined plant

The algorithm is based on the estimation of the total number of hours that the CSP plant can operate per day (THD); this can be done in advance before the dynamic simulation since the hourly values of direct irradiation for the location are known as an input data. Thanks to this, the hourly energy production of the

solar field ($Q_{SF,j}$) can be estimated as a function of hourly beam radiation and solar field efficiency, which in turns depends on the solar elevation and azimuth angles (10). By knowing the instantaneous thermal power demand from the power block ($Q_{PB,j}$), the THD can then be calculated by means of the equation below:

$$THD = \sum_{j=1}^{24} \frac{Q_{SF,j}}{Q_{PB,j}} \tag{5}$$

As stated before, the plant subject of this study is a hybrid plant in which PV and CSP work together to provide a single combined output and the CSP system has to vary its output in order to adapt and provide support for the PV generation**.** Due to the presence of PV during daytime the CSP plant might work at off-design conditions (part load) to allow the desired output to be reached, therefore resulting in a different storage utilization and thermal power demand of the PB with respect to a CSP alone case. Consequently, the hourly thermal demand of the PB that has to be provided by the solar field ($Q_{PB,j}$) changes according to the specific setpoint of the CSP plant, according to the following equation:

$$Q_{PB,j} = \frac{W_{el_i}}{W_{el_{nom}}} * Q_{th_{nom}} \tag{6}$$

Where W_{el_i} and $W_{el_{nom}}$ are the hourly and nominal electrical output of the CSP power block and $Q_{th_{nom}}$ its nominal thermal energy demand. The condition for whether using the storage or not is then the following:

$$Q_{SF,j} < Q_{PB,j} < \frac{W_{el_i}}{W_{el_{nom}}} * Q_{th_{nom}} \tag{7}$$

In case the incoming instantaneous power from the SF is less than the requested value ($Q_{SF,j} < Q_{PB,j}$) the storage is then used to supply the energy gap, at the condition that the amount of storage hours already utilized do not exceed the nominal storage capacity ($N_{TES} < TES_{cap}$). Every time the plant is assigned to operate for an hour, a counter N_{hrs} is updated. The loop keeps going until the counter does not exceed the maximum number of hours that the plant can operate in that day (THD) or when the current hour is not a tariff hour ($Op_{\_hr,j} = 0$), at which point the plant is shut off.

Once the plant is set to operate, the operation mode is chosen based on the available THD hours of that day and on the type of hourly tariff. In case the available THD are less than the number of peak hours of the day, the plant is dispatched in **operation mode 3**, with only PV during daytime and CSP to supply the peak hours. In the other case, the plant is dispatched at nominal output (**mode 1**) in case the current hour is a peak hour ($Peak_{,j} = 1$), otherwise at a fraction of it (**mode 2**).

The result of this algorithm is a selective pre-dispatch of the combined plant: the plant is set to operate whenever there is a price hour and there is enough energy incoming from the solar field. In case the solar field power is lacking, for instance due to a cloudy day, the storage is then utilized at the condition that supply for the peak hours can be granted; if not, the CSP plant then does not operate during hours of lower price in order to save storage and be able to provide the desired output during the peak hours.

The underlying assumption for the condition above is that the relation between thermal energy demand of the power block and its electrical output is approximated with a linear behavior. The accuracy of this assumption has been checked by performing trial dynamic simulation runs and plotting the resulting values of thermal and electrical power in the power block, as shown in the following graphs:

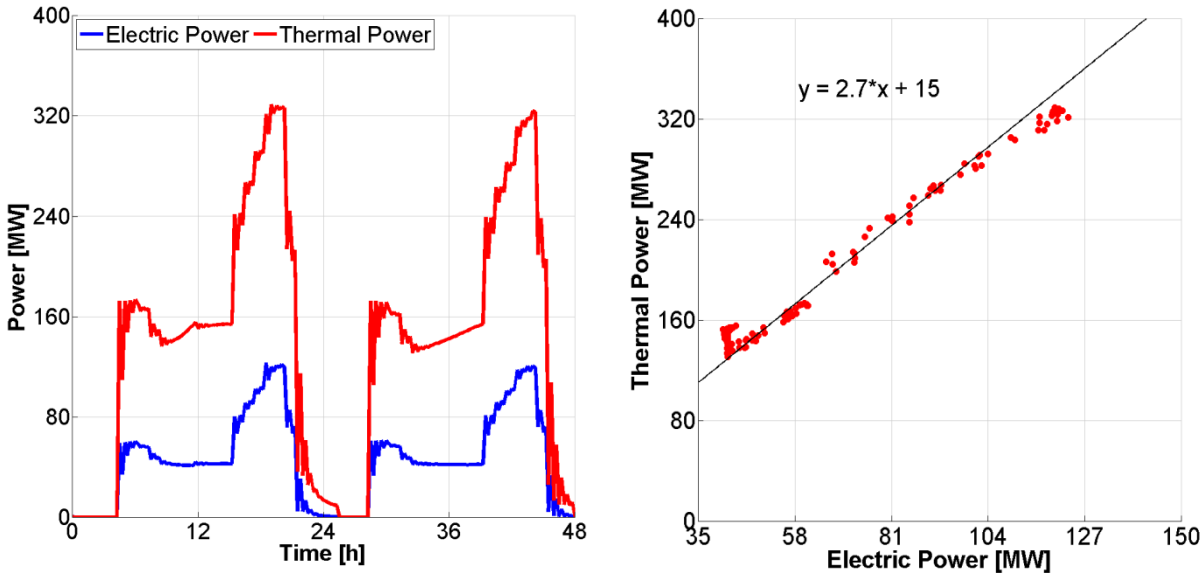

Figure 20 – Relation between thermal and electric power in the power block

As expected the thermal power is found to follow the behavior of the electric as a multiple of it, as shown in the left plot. When the thermal power is plotted as a function of the electric power for one day of operation (graph on the right), a linear behavior in the intermediate part-load range can be distinguished. Such approximation has been used only for the pre-assessment of the operational hours of the plant prior of the dynamic simulation. The actual off-design performance of the power block is taken into account by an efficiency curve for the steam turbine based on the Stodola Ellipse law (71).

For the PV-CSP case the hourly thermal power demand of the power block is reduced compared to the CSP alone case, due to the fact that PV is providing part of the desired output and the CSP plant is working at reduced load during this time. This results in improved savings of thermal energy storage that can be used to ensure more hours of operation at nominal output during peak periods.

3.7 Dynamic model

After both the PV and CSP power plants are sized and the dispatch planning is made, the next step consist of performing the dynamic simulation of the system for a whole year. As was mentioned before, the dynamic model is implemented in the TRNSYS environment due to the fact that CSP configurations, including solar tower configurations, are of complex nature and a MATLAB based calculation would prove to be difficult, slow and or/inaccurate. Furthermore, the STEC library in TRNSYS contains a number of built-in components that can facilitate the modelling of a solar power plant.

The dynamic simulation in TRNSYS is performed only for the CSP system. In fact, due to the nature of the PV model, the hourly energy output of the plant can be calculated directly in MATLAB, as was described in section 3.4.

3.7.1 TRNSYS inputs

The TRNSYS model components generally operate with a number of input data to produce a related number of outputs. The input variables of the whole system are provided through .txt files written in MATLAB, containing the results from the steady state calculation that was described in the previous sections. By using these files, TRNSYS carries out the dynamic simulation of the plant over the course of a year (by default) or over a specified time interval. It is important to realize that all the input files provided by the steady-state MATLAB model are sent to TRNSYS as fixed design values, which are not changed throughout the dynamic simulation process. The main files that TRNSYS reads as an input can be resumed as follows:

- **Simulation data:** Contains the desired number of hours of the simulation (8760h per year) and the chosen time step.
- **Weather data:** Contains the Typical Meteorological Year (TMY) weather data necessary for the transient calculations, including hourly irradiation values, solar azimuth and elevation values, ambient temperature and pressure conditions. These data are historical-based satellite measurements obtained from the Meteonorm (72) dataset for the location subject of the study in hourly values, and subsequently interpolated in the TRNSYS components for the specific time step of the transient simulation.
- **Design data:** Contains the steady state values for the STPP components, i.e. the nominal operating points. The input parameters include the sizing and nominal thermodynamic conditions of the turbines, the steam generation train, the condenser, the solar field efficiency matrix, the receiver, the storage tanks, etc.
- **PDS:** Contains the Pre-Defined Dispatch Strategy information. This includes the hourly output values for the steam turbines and the operation hours, which have been calculated according to the method explained in section **3.6.**
- **Price data:** Contains the hourly prices of electricity for the chosen location/market.

3.7.2 Control system

The key linkage between the PV and CSP models and for the correct application of the PDS is represented by the control system implemented in the TRNSYS plant layout. This system basically controls the dynamic behavior of plant by adjusting the molten salts mass flows and setting the dispatch of the storage tanks based on the inputs provided in the PDS file. As descried before, in the combined PV-CSP model the CSP plant has to dynamically adjust its output in response to PV fluctuations; this is initially done on an hourly basis in MATLAB to define the CSP setpoint at each hour of the year and determine the dispatch strategy planning accordingly. This information is then processed by the control system in TRNSYS to regulate all the plant's components to meet the desired CSP setpoint within the time step of the dynamic simulation.

To perform these tasks, a Proportional-Integral-Derivative controller (PID) is used, represented in TRNSYS by the built-in component type 23 (73). This component generally performs a loop feedback control, in which the measured process variable is evaluated in each loop and sent back as an input until its value converges to the value of the desired setpoint. In this case, the variable to be controlled is the instantaneous CSP power of the transient time step, while the setpoint to be reached is the hourly CSP output set in the PDS. The PID controller then provides a control signal as output, represented by the molten salts mass flow values that need to be sent from and to the hot and cold tanks.

3.7.2.1 Tuning of the controller

From basic control theory it is known that the control action of the PID controller is determined by the sum of three parameters, namely the proportional, integral and differential gain (74). The tuning of the PID controller consists of finding the right setting of these three parameters. Since this is usually of complicated analytical nature, in reality their values are found by trial and error until the desired behavior is found within an acceptable degree of error, as it will also be done in this model. The values that have been used in the final simulation are contained in Table 6.

Table 6 – Input parameters values used for the PID controller

Gain type	Value
Proportional	10000
Integral	0.2
Derivative	0
Model time step	0.2 [h]

The tuning of the PID controller represents one of the main issues associated to the combined model, due to the fact that the CSP plant has to adjust its output not only in response to PV fluctuations but also to variations in the hourly prices of electricity. Therefore, a significantly low response time is needed from the controller in order to match each hour with the proper planned output without significantly compromising the stability of the system. Increasing the proportional gain improves the response time of the controller and allows the error between the setpoint and the controlled variable to be decreased. However, this occurs at the expenses of stability, resulting in a more oscillatory output. The amplitude of the oscillations can in turn be decreased by increasing the value of integral gain, but at the expenses of the response time. The derivative term can also be useful to dampen the output oscillations but it is seldom used in practice because of its variable and unpredictable impact on system stability (75), as it was also experienced in this model. An example of the influence of these parameters on the combined plant output can be seen in Figure 21, for high (14000) and low (4000) values of proportional gain.

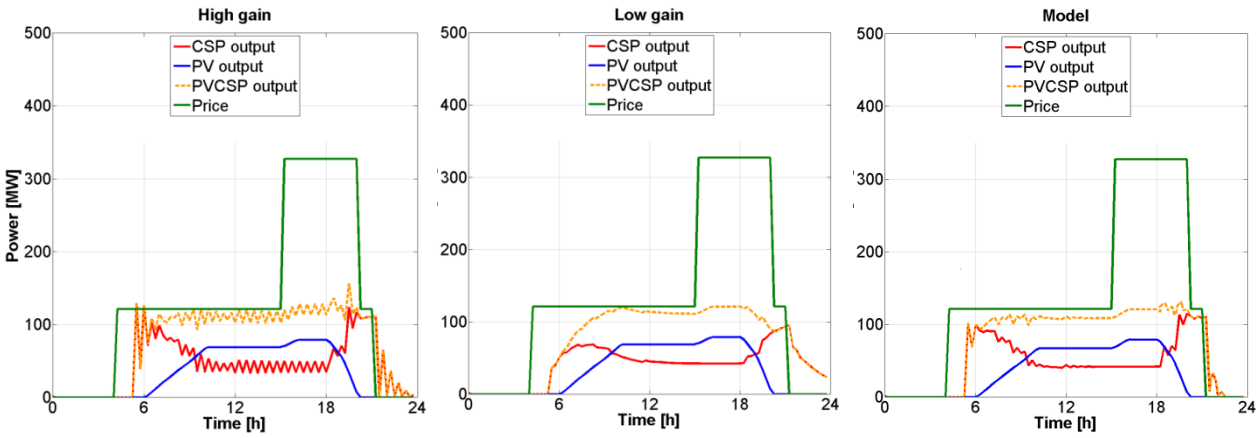

Figure 21 – TRNSYS output for high (a), low (b) and adopted (c) proportional gain of the PID controller.

With too high proportional gain (a), the output shows significant instability and oscillations, which are present also several hours after the shutdown of the plant. On the other hand, too low values of proportional gain (b) make the response time of the plant slow, failing to adjust in time to PV production and price variations. This occurs also during shutdown when a significant amount of power is still

produced after several hours. The case adopted in the model (c), shown in Table 6**,** still presents oscillations when CSP is ramping up/down, but with significantly lower amplitude and frequency with respect to the high gain case, without considerably compromising the response time.

The values shown in Table 6 have been found using a transient time step of 15 minutes. This is the lower limit value that has been chosen for the dynamic simulation; lower time steps would improve the overall stability and accuracy of the model, including the control, but the computational time would exceed the purpose of this thesis work.

3.7.3 TRNSYS output

The TRNSYS simulation results are projected in graphical format, showing the power values, TES levels and price values of the plant, amongst other important results. A representative example can be seen in Figure 22 and Figure 23**,** where a week of operation in summer is simulated for non-optimized combined and CSP alone plants.

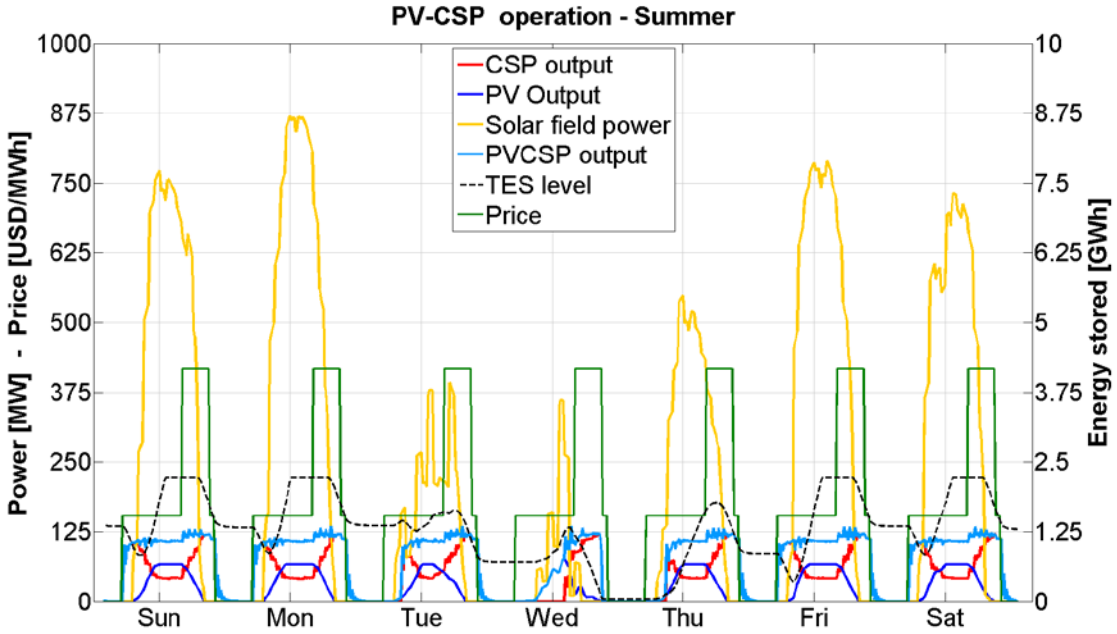

Figure 22 – Example of weekly dynamic operation of the PV-CSP plant.

This example is for a single run simulation of the PV-CSP combined model which does not represent an optimal plant configuration; therefore, it must only be considered as a representation. In the graph, the combined electrical power is shown in the light blue line, being the sum of the CSP (in red) and PV (in blue) outputs. The energy stored in the hot storage tank is represented by the dashed black line and the solar field power and tariff scheme by the golden and green lines respectively. It can be seen how the dispatch strategy influences the behavior of the plant; in days of low solar irradiation, such as Wednesday, the working hours of the CSP plant are reduced in order to save storage for the peak evening hours, which therefore can be dispatched at full output even in such days. This behavior corresponds to **operation mode 3** in Table 5 **.** On the other hand, during days of normal irradiation, the plant operates **in mode 1** (nominal output) during peak hours and **mode 2** (reduced output) during base hours.

The fact that this is not an optimum configuration can be seen in the level of the TES, which is still significantly high at the end of each day (excluding bad radiation days), showing that the solar field and/or the storage tanks are oversized. An example of operation of an optimized plant for the same week will be shown in the 'results' section.

In a similar fashion, the CSP alone dynamic operation for a plant of the same capacity can be introduced in Figure 23.

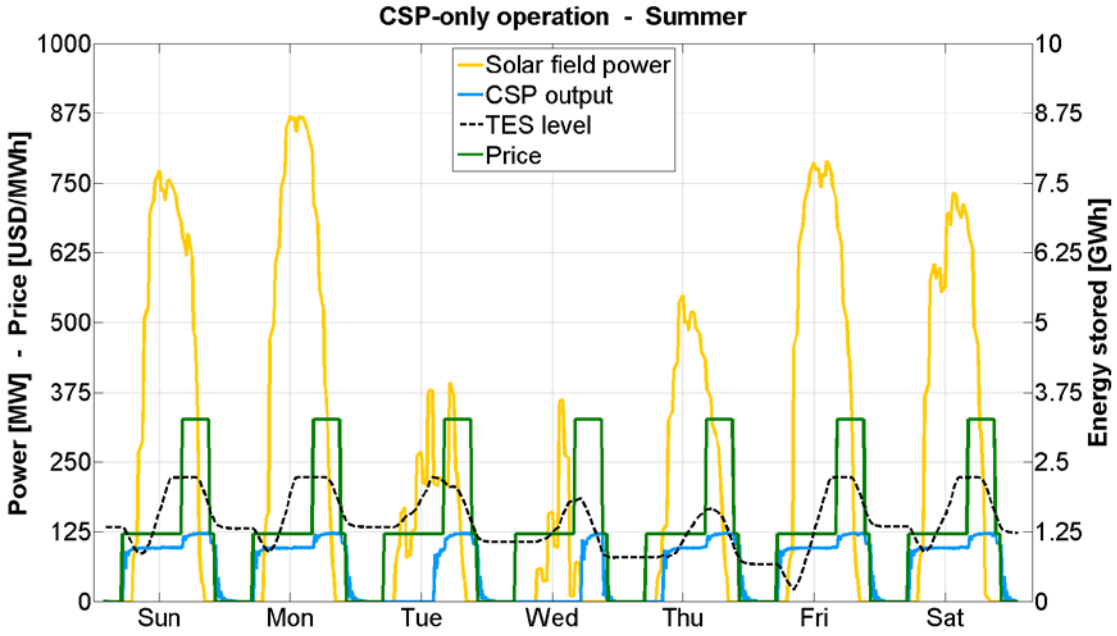

Figure 23 – Example of weekly dynamic operation of the CSP alone plant

In this case the output of the plant is obviously represented by only the CSP output. The dispatch strategy is the same as the PV-CSP case, as it involves the CSP side of the plant in any case. It can be seen at first glance that part load operation of the CSP plant is significantly reduced compared to the hybrid case, due to the absence of PV. On the other hand, this leads to a reduced number of operation hours especially in bad radiation days, as can be seen by comparing the outputs on Tuesday and Wednesday for the two cases. Accordingly, the consequences of these facts will be discussed in detail in the 'results' section for optimum plants configurations.

All the output data resulting from TRNSYS is then saved and sent back to MATLAB in the form of text files, to be read and processed for the calculation of the performance indicators, which will be described in detail in the next section.

3.8 Techno-economic calculations

After the dynamic simulations are complete, the data is exported back to MATLAB in order to perform the thermo-economic calculations and to calculate the performance indicators. Here, all the post-processing calculations are performed, which allow the most important economic parameters to be calculated.

In the PV model, the inputs are taken directly from the results of the MATLAB calculations and the performance indicators are subsequently derived as described in section 3.8.2. Regarding the CSP, the results coming from the TRNSYS simulation need to be taken; firstly MATLAB calls in the .txt output files from TRNSYS, read them and checks if the simulations were complete. The output txt files are:

- **Power File:** A file that contains the power values of the plant, including the net power output, the power from the solar field, the thermal output from the plant, the electrical consumption of the condenser, the energy stored in the TES, the thermal efficiency of the whole cycle, the solar

field efficiency, the total conversion efficiency and the work needed to run the pumps and the condenser. All of which is per the user defined simulation time step.

- **Price File:** A file that contains the tariffs and the dispatch strategy (whether or not the plant is operating for that given period), in terms of the user defined simulation time step.

Using these values the total annual energy yield, efficiency, revenues and operational hours can be calculated and used for the model validation and derivation of the previously mentioned performance indicators.

3.8.1 PDS indicators

After the data from the dynamic simulation are received, it is possible to validate the performance of the PDS, which means calculating a series of indicators that can be useful to see how well the dynamic model operation matches the planned operation made in MATLAB. The indicators that have been developed for this purpose are the following:

1. *Ratio between total PDS operation hours and total price hours*:

$$k1 = \frac{h_{PDS}}{h_{price}} * 100 \tag{8}$$

Measures the percentage of price hours the plant is planned to be operated over the year. It must be kept in mind that for the chosen case study the price hours must be used instead of the total hours of the year due to the fact that the implemented tariff scheme does not remunerate generation during nighttime.

2. *Ratio between total dynamic operation hours and total PDS operation hours*

$$k2 = \frac{h_{op}}{h_{PDS}} * 100 \tag{9}$$

Measures the percentage of planned operation hours matched in the dynamic operation over the year.

3. *Ratio between dynamic base operation hours and price base hours*

$$k3 = \frac{h_{op,base}}{h_{price,base}} * 100 \tag{10}$$

Measures the percentage of price base hours operated in the dynamic simulation over the year.

4. *Ratio between dynamic peak operation hours and price peak hours*

$$k4 = \frac{h_{op,peak}}{h_{price,peak}} * 100 \tag{11}$$

Measures the percentage of price peak hours operated in the dynamic simulation over the year.

5. *Capacity factor during base hours*

$$k5 = \frac{W_{el} * h_{op,base}}{W_{el_{nom}} * f_{load} * h_{price,base}} * 100 \quad (12)$$

Where f_{load} is the average between summer and winter load factors.

6. *Capacity factor during peak hours*

$$k6 = \frac{W_{el} * h_{op,peak}}{W_{el_{nom}} * h_{price,peak}} * 100 \quad (13)$$

3.8.2 Performance indicators

There are various indicators that are calculated when considering the performance of the plant, but the most important for the scope of this work are noted below. All the definitions and equations for these performance indicators are taken from (10) and (76).

- CAPEX
- OPEX
- IRR
- PPA
- LCOE

These parameters represent the vital information that is needed to perform feasibility studies in order assess the viability of a project for a specified location, which characterize the objective of the entire model.

In general, the procedure followed to estimate each cost component consists of taking costs that have been found in previous projects in the same location and scaling them to the desired plant capacity under study. A generic cost function adopted in the model for such purpose is shown in equation (14):

$$Cost_{calculated} = Cost_{ref} \left(\frac{CAP}{CAP_{ref}} \right)^{y} \quad (14)$$

Where the exponent y of the equation represents a simplification used to approximate a non-linear behavior of the cost functions with respect to the plant size. In the CSP model the exponent is changed according to the specific cost function. The reference values for each cost component of the plant and the corresponding scaling coefficients are taken from literature (26) (77).

3.8.2.1 CAPEX

The CAPEX is a measure of the total investment of the plant, shown by equations (15) and (16). For the combined plant, it is simply represented by the sum of the capital costs of the CSP and PV plants.

$$CAPEX_{CSP} = C_{direct,CSP} + C_{direct,CSP} \quad (15)$$

$$CAPEX_{PVCSP} = CAPEX_{CSP} + CAPEX_{PV} \quad (16)$$

The CAPEX is generally split into direct costs, related to the purchase and installation of plant equipment, and indirect costs, which include the spectrum of costs that are not encompassed in the previous category (land, taxes and engineering costs) as shown in equation (17).

$$CAPEX = C_{direct} + C_{indirect} \quad (17)$$

A general breakdown of the CAPEX components of both the PV and CSP plants is presented in the following section. A more detailed breakdown can be found in APPENDIX C.

3.8.2.2 CSP CAPEX

Equation 18 represents the upfront investment of the CSP plant. The direct component of the CAPEX comprises the investment associated to the power block (C_{PB}), solar field (C_{SF}), storage (C_{TES}), tower receiver (C_{rec}), balance of plant (C_{BOP}), land adaptation and contingency (C_{Site} and C_{Cont}) costs. The indirect CSP CAPEX covers all the remaining costs for the upfront investment that are not directly related to the installation and purchase of equipment. These costs mainly include the tax costs (C_{TAX}) plus the engineering, procurement and construction (C_{EPC}). Additional terms might include the purchase of land (C_{Land}).

$$CAPEX_{CSP} = C_{direct,CSP} + C_{direct,CSP} \quad (18)$$

$$C_{direct,CSP} = C_{PB} + C_{SF} + C_{TES} + C_{Tower} + C_{BOP} + C_{Site} + C_{Cont} \quad (19)$$

$$C_{indirect} = C_{EPC} + C_{Land} + C_{TAX} \quad (20)$$

3.8.2.3 PV CAPEX

On the PV side, the direct component of the CAPEX is made of the cost of the PV modules (C_{PV}), inverters (C_{Inv}), balance of system (C_{BOS}) and finally the tracking system ($C_{Tracking}$). The latter will be considered zero in the case of fixed-tilted arrays. As for the CSP case, the indirect cost in the case of the PV power plant is associated to the same variables (Equations 21, 22 and 23).

$$CAPEX_{PV} = C_{direct,PV} + C_{inderect,PV} \quad (21)$$

$$C_{direct,PV} = C_{PV} + C_{Inv} + C_{BOS} + C_{Tracking} \quad (22)$$

$$C_{indirect,PV} = C_{E\&D} + C_{Land} + C_{TAX} \quad (23)$$

3.8.2.4 OPEX

The OPEX, shown by equation (24), is the sum of the costs associated with plant operation and maintenance including labor, service costs, utility consumables and other miscellaneous costs. The operational expenditure of the hybrid plant is again calculated separately for the CSP and PV components.

$$OPEX_{PVCSP} = OPEX_{CSP} + OPEX_{PV} \tag{24}$$

3.8.2.5 CSP OPEX

The CSP OPEX includes four main variables as shown on equation (25). The costs of utility represent services like water and electricity, among others necessary to run the plant. The cost C_{serv} accounts for additional services not related to the plant operation. The miscellaneous costs, C_{misc} , accounts for the overheads on the operation. Finally, the fixed Operation and Maintenance (O&M) services are represented by C_{labor} and are related to the personnel necessary to operate and maintain the plant.

$$OPEX_{CSP} = C_{labor} + C_{serv} + C_{utility} + C_{Misc} + C_{Insurance} \tag{25}$$

A detailed description of each of these components can be found in APPENDIX C.

3.8.2.6 PV OPEX

For the OPEX in the PV power plant the approach is the same. The difference is that the utility services are included in the labor variable. It also includes PV panel cleaning, power plant monitoring and inverters maintenance. Additionally, overheads on daily operations are also considered.

$$OPEX_{PV} = C_{labor,PV} + C_{Insurance,PV} \tag{26}$$

3.8.2.7 Internal rate of return (IRR)

The internal rate of return (IRR) represents an indicator of fundamental importance for economic evaluations of projects. It is used to measure the relative profitability of the plant. Its value descends from the Net Present Value (NPV), which can be defined as the difference between the present value of cash inflows and the present value of cash outflows, as shown in equation (27):

$$NPV = \left\{ \begin{array}{l} -\sum_{t=0}^{n_{con}-1} \frac{CAPEX}{n_{con}(1+i)^t} \\ +\sum_{t=n_{con}}^{n_{con}+n_{op}-1} \frac{REV - OPEX}{(1+i)^t} \\ -\sum_{t=n_{con}+n_{op}}^{n_{con}+n_{op}+n_{dec}-1} \frac{C_{dec}}{n_{dec}(1+i)^t} \end{array} \right\} \quad (27)$$

Where REV are the annual revenues from the selling of electricity, i the real discount rate and C_{dec} the decommissioning cost of the plant. n_{con} represents the construction time of the plant, n_{op} its operational time and n_{con} its decommissioning time. For this study, the decommissioning cost or salvage value was not taken into account for the CSP technology as a clear picture of these values does not exist yet, due to the recentness of the solar tower technology (26). From the NPV, the IRR is calculated as the discount rate that zeros all of the cash flows at the end of the power plant lifetime, calculation that must be performed by means an iterative algorithm. In this thesis work, a desired value of IRR will be fixed as an input, which will be used to derive the corresponding prices of electricity that allow the finding of a suitable power purchase agreement for the plant, as described in the next section.

3.8.2.8 Levelised Cost of Electricity (LCOE)

The levelised cost of electricity can be defined as the minimum price of electricity which, over the entire lifetime of the power plant, generates enough revenues to pay back the CAPEX, cover the OPEX and generate enough cash for plant decommissioning. In other terms, it is the electricity price needed for the plant to break-even over its lifetime. In the model, the LCOE is calculated according to the following equation:

$$LCOE_{PV-CSP} = \frac{CAPEX_{CSP} + \sum_{t=1}^{n} \frac{OPEX_{CSP}}{(1+i)^t} + CAPEX_{PV} + \sum_{t=1}^{n} \frac{OPEX_{PV}}{(1+i)^n}}{\sum_{t=1}^{n} \frac{FYE_{CSP} + FYE_{PV} \times (1-SDR)^t}{(1+i)^t}} \quad (28)$$

FYE_{CSP} and FYE_{PV} correspond to the first year electrical output of the CSP and PV components respectively. Due to fact that the performance of PV systems degrades with time, a degradation factor (SDR) is taken into account (78) (79).Its value was defined from literature as 0.79% of the nominal electricity production (80).

Despite the fact that this is the most common indicator used for comparing different technologies among themselves, its use when hourly variations of electricity prices are present, such as in this case study, does not represent a fair mean of economic assessment for the plant, since the actual time of production is not taken into account in this indicator. Instead, the comparison will be carried out using other economic indicators which take into account the time of production of the plant, such as IRR and PPA, defined in the next section.

3.8.2.9 Power Purchase Agreement (PPA)

One of the main goals of this thesis work lies in the determination of the optimum electricity price scheme that must be applied in order to make the proposed designs profitable. At the present state, most of the utility scale current and planned solar projects operate under a Power Purchase Agreement (PPA) (81). A PPA is generally a long term agreement between the buyer and seller of electricity in which a fixed price is granted for the produced electricity for the entire duration of the contract, regardless of future market conditions. In contrast to the LCOE, a PPA price represents not just the cost of generating electricity but the real selling tariff were tax payments and investors returns are taken into account (26). An example of PPA in the context of solar energy is the current price scheme applied for CSP in South Africa under the REIPPP program, which constitutes the starting price structure of this work as well.

The structure of the REIPPP 4 price scheme was explained in section **3.23.2.** In the REIPPP 4 case the PPA can be determined as the weighted average between the base tariff applied during daytime and the peak tariff applied during peak hours:

$$PPA_{REIPP4} = \frac{Base\ tariff * h_{base} + Peak\ tariff * h_{peak}}{h_{price}} \tag{29}$$

In which h_{base} and h_{peak} are the number of hours in which the base tariff and peak tariffs are applied, weighted on the total number of price hours h_{price}. Starting from the structure of the REIPPP 4 tariff scheme, the objective of the model is to calculate a PPA value that will be able to guarantee a predetermined profit for the plant, i.e. a desirable IRR value, for each given plant design. The procedure then boils down to reversing the NPV and IRR calculation that was explained in the previous section:

1) Fix desired IRR value
2) NPV calculation
3) Annual plant revenues
4) Hourly electricity prices
5) PPA

It must be noted that in order to make the computation of the desired hourly prices possible, a fixed price scheme is necessary. Therefore, for this calculation the tariff scheme of the REIPPP 4 program was employed (Figure 15), where the peak prices occur at the same hours of the day for the entire year and are a multiple (2.7 times) of the base hours prices.

Since the IRR is defined as the value of the discount rate that makes the sum of all cash flows (Net Present Value) along the lifetime of the plant equal to zero, and its value is fixed as an input data, it is possible to determine the annual revenues of the plant from equations (30) and (31):

$$NPV = \left(\sum_{t=1}^{n} \frac{REV_t}{(1+IRR)^t}\right) - CAPEX = 0 \tag{30}$$

$$REV = \left(\sum_{i=1}^{8760} E_{gen_i} * Price_i \right) * f_{av} \; - OPEX \tag{31}$$

Where E_{gen_i} is the hourly value of the plant energy yield and f_{av} the annual availability factor. Since all the other terms in equation (31) are known and the tariff scheme is fixed, the hourly base electricity price $Price_i$ can then be treated as an unknown and its value derived along with the desired base and peak tariffs:

$$Base\ tariff = \ Price_i \tag{32}$$

$$Peak\ tariff = 2.7 * Price_i \tag{33}$$

Therefore equation (29) can be applied.

The underlying condition behind the PPA calculation is the choice of a proper IRR value that would result in a profitable operation for the plant. From basic finance theory, a project is defined to be profitable when its IRR exceeds the value of the market discount rate (81). Accordingly, the IRR input value must be selected to meet this condition for the chosen location.

3.9 Model Verification

As mentioned in sections 3.3 and 3.4 both the CSP and PV plants models have been individually validated by their respective authors. To verify the proper functioning of the PV-CSP combined model, an additional verification was performed. Such verification was carried out by performing a market research about existing planned/under constructions PV-CSP hybrid projects and using the gathered data to compare the results obtained from the model itself.

For such purpose, the information obtained for the Copiapó PV-CSP project was used. Such plant was announced by CSP developer Solar Reserve to provide stable baseload power for the mining industry located in the region of Copiapó, located in the Atacama Desert in norther Chile (36). The technical specifications of such plant are presented in Table 7. As can be seen, the Copiapó project consists of two CSP plants of 130 MW gross capacities each. Due to the fact that the DYESOPT tool can simulate only one CSP plant at a time, the values of total capacity, energy yield and CAPEX of Copiapó were therefore halved in order to perform the comparison with DYESOPT. Furthermore, since Copipaó is a baseload power plant, the PDS that has been developed for intermediate and peaking operation was not used in this case and the PV-CSP model was dispatched for baseload instead.

Table 7 – Reference technical data for the planned PV-CSP plant in Copiapó (36)

Parameter	Value	Unit
Total capacity	410	MW
CSP Capacity	2x130	MW
PV Capacity	150	MW
Power output	220 MW typical (260 MW max/200 MW min)	MW
Heliostat area	115	m^2
Storage capacity	14	h
Tracking	Fixed tilt (winter design) -	-
Net electricity output	1700+	GWh
Capacity factor	Baseload	%
No. of heliostats	20,000 – 35,000	-
Field aperture	2,656,000	m^2
Project cost	2000	milUSD

Table 8 shows the input design parameters that have been used to perform the verification of the model. As information about certain parameters was not available (solar multiple, PV and inverter type and tilt angle of the modules), their values were assumed based on typical values employed for such applications and on the available PV and Inverters modules implemented in the tool.

Table 8 – Design parameters for the Copiapó project and the DYESOPT model

Design Parameters	Copiapó Project	DYESOPT
Location	27°22'S 70°20'W	27°22'S 70°20'W
Total capacity [MW]	205	205
CSP Capacity [MW]	130	130
PV Capacity [MW]	75	75
Power output [MW]	110	110
Heliostat area [m^2]	115	115
Storage capacity [h]	14	14
Solar multiple	*Unknown*	2.1
PV module type	*Unknown*	Hanwha Solar HLS60 SunPower E20 327W
Inverter type	*Unknown*	Ingecon Sunpower Max
Tracking	Fixed tilt (winter design)	38° (Tilt angle)

The results of a one year dynamic simulation are presented in Table 9 for two different PV modules available in DYESOPT. The relative errors between the real values from the project and the simulated one are also reported, if available.

The obtained results generally show agreement with the project data. The type of PV modules was found to have an influence mostly in the CAPEX side, as expected, and the best agreement with the real data was found using the Hanwha Solar HLS60 modules.

The relative error associated to net electricity output is below 10%, which can be considered acceptable given the fact that the data source of DNI used in the real project is unknown and the one adopted in DYESOPT (Meteonorm (72)) relies on interpolation of satellite data of the closest available location. Furthermore, the tilt angle of the PV modules was unknown and it was approximated to a value that best approached a winter design.

The number of heliostats was found to be within the estimated range; however, the results were obtained using a solar multiple of 2.1, as the one for the real project is unknown. The total CAPEX calculated by DYESOPT shows good agreement with the data from the market watch when the Hanwha modules are used. The annual OPEX is reasonable when compared to available references (26). Lastly, the LCOE is in line with the most recent PPAs awarded to PV-CSP projects in Chile (82).

Table 9 – Results of the dynamic simulation run using two different PV modules

Results	**Copiapó Project**	**DYESOPT (Hanwha)**	**DYESOPT (SunPower)**	**Relative error [%]**
Net electricity output [GWh]	850+	777.77	775.68	8.5-8.7
Capacity factor [%]	Baseload	81	80	-
No. of heliostats	10,000 – 17,500	11,606	10,930	-
Field aperture [m^2]	~ 1,330,000	1,330,000	1,260,000	0-5.3
No. of PV modules	-	312,805	260,805	-
No. PV Arrays	-	75	72	-
No. module per string	-	19	13	-
Total CAPEX [milUSD]	1000	1062.62	1194.61	6.3-19
Annual OPEX [milUSD]	-	13.75	14.27	-
LCOE [USD/MWh]	-	130.61	145.33	-

3.10 Multi-Objective Optimization

The multi objective optimization represents the final stage of the simulation work. As suggested by the name in the multi-objective optimization a number of objectives are simultaneously optimized. However, many times these objectives are conflicting to each other, that the optimal solution of an objective function is different from that of the other. By solving these problems (constrained or unconstrained), the solution gives rise to trade-off curves, known as Pareto curves (42).

In the context of DYESOPT the Queueing Multi-Objective Optimiser (QMOO) (83) tool by EPFL is implemented to carry out the multi-objective optimization.

Table 10 shows the parameters of the CSP and PV plants that have been set as decision variable for the optimizer. For each variable, a range of values within which it can vary has been set.

Table 10 – Input variables for the multi-objective optimization.

Decision variables		
Parameter	**Range**	**Units**
CSP power plant		
Net power output	[80 - 250]	[MW]
Solar multiple	[1 - 3]	[-]
Heliostat mirror area	[60 - 120]	[m^2]
Storage size	[4 - 10]	[h]
Tower height	[145 - 280]	[m]
Receiver height	[10 - 25]	[m]
Receiver diameter	[8 - 22]	[m]
Summer load factor	[0.5 - 1]	[-]
Winter load factor	[0.5 - 1]	[-]
PV power plant		
Net AC capacity[1]	[20 - 150]	[MW]
PV module type[2]	[1 - 3]	[-]
Inverter model	[1 - 3]	[-]
Tilt angle	[20 - 50]	[degrees]
Tracking[3]	[1 - 4]	[-]
PV-CSP power plant		
Net power output	[80 - 250]	[MW]
Summer load factor	[0.5 - 1]	[-]
Winter load factor	[0.5 - 1]	[-]

[1] [20-500] for the PV alone case

[2] See APPENDIX C

[3] 1: Single axis North-South 2: Single axis East-West, 3: Double axis, 4: Fixed tilt

In Table 11 the chosen objective functions are shown. For this study the objective is to minimize both the PPA and CAPEX that correspond to a fixed level of profitability of the plant, represented by an IRR of 15%.

Table 11 – Objective functions for the multi-objective optimization

Objective functions		
Parameter	**Units**	**Objective**
PPA	[USD/MWh]	Minimize
CAPEX	[milUSD]	Minimize

Due to the fact the CAPEX of the plant is already taken into account in the calculation of the PPA (equation 30), it would have been possible to perform an optimization with PPA as the only objective function. However, since the CAPEX is also representative of the level of risk involved in a project, it has been chosen as a separate objective function in order to take into account such aspect and avoid unrealistic CAPEX values to be achieved in the final outcome of the optimization.

4 Results and discussion

This section contains the final results of the multi objective optimization that has been performed for all the cases that have been taken into account, namely hybrid PV-CSP, CSP alone and PV alone. The results are presented individually for each case featuring optimization plots containing Pareto fronts of PPA and CAPEX trade-offs. The ranges considered for each parameter of the CSP and PV plants during the multi objective optimization are shown in

Table 10, while the economic and location-related input parameters are contained in Table 3 and Table 4. All the obtained PPA values are referred to a fixed IRR of 15%, choice that was justified in section 3.8.2.9.

A specific optimum plant was selected in each case and its corresponding point in the Pareto front has been highlighted (**A**, **B** and **C** for PV-CSP, CSP alone and PV alone respectively). Each optimum plant has been chosen to have the same capacity of 120 MW in all cases to allow a clearer comparative analysis to be performed. The choice of this capacity is due to the fact that it is similar to capacities of real plants currently operating or under construction (39) (84) (85). Among all plants of same capacity in the Pareto front, the choice was then restricted to the one yielding the best performance, i.e. minimum PPA. The most important parameters associated to the discussed optimum plants can be found in APPENDIX A.

Based on the obtained results, after each set of plots a general discussion together with a comparative analysis between the three cases is then performed, allowing the reader to clearly understand the differences between each case as well as the overall trend.

4.1 Installed capacity

Figure 24 represents the CAPEX vs PPA trade-off curves for each case, with respect to the net installed capacity, represented by different colors in the graph. All the curves were obtained when stopping the optimizer after approximately 2000 iterations. The single 120 MW plant configurations that have been selected are represented by the capital letters '**A'**, '**B**' and '**C**' in the PV-CSP, CSP alone and PV alone respectively.

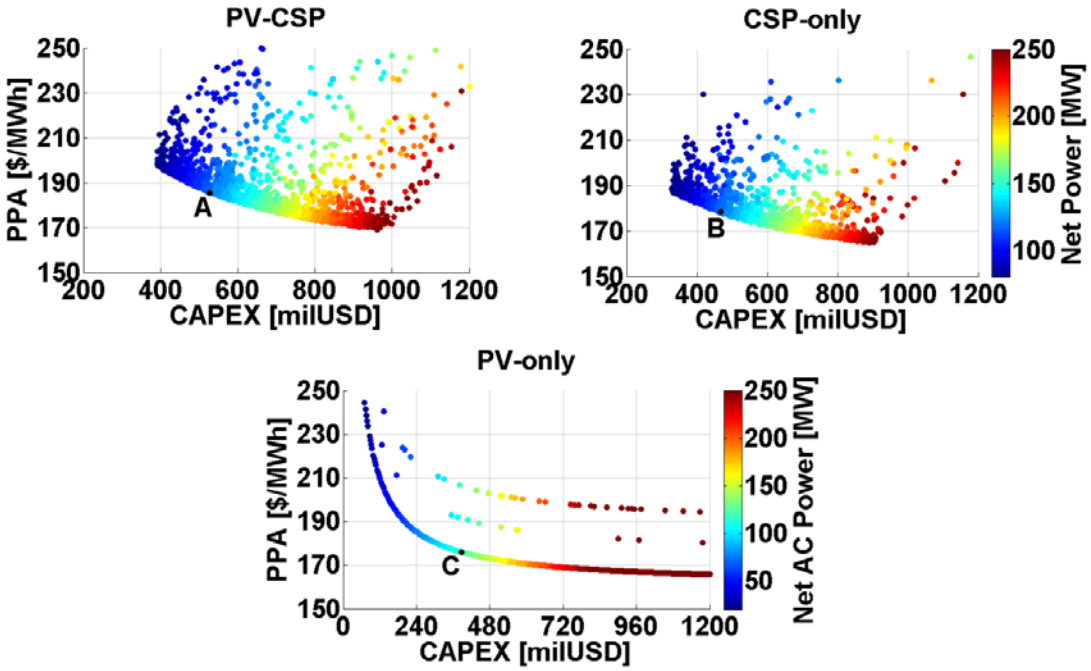

Figure 24 – PPA-CAPEX trade-off with respect to the net power output for all considered cases

The plot shows how different profitability levels can be reached with different installed capacities. In general, plants with higher capacities result in lower PPAs for the same desired level of profitability (15% IRR). This result is expected due to the fact that with increasing capacity, economies of scale allow the increment in CAPEX to be offset by the higher amount of revenues generated in a year with respect to a plant of lower capacity. It must be noted though that for high capacities in all cases the decrease in PPA occurs at the expense of an increasingly higher increment in CAPEX. Therefore, increasing the plant capacity would guarantee higher cash flows but also add a higher risk factor for investors due to the large capital expenditure. Furthermore, a maximum limit in CSP capacity size exists due to the increase in optical losses in the solar field (higher distance between the heliostats and the tower) at large installed capacities, resulting in increasingly higher solar filed sizes. Since the solar field is the main cost component of the CSP plant (28), the CAPEX is therefore negatively affected, as already found in previous optimization studies on peaking CSP power plants (10). Comparing the three cases, it can be seen that the PV-CSP Pareto front lies on higher PPA values than the CSP and PV alone plants. This is also confirmed by comparing the PPA values of the selected optimum plants:

Table 12 – PPA and CAPEX results for the selected optimums

Parameter	Values			Units
	A	**B**	**C**	
PPA	185.50	178.44	175.90	[USD/MWh]
CAPEX	527.77	467.3	386.67	[milUSD]
Net Energy Yield				[GWhe/yr]

The results gathered in Table 12 show that for the same capacity of 120 MW the best result is yielded by the PV alone configuration, both in terms of minimum PPA and CAPEX.

4.2 Load factors

Figure 25 and Figure 26 illustrative of the different load factors levels of the PV-CSP and CSP alone plants during winter (left) and summer (right). As the reader might recall, the model allows the plant to vary its output during the day and work at decreased output during non-peak hours. The percentage of the nominal output at which the plant is working during this time is in fact represented by the load factor, plotted with different colors in the plots.

It can be seen that in both cases the load factors generally converge to relatively high values, between 80 and 100% of the nominal output, meaning that the output of the optimum plants always tend to be close to nominal. Load factors in winter tend to be lower than in summer as expected, due to the fact that poorer solar irradiation is present in winter, thus being more convenient for the plant to decrease its output during daytime to save storage for peak times.

The CSP alone optimum model is able work at lower load factors than the PV-CSP case, especially in winter, when the difference with the PV-CSP case is around 10% as Table 13 shows. This behavior was expected because, as already mentioned in section **3.5**, in the PV-CSP combined operation the CSP plant works at part load during daytime to accommodate the PV output. Therefore, a further decrease of the combined output would result in the turbine approaching too low points of operation, resulting in both high PV curtailments and low efficiencies of the thermal cycle. On the other hand, in absence of PV penetration the CSP alone plant has a higher margin for decreasing its output without approaching the minimum operation point of the turbine.

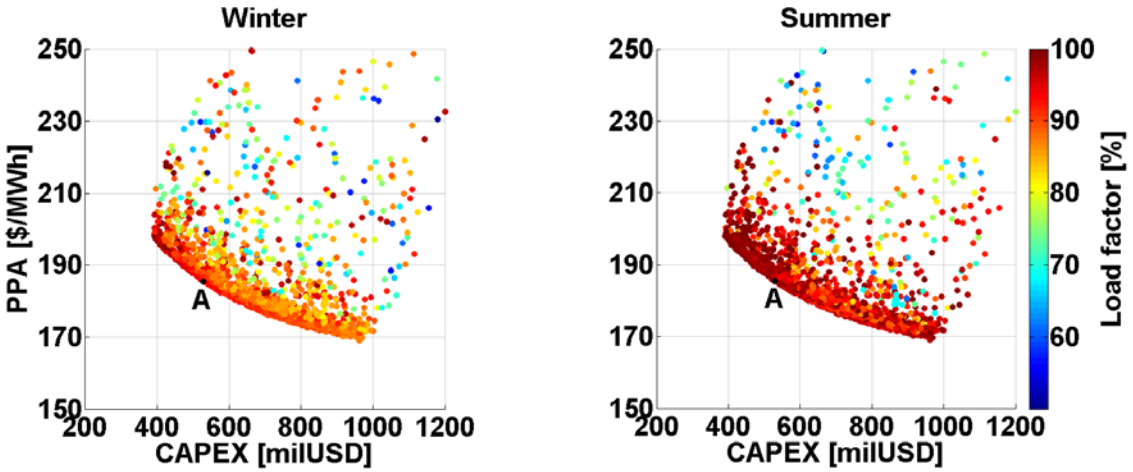

Figure 25 – PV-CSP trade-off for summer and winter load factors

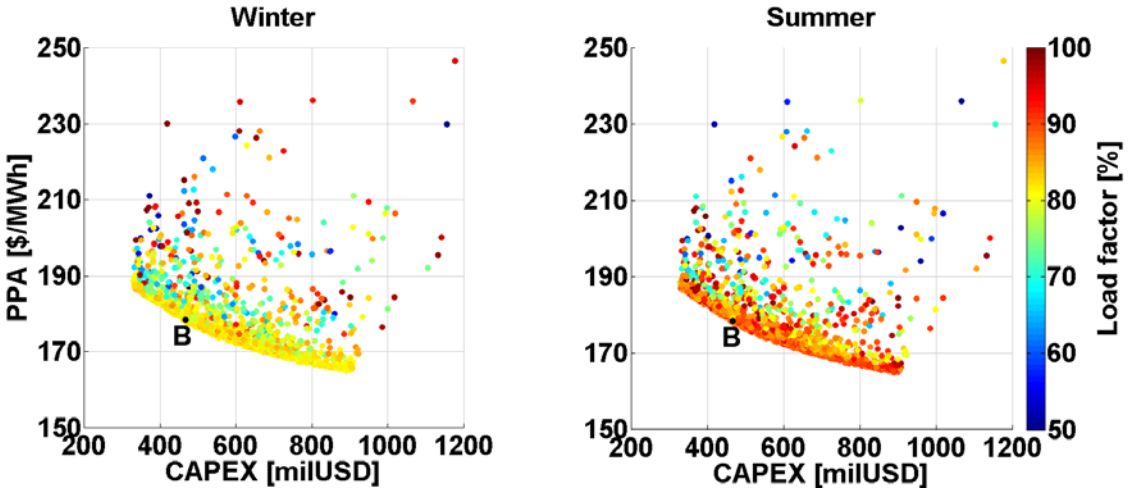

Figure 26 – CSP alone trade-offs for summer and winter load factors

Table 13 – Summer and winter load factors results of the selected optimums

Parameter	Values		Units
	A	**B**	
Summer load factor	96.12	91.66	[%]
Winter load factor	93.71	82.14	[%]

4.3 Storage, solar multiple, PV penetration

Figure 27 gathers further trade-off curves associated with the most important parameters of the hybrid plant. Due to the fact that the same trends were found for the CSP alone case, only the trade-off curves of the PV_CSP configuration are shown. In Figure 27a the storage influence can be seen, in Figure 27b the solar multiple, in Figure 27c the penetration of PV with respect to CSP can be observed and finally in Figure 27d the influence of the capacity factor is shown. The CSP alone and PV-CSP optimums converged to the same configurations of storage and solar multiple, therefore the plots reported here can be representative of both cases.

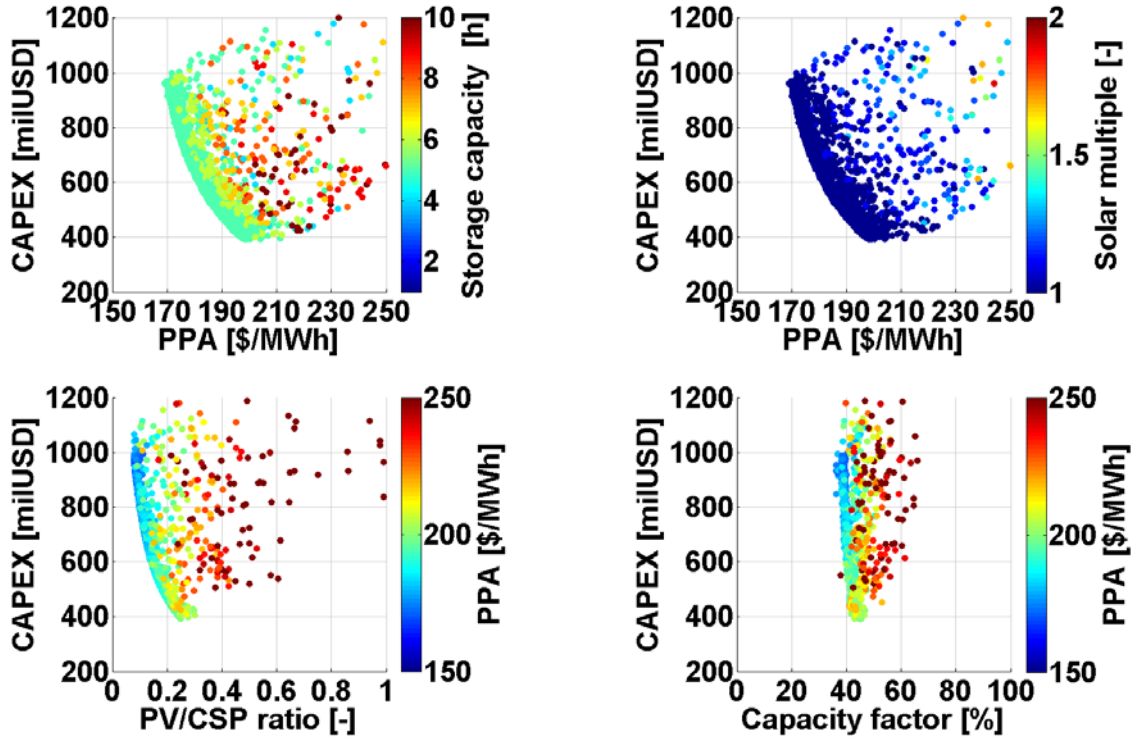

Figure 27 – Pareto fronts for various parameters of the PV-CSP plant

The analysis of the above graphs illustrates that the optimizer tends to converge to well-defined plant configurations. In fact, the Pareto fronts converge to storage values of five hours, solar multiple of 1, minimum PV penetration levels and capacity factors between 40% and 50 %. The same values were found for CSP-only optimums, except for the PV penetration, which does not apply and the capacity factor, which will be explained in more detail.

The found configurations are directly linked to the adopted tariff scheme. The value of storage capacity is justified by the fact that five peak hours are present every day. A lower storage capacity would not allow the plant to guarantee full operation during peak periods, while a higher value would not influence the capacity factor during this time, therefore adding extra cost to the system. Solar multiples tend to 1, as it was already found in previous studies about CSP peaking plants (10). Higher SM values are in fact associated with larger storage systems, more suitable for baseload operation. An interesting result is the fact that the PV capacity is minimized; the optimum plants therefore tend to converge to CSP-only power plants, indicating that for the applied type of operation a pure CSP system might be more suitable.

4.4 Capacity factor

Figure 28 presents the trade-off curves obtained with respect to the capacity factor in each case. The specific capacity factor values for the selected optimums are shown in Table 14.

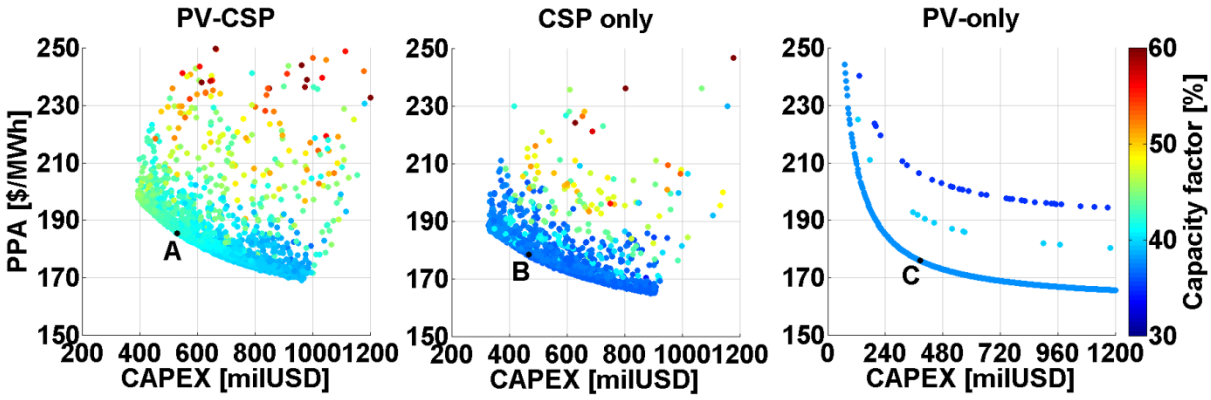

Figure 28 – PPA-CAPEX tradeoff with respect to the capacity factor for all considered cases

The found annual capacity factor values lying in the Pareto front are comprised between 35and 45% in all cases. Such values can be expected for such a peaking/intermediate load plant, considering the fact that the plant can operate only during price hours, which account for 60% of the total hours of the day, and only 20% of them are peak hours, which are the ones being prioritized by the PDS.

Table 14 – Capacity factor values for the selected optimums

Parameter	Values			Units
	A	B	C	
Capacity factor	42	36	38	[%]

When comparing plants of the same capacity, the PV-CSP system is the one that performs best in terms of capacity factor, with a value of 42% against 36% and 38% of the CSP and PV-only configurations. Such difference is achieved thanks to the presence of PV in the operation of the combined plant. In fact, part of the output of the during daytime is made by the PV system, thus leading to improved savings in thermal energy storage on the CSP side, allowing the plant to work at the desired output for an increased range of hours. This can be seen by comparing Figure 28 with the results represented in Figure 27c for the PV/CSP ratio: the highest PV penetrations in Figure 27c correspond to the points of highest capacity factor in the PV-CSP case of Figure 28 (CAPEX of ~400 milUSD). On the other hand, with the same output, storage capacity and solar multiple sizes, the CSP alone plant will be dispatched by the PDS for a reduced amount of time during daytime in order to be able to meet the evening peak hours , thus resulting in lower overall capacity factors. The PV alone plant would be expected to score the lowest performance among all, although it can be seen that in reality it yields same or higher capacity factors than the CSP alone case. However, it must be noted that a PDS that prioritizes peak hours is not implemented for the PV alone plant, due to the fact that peak hours are located during non-sun periods and the plant lacks an electrical storage system. Therefore, contrarily to PV-CSP and CSP-only, optimized PV-only configurations tend to maximize capacity factors during daytime. Indeed for such operation optimum PV plant configurations all feature single or double axis tracking systems, as can be seen in APPENDIX A.

4.5 Dynamic operation

Figure 29**,** Figure 30 and Figure 31 show the weekly dynamic operation of the selected optimum plant configuration **A**, **B** and **C** during a week. The week that has been plotted is the same featuring the plots contained in section 3.7.3, allowing the reader to see the difference in operation between non-optimum and optimum plant configurations. The electricity prices plotted in green are the ones corresponding to the PPA of the optimum plant, while the ones corresponding to the non-optimum plant are the current REIPPP prices.

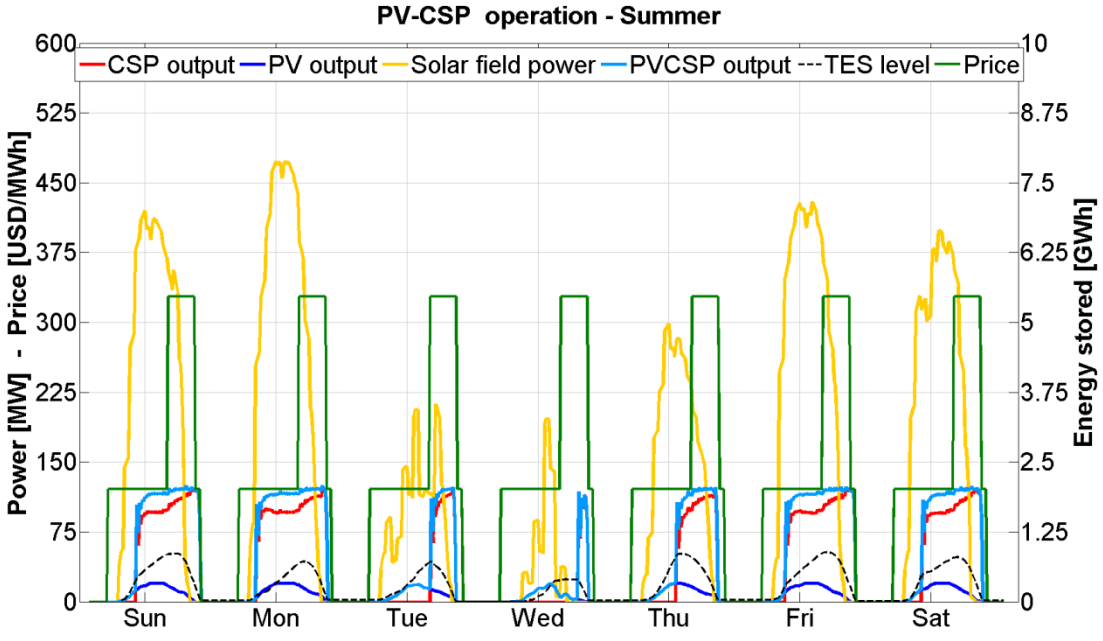

Figure 29 – Weekly operation of the selected PV-CSP optimum (A)

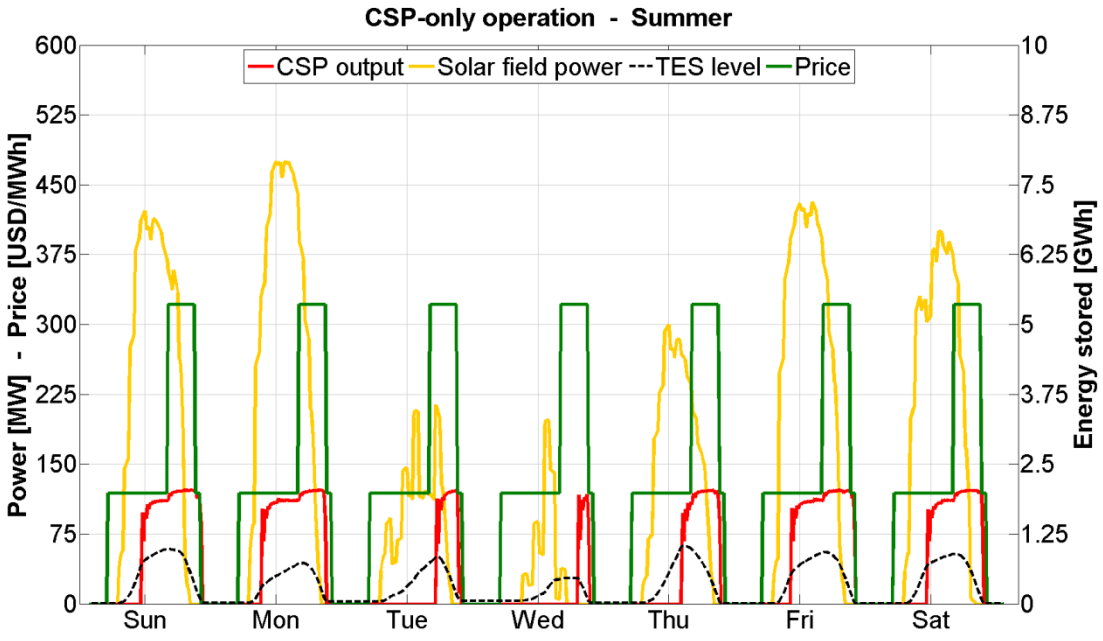

Figure 30 – Weekly operation of the selected CSP alone optimum (B)

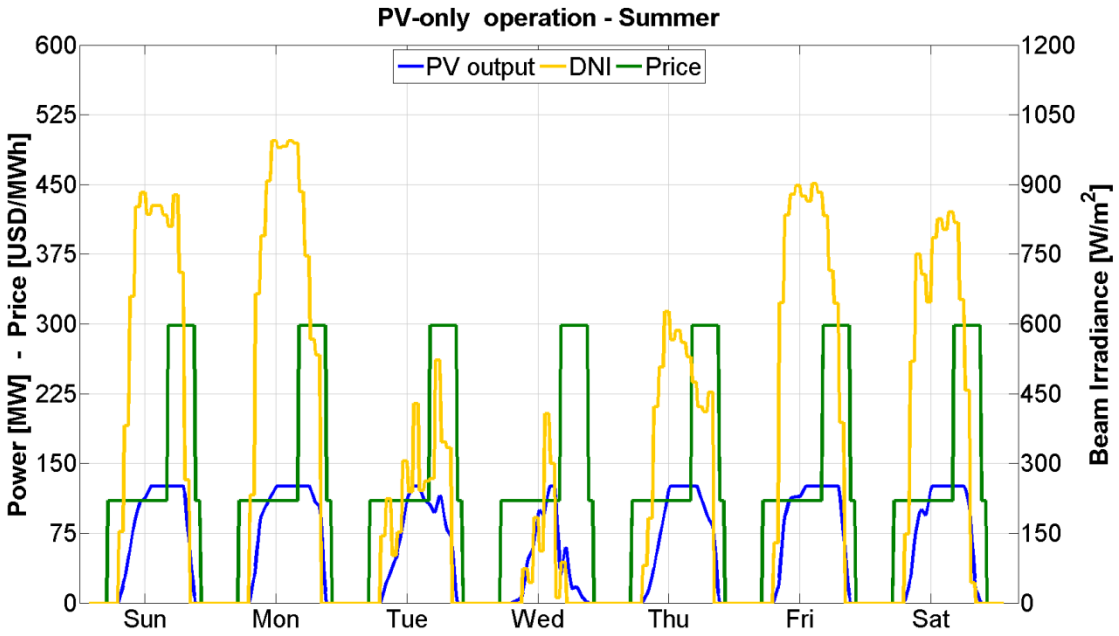

Figure 31 - Weekly operation of the selected CSP alone optimum (C)

The graphs allow the dispatch strategy of the combined and CSP alone plant to be seen during the dynamic simulation, for both good and bad days of radiation. In the PV alone case, no PDS was applied and the plant generates electricity purely based hourly solar irradiation. It can be observed that the optimum plant configurations do not cover the whole range of price hours in both the hybrid and CSP alone cases. Even during days of high insolation, such as Monday and Friday, the PDS sets the output of the plant to zero in the first price hours of the day, in order to save storage for peak hours, which in this way are always fully matched. The storage utilization is maximized, being the hot tank fully discharged at the end of each day. When a low radiation day is encountered, as on Tuesday and Wednesday, the combined plant enters in **operation mode 3**, dispatching only the PV during daytime and saving the CSP for the peak evening hours. The difference between daytime and evening output levels is minimal, fact already discussed in Figure 25 and Figure 26**.**

Dynamic operation of the optimum CSP plant resembles the one of PV-CSP, with the same PDS being applied. The resemblance is a consequence of the fact that the optimum PV-CSP configurations tend to minimize the PV penetration, therefore resembling a CSP alone power plant. Even though operation during peak hours is ensured by both the PV-CSP and CSP alone plants, the latter operates for a lesser amount of time during base hours, as already mentioned in the discussion of the capacity factors. This can be confirmed quantitatively by looking at Table 15, containing the annual dispatch indicators of each case.

Table 15 – Dispatch indicators for the selected optimums

Indicator		Values [%]		
		PV-CSP	**CSP alone**	**PV alone**
k1	PDS hours to price hours	62.87	57.05	- (65.33)
k2	PDS hours to dynamic operation hours	95.53	96.03	-
k3	Dynamic to price base hours	44.82	39.51	61.52
k4	Dynamic to price peak hours	98.01	97.75	74.45
k5	Base hours capacity factor	44.80	37.60	54.36
k6	Peak hours capacity factor	96.92	95.78	65.03

Indicator k1 shows that the operational hours' range of all cases is set between 57% and 65% of the actual tariff hours during the year. For the PV alone case the PDS hours were replaced with the actual operational hours of the plant, due to the fact that a PDS is not applied. The price hours that are discarded by the PDS are mostly base tariff hours, while the peak hours are almost always met, as shown by indicators k3 and k4. This proves that the PDS of optimum plants is effective in prioritizing peak tariff hours. Furthermore, the values of capacity factors k5 and k6 show that the PV-CSP and CSP alone plants are able to work at the desired output during most of the operation hours, being the relative error between k3-k5 and k4-k6 less than 2% in both cases. The PDS is further validated by indicator k2, showing that the mismatch between the planned hours of operation and the actual hours of operation during the dynamic simulation is less than 5% in all cases.

By further analyzing the indicators it can be seen that PV-CSP plant is the one that performs best in meeting the peak hours, with a value 98% value of k4. The CSP alone plant performs similarly during peaks, while reducing operation during base hours, as shown by indicators k3 and k5. On the other hand, the PV alone power plant maximizes operation during base hours, resulting in a 61.52% value in the k3 indicator, much higher than the PV-CSP and CSP alone cases. Conversely, as expected the PV power plant performs worse in meeting peak hours at nominal output, with only 65% peak hours capacity factor compared to the 96.92% and 95.78% values of the PV-CSP and CSP alone configurations.

To conclude, Table 16 gathers the most important results that have been discussed in this section, for the three optimum configurations that have been discussed. More insights about the specific parameters of each optimum can be found in APPENDIX A.

Table 16 – Discussed results for the optimums selected in each case

Parameter	Values			Units
	PV-CSP (A)	**CSP alone (B)**	**PV alone (C)**	
PPA	185.50	178.44	175.90	[USD/MWh]
CAPEX	527.77	467.3	386.67	[milUSD]
Net Energy Yield	436.51	383.48	413.60	[GWhe/yr]
Capacity factor	42	36	38	[%]
Storage capacity	5	5	-	[h]
Solar multiple	1.0	1.0	-	[-]
Summer load factor	96.12	91.66	-	[%]
Winter load factor	93.71	82.14	-	[%]
Base hours capacity factor	44.80	37.60	54.36	[%]
Peak hours capacity factor	96.92	95.78	65.03	[%]

5 Conclusions

A techno-economic analysis of a combined PV-CSP power plant for intermediate and peak load operation under a two-tier tariff scheme in South Africa was performed. The analysis has been conducted by developing a suitable dispatch strategy for maximizing the profitability of the plant, by prioritizing peaking periods without compromising intermediate load operation. By fixing a desired level of profitability for the plant, represented by an Internal Rate of Return (IRR) of 15%, a multi-objective optimization was conducted in order to find trade-off curves between CAPEX and PPA values, among other indicators, that would guarantee such profitability. The results were then compared with CSP alone and PV alone optimum configurations.

For the same profitability level, it was found that better economic performance (lower PPA values) was reached with increasing installed capacity in all PV-CSP, CSP alone and PV alone cases. A maximum limit was however observed towards high capacity values, therefore posing a limit in the economic convenience of increasing capacity to decrease the PPA, due to significant corresponding CAPEX increments. Optimum plants configurations were found to be well defined and similar between the PV-CSP and CSP alone cases, converging to values of five hours of storage and solar multiples of one. In the PV-CSP case, the optimizer minimized PV penetration with respect to CSP, thus suggesting that for the chosen way of operation a CSP alone plant might be more suitable. PV alone optimums all featured tracking systems to maximize operation during daytime price hours, while fixed tilt configurations were discarded by the optimizer.

The CSP alone plant was found be more flexible in the capability of lowering its output during non-peak hours, while the presence of PV in the hybrid plant resulted in part load operation of the CSP system, thus preventing the output of the combined plant to be lowered to the same limit. This fact is although offset by improved savings of thermal energy storage of the PV-CSP plant with respect the CSP alone case, due to the fact that part of the output of the combined plant is provided by PV during daytime.

Several indicators were developed for measuring the capability of the plant of meeting the pre-defined dispatch strategy. The pre-defined dispatch strategy has been validated by resulting in values higher than 95% agreement between the PDS and the dynamic operation in all cases. The PV-CSP plant performed similarly to the CSP alone during peak hours, while scoring higher capacity factors during base tariff hours. On the other hand, the PV alone configuration maximized operation during daytime base hours, while proving inefficient in meeting peak periods at firm capacity as expected.

The obtained results showed that for the selected operational strategy, the hybrid PV-CSP configuration yielded the worst performance in the corresponding PPA and CAPEX indicators necessary to reach the desired profitability level, compared to the CSP and PV alone cases. The PV-CSP plant however performed better than the other technologies in terms of capacity factor and dispatch indicators. This highlights the fact that the value of a PV-CSP configuration increases when certain constraints are applied, such as maximizing the capacity factor, as for base load applications, or in case the plant needs to guarantee production for a fixed number of hours every day, as can happen in real load-following power plants. On the other hand, for a peaking dispatch strategy with no such constraints, the CSP alone optimum configuration proved to be a better option in terms of economic performance. The PV alone case yielded the lowest PPA and CAPEX among all cases, despite the fact that no dispatch strategy can be applied for the PV plant alone and peak hours are rarely dispatched, due to their location within non-sun hours. The drawback of a PV only configuration lies in the fact that a tracking system is needed to maximize production during daytime, thus adding complexity to the plant, while fixed-tilt configurations

were discarded by the optimizer. Furthermore, the PV alone plant would be unable to perform if operational constraints were applied, such as guaranteeing a firm output level during the day, varying the output on an hourly basis, guaranteeing production during peak hours or for a fixed amount hours per day.

6 Model limitations and future work

The present thesis work can be further refined by considering and investigating cases that time constrainst did not allow to take into account . Ther most important prompts for potential improvements, together with limitations associated to the model that have been identified by the author are the following:

- Run a multi-objective optimization for a case where constraints are applied on the PDS, in terms of a fixed minimum number of operational hours per day, i.e. a **fixed capacity factor**.

- Implement a model for **electrical storage** in the PV-only power plant, so that the same PDS as the PV-CSP and CSP alone cases can be applied.

- Implement a **refined financial model** for the PPA calculation which considers different financing options and hourly tariff structures. Investigate the impact of different PPAs applied to the PV and CSP separately.

- Investigate a case in which PV and CSP are partially **decoupled**, i.e. PV is not curtailed when the minimum working point of the turbine is reached but CSP is shut down instead.

- Take into account **ramp-up and down times**. In real power plants operations based on steam cycles, the turbine block needs a certain amount of time to reach the nominal point of operation at startup, or to adjust its output to different demand levels during operation. For this modelling work such delay times were not fully taken into account and the plant was assumed to be able to adjust its output fast enough to reach the desired output at the planned hours in the pre-defined dispatch strategy.

- The effect of **daily startups** on the performance and lifetime of the turbine was not considered in this thesis work. Due to the nature of the implemented dispatch strategy, both the PV-CSP and CSP alone plants do not operate continuously during the year but experience daily startups instead. Therefore, a study of the impact of these frequent startups on the degradation of the power block shall be performed.

- Investigate the effect of **extended part load operation** on the performance and lifetime of the power block. As it is well acknowledged, steam turbines should be operated as close as possible to nominal conditions not only for efficiency reasons but also to minimize system degradation over long periods.

- **Dispatch strategy**: The developed dispatch strategy is based on a weather file containing hourly values of irradiation extrapolated from historical data from commercially available software (Meteonorm). Based on this data, the choice of the total daily operational hours (THD) of the hybrid and CSP alone plants was thus defined in advance for the whole year before the dynamic simulation, following the algorithm that was explained in section 3.6. In reality, power plants are dispatched following a day-ahead strategy, in which the operating hours of the following day are decided based on the weather forecast and the storage availability of the day before.

- **TRNSYS oscillations and PID controller**: implement specific tuning methods to improve the controller's stability: step response method, frequency response method etc.

Bibliography

1. **IEA.** *World Energy Outlook 2014 Factsheet.* Paris : International Energy Agency, 2014.

2. —. *Tracking Clean Energy Progress 2015.* Paris : International Energy Agency, 2015.

3. —. *Technology Roadmap: Solar Photovoltaic Energy.* Paris : International Energy Agency, 2014.

4. —. *Technology Roadmap: Solar Thermal Energy.* Paris : International Energy Agency, 2014.

5. **James Spelling, Björn Laumert.** *Thermo-economic Evaluation of Solar Thermal and Photovoltaic Hybridization Options for Combined-Cycle Power Plants.* s.l. : Journal of Engineering for Gas Turbines and Power, 2015.

6. **Green Adam, Dunn Rebecca, Dent Jolyon, Diep Charles.** *High Capacity Factor CSP-PV Hybrid Systems.* Santa Monica : SolarReserve, 2015.

7. **C.Silinga, P. Gauché.** *Scenarios for a South African CSP peaking system in the short term.* s.l. : Elsevier, 2013.

8. **C.Silingaa, P. Gauché, J. Rudman and T. Cebecauer.** *The South African REIPPP two-tier CSP tariff: Implications for a proposed hybrid CSP peaking system.* s.l. : Elsevier, 2014.

9. *Optimization of thermal energy storage integration strategies for peak power production by concentrating solar power plants.* **Guedez, R., et al., et al.** 49, Stockholm : Elsevier Ltd, 2013.

10. **Guedez, Rafael, et al., et al.** *A Methodology for Determining Optimum Solar Tower Plant Configurations and Operating Strategies to Maximise Profits Based on Hourly Electricity Market Prices.* San Diego : ASME, 2015.

11. **Castillo, Luis.** *Techno-economic Analysis of Combined Hybrid Concentrating Solar and Photovoltaic Power Plants: a case study for optimizing solar energy integration into the South African electricity grid.* Stockholm : KTH, 2014.

12. **Spelling, James.** *Hybrid Solar Gas-Turbine Power Plants: A Thermoeconomic Analysis.* Stockholm : KTH, 2013.

13. **Sandia National Laboratories.** Energy and Climate, Secure & Sustainable Energy Future. *Energy and Climate, Secure & Sustainable Energy Future.* [Online] 2015. [Cited: 9 May 2015.] http://energy.sandia.gov/infrastructure-security/electric-systems/renewable-energy/how-a-grid-manager-meets-demand-load.

14. **Bhattacharyya, Subhes C.** *Energy Economics: Concepts, Issues, Markets and Governance.* s.l. : Springer, 2011.

15. **Kalogirou, Soteris A.** *Solar Energy Engineering: Process and Systems.* 2nd. s.l. : Elsevier Ltd, 2014.

16. **Notton, G., Lazarov, V. and Stoyanov, L.** *Optimal sizing of a grid-connected PV system for various PV module technologies and inclinations, inverter efficiency characteristics and locations.* Ajaccio, Sofia : Elsevier Ltd, 2010.

17. **AM Solar Inc.** Standard Test Conditions (STC) vs. Normal Operating Cell temperature (NOCT). *AM Solar.* [Online] AM Solar, 2015. [Cited: 09 February 2015.] http://www.amsolar.com/home/amr/page_164.

18. **Wholesale Solar.** Wholesale Solar. [Online] [Cited: 13 February 2015.] http://www.wholesalesolar.com/deep-cycle-battery-info.html.

19. **Poullikkas, Andreas.** *A comparative overview of large-scale battery systems for electricity storage.* 2013.

20. **Helder Lopes Ferreira, Raquel Garde, Gianluca Fulli, Wil Kling, Joao Pecas Lopes.** *Characterisation of electrical energy storage technologies.* 2013.

21. **Grietus Mulder, Daan Six, Bert Claessens, Thijs Broes, Noshin Omar, Joeri Van Mierlo.** *Battery energy storage systems: Assessment for small-scalerenewable energy integration.* s.l. : Elsevier, 2010.

22. **Erik Wesoff.** Greentechmedia. [Online] 12 November 2014. [Cited: 13 February 2015.] http://www.greentechmedia.com/articles/read/The-Worlds-Biggest-Battery-is-Being-Built-in-Southern-California.

23. **Breyer, Ch., et al., et al.** *Economics of Hybrid PV-Fossil Power Plants.* 2011.

24. **Khelif A., Talha A., Belhamel M., Hadj Arab A.** *Feasibility study of hybrid Diesel–PV power plants in the southern of Algeria: Case study on AFRA power plant.* 2012.

25. **Dekker J., Nthontho M., Chowdhury S., Chowdhury S.P.** *Economic analysis of PV/diesel hybrid power systems in different climatic zones of South Africa.* 2012.

26. **CSP Today.** *CSP Solar Tower Report 2014: Cost, Performance and Thermal Storage.* s.l. : CSP Today, 2014.

27. **Guedez R., Topel M., Spelling J., Laumert B.** *Enhancing the profitability of solar tower power plants through thermoeconomic analysis based on multi-objective optimization.* Beijing : Elsevier Ltd, 2014.

28. **IRENA.** *Concentrating Solar Power, Renewable Energy Technologies: Cost Analysis Series.* Abu Dhabi : IRENA Secretariat, 2012.

29. **J. Duffie, W. Beckmann.** *Solar Engineering of Thermal Processes.* 3rd Edition. s.l. : John Wiley & Sons, 2006.

30. **Guedez, Rafael.** Multi-Objective Optimization: A review on optimization techniques and application to CSP design. Stockholm : s.n., 2015.

31. **Concentrating Solar Power Alliance.** *The Economic and Reliability Benefits of CSP with Thermal Energy Storage: Recent Studies and Research Needs.* s.l. : CSP Alliance, 2012.

32. **Steinmann, W.-D.** Thermal Energy Storage Systems for Concentrating Solar Power (CSP) Technology. [book auth.] Keith Lovegrove and W Stein. *Concentrating Solar Power Technology: Power, Developments and Applications.* s.l. : Woodhead Ltd, 2015.

33. **Renewable Energy World.** *Renewable Energy World.* [Online] 14 October 2011. [Cited: Tuesday February 2015.] http://www.renewableenergyworld.com/rea/news/article/2011/10/gemasolar-achieves-24-hour-operation.

34. **Rodriguez, I.** Solar Thermal Energy Lecture Notes. 2014.

35. **Ushak, S., Fernandez, A.G. and Gradega, M.** Using Molten Salts and Other Liquid Sensible Storage Media in Thermal Energy Storage (TES) Systems. [book auth.] Luisa Cabeza. *Advances in Thermal Energy Storage Systems: Methods and Applications.* s.l. : Elsevier Ltd, 2015.

36. **SolarReserve.** *Meeting Mining's Need for Baseload Power with Solar Thermal with Storage.* Toronto : SolarReserve, 2014.

37. **Abengoa Solar.** Atacama 1: factsheet. [Online] 2015. [Cited: 16 March 2015.] http://www.abengoa.com/export/sites/abengoa_corp/resources/pdf/noticias_y_publicaciones/destacado_cerro_dominador/Factsheet_Cerro_Dominador_en.pdf.

38. **Chilean Environmental Assessment Service.** *Environmental Impact Statement: Atacama 2 Solar Plant.* s.l. : Government of Chile, 2014.

39. **CSP Today Global Tracker.** Solar Reserve Redstone CSP tower plant. *CSP Today Global Tracker.* [Online] 2014. www.csptoday.com.

40. **Golden Associates.** *Draft Scoping Report: Proposed Solar Power Development on the Remaining Extent of Farm Bokpoort 390, Northern Cape.* s.l. : Golden Associates, 2015.

41. **CSP World.** CSP World Map - Ashalim CSP Plant 2. *CSP World.* [Online] 2012. [Cited: 10 March 2015.] http://www.csp-world.com/cspworldmap/ashalim-csp-plant-2.

42. **Lihui Wang, Amos H. C. Ng, Kalyanmoy Deb.** *Multi-Objective Optimization Using Evolutionary Algorithms: An introduction.* s.l. : Springer, 2011.

43. **SolarGIS.** Solar Radiation Maps: GHI. *SolarGIS*. [Online] SolarGIS, 2015. [Cited: 09 February 2015.] http://solargis.info/doc/free-solar-radiation-maps-GHI#U.

44. **CSP Today.** *CSP Today Markets Report 2014.* s.l. : CSP Today, 2014.

45. **Deign, Jason.** *Could CSP compete for peaker power?* s.l. : CSP Today, 2015.

46. **Department of Energy of South Africa.** Integrated Resource Plan Update. *Government Gazette.* 2014.

47. **IRP.** *Integrated Resource Plan for electricity 2010 - 2030.* s.l. : Government Gazette, Republic of South Africa, 2011.

48. **CSP Today.** CSP Today Global Tracker. *CSP Today.* [Online] CSP Today, 2015. [Cited: 10 February 2015.] http://social.csptoday.com/tracker/projects.

49. **Morin, G.** Optimisation of concentrating solar power (CSP) plant designs through integrated techno-economic modelling. *Concentrating Solar Power Technology.* s.l. : Woodhead Publishing, 2012, pp. 594-535.

50. **Topel, Monika.** Modeling Tools. [Online] KTH, 02 02 2015. [Cited: 06 02 2015.] https://www.kth.se/en/itm/inst/energiteknik/forskning/kraft_varme/ekv-researchgroups/csp-group/modeling-tools-1.493747.

51. **Department of Energy of South Africa.** Renewable Energy Independent Power Producer Procurement Programme (REIPPPP). [Online] 2014. http://www.ipprenewables.co.za/.

52. **R. Guédez, M. Topel, J. Spelling , B. Laumert.** *Enhancing the profitability of solar tower power plants through thermoeconomic analysis based on multi-objective optimization.* Beijing : Proceedings of the International SolarPACES Conference, 2014.

53. **Kistler, B. L.** *A user manual for DELSOL3: A computer code for calculating the optical performance and optimal system design for solar thermal central receiver plants.* Albuquerque : Sandia National Laboratories, 1986.

54. **Collado, F.** *Quick Evaluation of the Annual Heliostat Field Efficiency.* s.l. : Solar Energy Volume 82, 2008. pp. 379 – 384.

55. **P. Gilman, N. Blair, M. Mehos.** *Solar advisor model user guide for version 2.0.* Golden : NREL/TP-670-43704, 2008.

56. **F. Incropera, D.DeWitt , T. Bergman.** *Fundamentals of Heat and Mass Transfer.* New York : John Wiley & Sons, 2007.

57. **Staine, F.** *Intégration énergetique des procedes industriels par la method du pincement etendue aux facteurs exergetiques.* Lausanne : Swiss Federal Technology Institute, 1995.

58. **Thermoflow.** Thermoflex modular program for thermal power systems. [Online] 2014. www.thermoflow.com.

59. **UW-M, Solar Energy Laboratory at.** *TRNSYS 17 a Transient System Simulation program.* Madison, : s.n., 2015.

60. **Schwarzbözl, P.** *STEC: A TRNSYS Model Library for Solar Thermal Electric Components.* 2006.

61. **J. Spelling, B. Laumert, T. Fransson.** *Optimal Gas-Turbine Design for Hybrid Solar Power Plant Operation.* s.l. : Journal of Engineering for Gas Turbines and Power, 2012.

62. **S. Shahril, R. Titik and M. Ismail.** *Sizing Grid-Connected Photovoltaic System Using Genetic Algorithm.* s.l. : Langkawi : IEEE, 2011.

63. **M. Mattei, G. Notton, C. Cristofari, M. Muselli, P. Poggi.** *Calculation of the polycrystalline PV module temperature using a simple method of energy balance.* s.l. : Science Direct, 2005.

64. **A. Mohamed, R. Hasimah, H. Mohammad, R. Saidur.** *Climate Based Empirical Model for PV Module Temperature Estimation in Tropical Environment.* s.l. : Applied Solar Energy, 2013.

65. **Klucher, T. M.** *Evaluation of Models to Predict Insolation on Tilted Surfaces.* s.l. : Great Britain : Solar Energy, 1979.

66. **W. De Soto, S.A. Klein, W.A. Beckman.** *Improvement and validation of a model for photovoltaic array performance.* s.l. : Wisconsin-MadisoN : Science Direct, 2005.

67. **Spelling, James.** *Solar Power Technologies - Solar Fundamentals.* Stockholm : KTH, 2012.

68. **G. Velasco, R. Piqué, F. Guinjoan, F. Casellas and J. de la Hoz.** *Power sizing factor design of central inverter PV grid-connected systems: a simulation approach.* 2010.

69. **Turbomachinery International.** Impact of low load operation on steam plant lifetime. *TurbomachineryMag.* [Online] 20 Septmeber 2014. [Cited: 20 July 2015.] http://www.turbomachinerymag.com/blog/content/impact-low-load-operation-steam-plant-lifetime.

70. **Balling, Lothar.** *Flexible Future for Combined Cycle.* s.l. : Modern Power System, 2010. pp. pp. 61-65.

71. **Cooke, D.** *Modeling of Off-Design Turbine Pressures by Stodola's Ellipse.* Richmond : Energy Incorporated, 1983.

72. **Meteotest.** Meteonorm - Irradiation data for every place on Earth. *Meteonorm.* [Online] 2015. http://meteonorm.com/.

73. **TRNSYS.** *Mathematical Reference: Volume 4.* s.l. : Wisconsin-Madison, 2011.

74. **Karl Johan Aström, Richard M. Murray.** *Feedback Systems.* s.l. : Princeton University Press, 2009.

75. **Kiam Heong Ang, Gregory Chong, Yun Li.** *PID Control System Analysis, Design and Technology.* s.l. : University of Glasgow, 2007.

76. *Enhancing the profitability of solar tower power plants through thermoeconomic analysis based on multi-objective optimization.* **Guedez, R., et al., et al.** Beijing : Elsevier Ltd, 2014.

77. **Turchi, Craig S and Wagner, Michael J.** *POWER TOWER REFERENCE PLANT FOR COST MODELING WITH THE SYSTEM ADVISOR MODEL (SAM).* 2012.

78. **Darling, Seth B., et al., et al.** *Assumptions and the Levelized Cost of Energy for Photovoltaics.* 2011. pp. 3133-3139.

79. **Campbell, Matthew.** *Charting the Progress of PV Power Plant Energy generating Costs to Unsubsidised Levels, Introducing the PV - LCOE Framework.* Richmond : SunPower Corporation, 2011.

80. **Jordan, Dirk C and Kurtz, Sarah R.** *Photovoltaic Degradation Rates — An Analytical Review.* s.l. : NREL.

81. **A. Thumann, E. A. Woodroof.** *Energy Project Financing:Resources and Strategies for Success.* s.l. : The Fairmont Press, Inc, 2008.

82. **HeliosCSP.** HeliosCSP. [Online] 31 12 2014. [Cited: 10 04 2015.] http://www.helioscsp.com/noticia.php?id_not=2835.

83. **Leyland, Geoffrey Basil.** *Multi-objective optimisation applied to industrial energy problems.* Lousanne : EPFL, 2002.

84. Israel's 121 MW Ashalim Plot B plant set for50% expansion but regulation stunts other projects. *CSP Today Global Tracker.* [Online] 10 July 2015. [Cited: 18 July 2015.] http://social.csptoday.com/markets/israel%E2%80%99s-121-mw-ashalim-plot-b-plant-set-50-expansion-regulation-stunts-other-projects.

85. Copiapó. *Solar Reserve.* [Online] 2015. http://www.solarreserve.com/en/global-projects/csp/copiapo.

86. **Taylor, Michael.** *Renewable Power Generation Cost in 2014.* s.l. : IRENA, 2015.

87. **Ahlfeldt, Chris.** *The Localisation Potential of Photovoltaics (PV) and a Strategy to Support Large Scale Roll-Out in South Africa.* s.l. : EScience Associates, 2013.

88. **Smith, Stephen.** PV Trackers. *SolarPro Magazine.* 13 March 2014, pp. 1-4.

89. **Barbose, Galen, Weaver, Samantha and Darghouth, Naim.** *Tracking the Sun VII: An Historical Summary of the Installed Price of Photovoltaics in the United States from 1998 to 2013.* s.l. : SunShot, 2014.

90. **Barbose, Galen, et al., et al.** *Tracking the Sun VI: An Historical Summary of the Installed Price of Photovoltaics in the United States from 1998 to 2012.* s.l. : SunShot, 2013.

91. **Harder, E.** *The costs and benefits of large-scale solar photovoltaic power production in Abu Dhabi, United Arab Emirates.*

92. **Tidball Rick, Bluestein Joel, Rodriguez Nick, Knoke Stu.** *Cost and Performance Assumptions for Modeling Electricity Generation Technologies.* s.l. : NREL.

93. **Speer, Bethany, Mendelsohn, Michael and Cory, Karlynn.** *Insuring Solar Photovoltaics: Challenges and Possible Solutions.* s.l. : NREL, 2010.

7 Appendix

APPENDIX A: OPTIMUM PLANTS CONFIGURATIONS

Table 17 – Selected PV-CSP optimum plant configuration (A).

Parameter	Value	Units
	PV-CSP power plant (A)	
	Solar field	
Solar multiple	1.0	[-]
Heliostat mirror area	107	[m²]
Number of heliostats	6476	[-]
Field aperture area	692932	[m²]
Average solar field efficiency	61.82	[%]
	Receiver/Tower	
Tower height	174	[m]
Receiver height	12	[m]
Receiver diameter	8	[m]
	TES	
Storage size	5	[h]
Energy capacity	1588	[MWh_{th}]
	Power block	
Net power output	120	[MW]
Gross power output	139.1	[MW]
Parasitic consumption	19.1	[MW]
Nominal cycle thermal efficiency	38.2	[%]
Summer load factor	96.12	[%]
Winter load factor	93.71	[%]
	PV	
AC output	20	[MW]
DC output	23.3	[MW]
Module type	1	[-]
Inverter model	1	[-]
Tilt angle	38	[degrees]
Number of modules	95267	[-]
Number of arrays/inverters	25	[-]

Table 18 – Selected optimum CSP-only plant configuration (B).

Parameter	Value	Units
CSP only power plant (B)		
Solar field		
Solar multiple	1.0	[-]
Heliostat mirror area	92	[m^2]
Number of heliostats	7642	[-]
Field aperture area	703064	[m^2]
Average solar field efficiency	61.22	[%]
Receiver/Tower		
Tower height	163	[m]
Receiver height	12	[m]
Receiver diameter	8	[m]
TES		
Storage size	5	[h]
Energy capacity	1586	[MWh_{th}]
Power Block		
Net power output	120	[MW]
Gross power output	139	[MW]
Parasitic consumption	19	[MW]
Nominal cycle thermal efficiency	38.2	[%]
Average power cycle thermal efficiency	36.96	[%]
Average sun to electricity efficiency	19.71	[%]
Summer load factor	91.66	[%]
Winter load factor	82.14	[%]

Table 19 – Selected optimum PV-only plant configuration (C).

Parameter	Value	Units
	PV only power plant (C)	
Net AC output	120	[MW]
DC output	143.2	[MW]
PV module type	3	[-]
Inverter model	3	[-]
Tilt angle	50	[degrees]
Tracking mode	1	[-]
Number of modules	485385	[-]
Number of arrays/inverters	126	[-]

APPENDIX B: DYESOPT FUNCTIONS

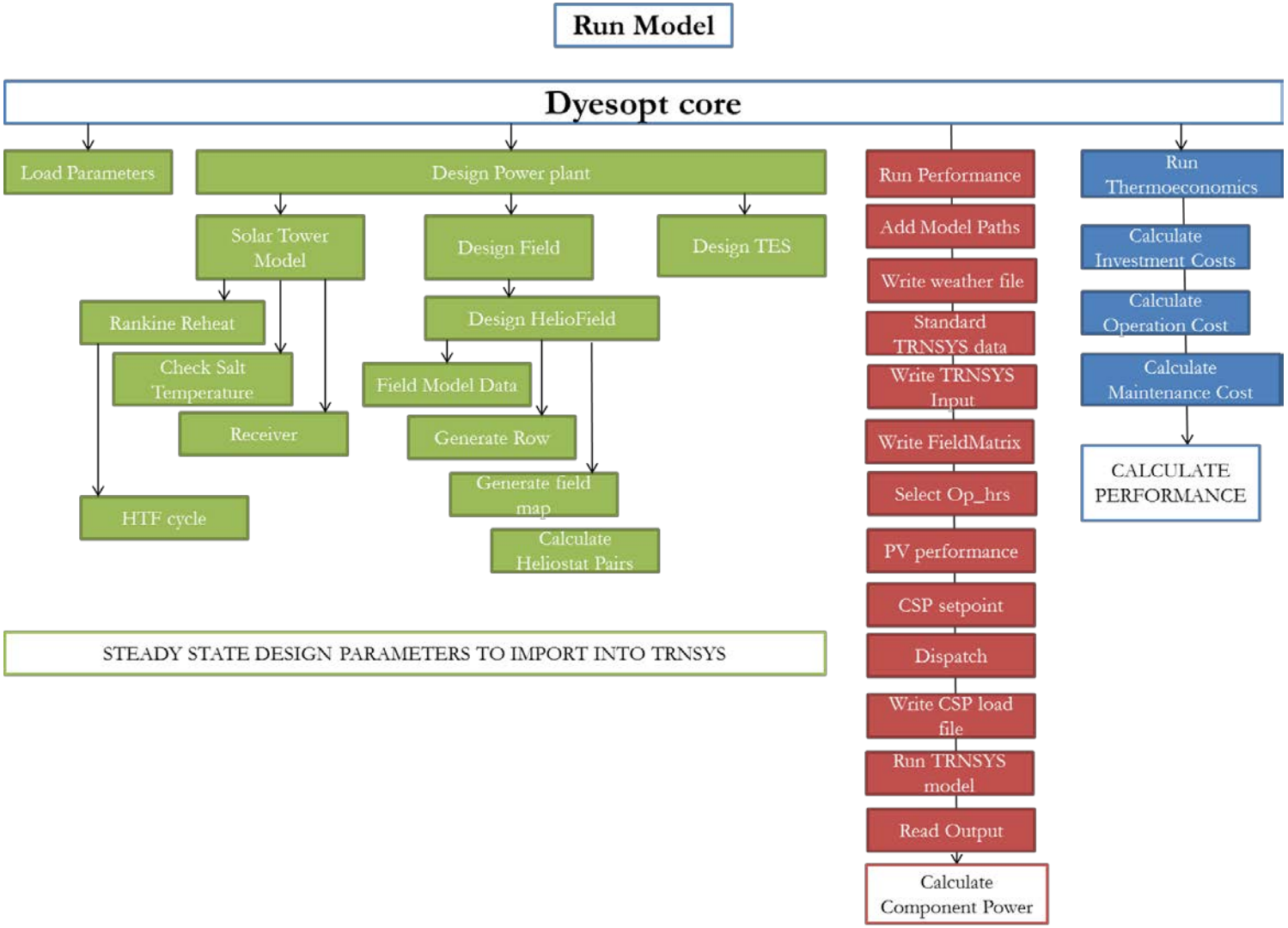

Figure 32 - Maltab functions for the STPP plant

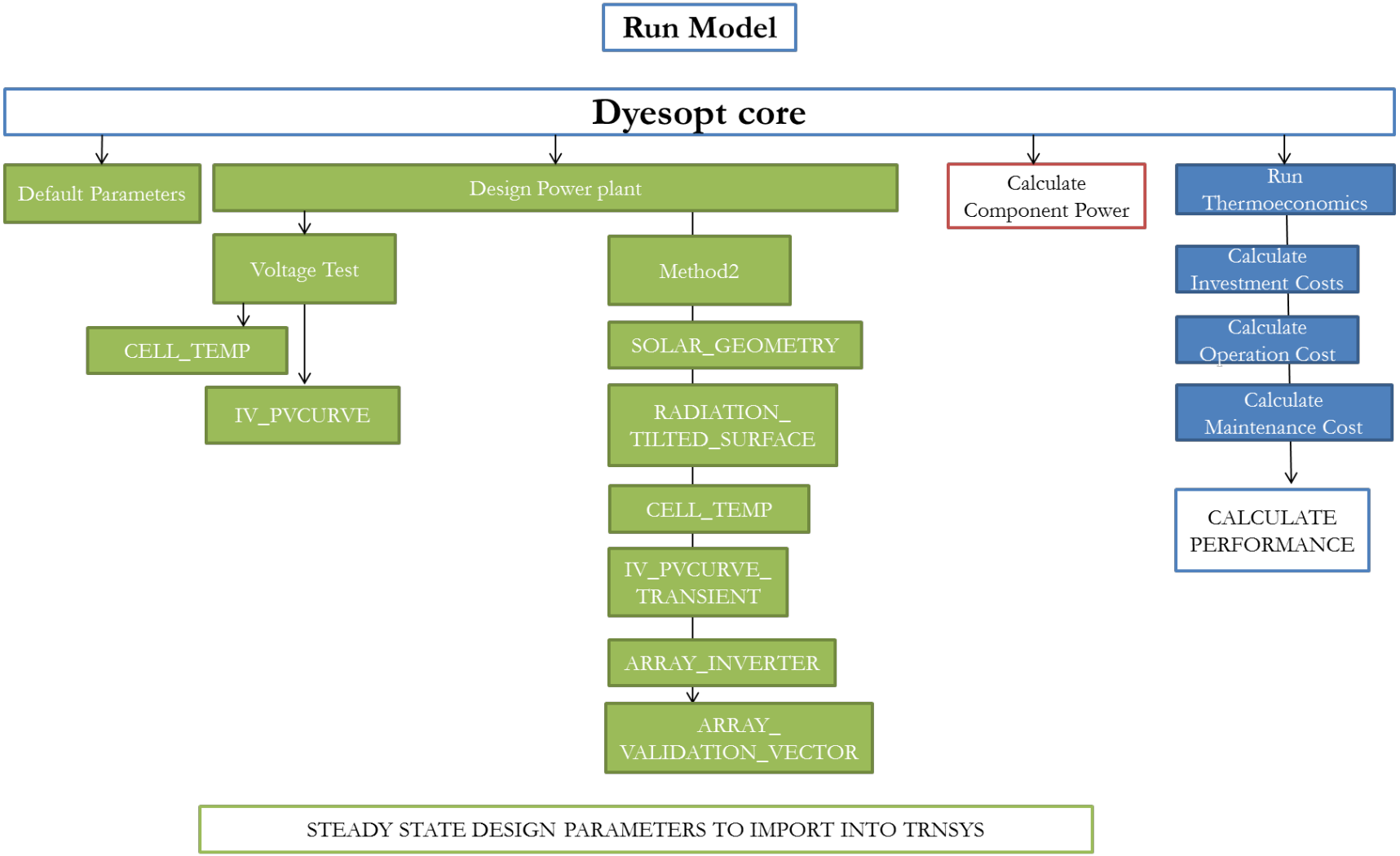

Figure 33 – Matlab functions for the PV plant.

APPENDIX C: CSP COST FUNCTIONS

$$CAPEX_{CSP} = C_{direct,CSP} + C_{direct,CSP}$$

Direct CAPEX

$$C_{direct,CSP} = C_{PB} + C_{SF} + C_{TES} + C_{Tower} + C_{BOP} + C_{Site} + C_{Cont}$$

$$C_{PB} = \left\{ \left[\left(\frac{IC_{gross}}{IC_{gross,ref}} \right)^{yPB,1} \right] \times \left[\left(\frac{p_{in,HPT}}{p_{in,HPT,ref}} \right)^{yPB,2} \right] \right\} \times \left[C_{PB,ref} - C_{PH,ref} \left(1 - \frac{N_{PH}}{N_{PH,ref}} \right)^{yPB,3} \right]$$

$$C_{SF} = C_{SF,ref} \left(\frac{A_{SF}}{A_{SA,ref}} \right)^{ySF,1}$$

$$C_{TES} = \left\{ C_{Salts,ref} \left(\frac{TES_{Cap}}{TES_{Cap,ref}} \right) + \left[C_{TESsys,ref} \left(\frac{TES_{Cap}}{TES_{Cap,ref}} \right)^{yTES,1} \right] \right\}$$

$$C_{rec} = C_{rec,ref} \left(\frac{Q_{rec}}{Q_{rec,ref}} \right)^{yrec,1} \left(\frac{A_{rec}}{A_{rec,nom}} \right)^{yrec,2}$$

$$C_{Tower} = a_{Tower} \times T_h^{\ 2} + b_{Tower} \times T_h + C_{Tower}$$

$$C_{BOP} = C_{BOP,ref} \left(\frac{IC_{gross}}{IC_{gross,ref}} \right)^{yBOP,1}$$

$$C_{Site} = \left\{ C_{Site,ref} \left(\frac{A_{Land}}{A_{Land,ref}} \right)^{ySite,1} - C_{Pond,ref} \left[1 - \left(\frac{IC_{gross}}{IC_{gross,ref}} \right)^{ySite,2} \right] \right\}$$

$$C_{cont} = X_{cont,\%} \times C_{direct}$$

Table 20 – Technical reference values used in the direct CSP CAPEX cost functions

Cost	Ref Unit	South Africa	Reference Source
Power Block	IC_{Gross} [MW]	55	(26)
	$P_{inHPT,ref}$ [bar]	105	(26)
	$N_{PH,ref}$ [USD]	4	(26)
	$C_{PB,ref}$ [USD]	34,218,257	(26)
	$C_{PH,ref}$ [USD]	1,107,501	(26)
	$y_{PB,1}$	0.8	(77)
	$y_{PB,2}$	0.1	(77)
	$y_{PB,3}$	0.75	(77)
Solar Field	$A_{SF,ref}$ [m,^{2}]	435,735	(26)
	$C_{SF,ref}$ [USD]	53,147,708	(26)
	y_{SF}	1	(77)
TES	$TES_{cap,ref}$ [MW_{th}]	405.9	(26)
	$C_{salts,ref}$ [USD]	393,255	(26)
	$C_{TESsys,ref}$ [USD]	10,467,834	(26)
	y_{TES}	0.8	(77)
Receiver	$Q_{rec,ref}$ [MW_{th}]	241.1	(26)
	$A_{rec,ref}$ [m^2]	130	(26)
	$C_{rec,ref}$ [USD]	8,665,491	(26)
	$y_{rec,1}$	0.7	(77)
	$y_{rec,2}$	- 0.2	(77)
Tower	a_{Tower}	1835.7	(26)
	b_{Tower}	285868	(26)
	c_{Tower} [USD]	$ 11,082,338	(26)
BOP	$C_{BOP,ref}$ [USD]	$ 17,197,746	(26)
	y_{BOP}	0.8	(77)
Site	$A_{land,ref}$ [m^2]	2,430,000	(26)
	$C_{site,ref}$ [USD]	22,541,514	(26)
	$C_{Ponds,ref}$ [USD]	101,849	(26)
	$y_{Site,1}$	0.9	(77)
	$y_{Site,2}$	0.9	(77)
Contingency	$X_{cont,\%}$ [%]	7	(26)

Indirect CAPEX

$$C_{indirect} = C_{EPC} + C_{Land} + C_{TAX}$$

$$C_{EPC} = X_{EPC,\%} \times CAPEX_{ref} \left(\frac{CAPEX}{CAPEX_{ref}} \right)^{yEPC,1}$$

$$C_{Land} = A_{Land} \times C_{Land,ref}$$

$$C_{TAX} = C_{direct,CSP} \times \delta_{TAX,CAPEX} \times X_{TAX,\%}$$

Table 21 – Technical reference values used in the indirect CSP CAPEX cost functions

Cost	Ref Unit	South Africa	Reference
EPC	$X_{EPC,\%}$ [%]		(26)
	$CAPEX_{ref}$ [USD]	208,878,385	(26)
	y_{EPC}	0.9	(77)
Land	$C_{land/m^2,ref}$ [m²/MW]	0.5	(26)
Tax	$X_{tax,\%}$ [%]	28	(26)
	$\delta_{tax,CAPEX}$	0.78	(26)

CSP OPEX REFERENCE COSTS

$$OPEX_{CSP} = C_{Labor} + C_{Serv} + C_{Utility} + C_{Misc} + C_{Insurance}$$

$$C_{Labor} = C_{Lab,adm} + C_{Lab,op} + C_{Lab,Maint.PB} + C_{Lab,Maint.SF}$$

$$C_{Lab,op} = C_{Lab,op,refPB} + C_{Lab,op,refSF} \left[\left(\frac{A_{SF}}{A_{AS,ref}} \right)^{yLab1} \right]$$

$$C_{Lab,Maint.PB} = C_{Lab,Maint.PB,ref1} + C_{Lab.Maint.PB,ref2} \left[\left(\frac{IC_{gross}}{IC_{gross,ref}} \right)^{yLab2} \right]$$

$$C_{Lab,Maint.SF} = C_{Lab,Maint.SF,ref1} + C_{Lab,Maint.SF,ref2} \left[\left(\frac{A_{SF}}{A_{SF,ref}} \right)^{yLab3} \right]$$

$$C_{Serv} = C_{Serv,ref} \left(\frac{IC_{gross}}{IC_{gross,ref}} \right)^{yServ,1}$$

$$C_{Utility} = \left(C_{Wtr,ref} + C_{el,ref}\right) \times \left(\frac{IC_{gross}}{IC_{gross,ref}}\right)^{yuti,1}$$

$$C_{Misc} = \left\{ \begin{array}{l} C_{Misc.Site,ref}\left(\frac{A_{SF}}{A_{SF,ref}}\right)^{yMisc,1} + C_{Misc.SF,ref}\left(\frac{A_{SF}}{A_{SF,ref}}\right)^{yMisc,2} \\ + C_{Misc.rec,ref}\left(\frac{Q_{rec}}{Q_{rec,ref}}\right)^{yMisc,4} + C_{Misc.TES,ref}\left(\frac{TES_{CAP}}{TES_{CAP,ref}}\right)^{yMisc,5} \\ + C_{Misc.PB,ref}\left(\frac{IC_{gross}}{IC_{gross,ref}}\right)^{yMisc,3} \end{array} \right\}$$

Table 22 – Technical reference values used in the CSP OPEX cost functions

Cost	Ref Unit	South Africa	Reference
Labour	$C_{lab,adm}$ [USD]	15,000	(26)
	$C_{lab_o,ref_{PB}}$ [USD]	555,000	(26)
	$C_{lab_o,ref_{SF}}$ [USD]	11,000	(26)
	$y_{lab,1}$	1	(77)
	$C_{lab_{M,PB},ref_1}$ [USD]	12,000	(26)
	$C_{lab_{M,PB},ref_2}$ [USD]	36,000	(26)
	$y_{lab,2}$	0.7	(77)
	$C_{lab_{M,SF},ref_1}$ [USD]	36,000	(26)
	$C_{lab_{M,SF},ref_2}$ [USD]	36,000	(26)
	$y_{lab,3}$	0.7	(77)
Services	$C_{ser,ref}$ [USD]	218,221	(26)
	y_{ser}	1	(77)
Utility	$C_{wtr,ref}$ [USD]	87,192	(26)
	$C_{el,ref}$ [USD]	121,567	(26)
	y_{uti}	1	(77)
Miscellaneous	$C_{misc_{Site},ref}$ [USD]	152,620	(26)
	$C_{misc_{SF},ref}$ [USD]	510,022	(26)
	$C_{misc_{rec},ref}$ [USD]	164,202	(26)
	$C_{misc_{TES},ref}$ [USD]	121,390	(26)
	$C_{misc_{PB},ref}$ [USD]	240,251	(26)
	$y_{misc,1}$	1	(77)
	$y_{misc,2}$	1	(77)
	$y_{misc,3}$	1	(77)
	$y_{misc,4}$	0.7	(77)
	$y_{misc,5}$	0.7	(77)

APPENDIX D: PV COST FUNCTIONS

$$CAPEX_{PV} = C_{direct,PV} + C_{inderect,PV}$$

Direct CAPEX

$$C_{direct,PV} = C_{PV} + C_{Inv} + C_{BOS} + C_{Tracking}$$

$$C_{PVModules} = C_{PVModules,ref} \times IC_{DC}$$

$$C_{Inv} = C_{Inv,ref} \times IC_{DC}$$

$$C_{BOS} = C_{BOS,ref} \times IC_{DC}$$

$$C_{Tracking} = C_{Tracking,ref} \times IC_{DC}$$

Table 23 – Technical reference values used in the direct PV CAPEX cost functions

Cost	Ref Unit	South Africa	Reference	Comments
PV modules	$C_{PV,ref}$ [USD/$W_{p,DC}$]	0.54 - 1.82	Suppliers quotations	The lower value represents the benchmark value obtained for PV modules in the quotation and the higher values the most expensive one
Inverters	$C_{Inv,ref}$ [USD/$W_{p,DC}$]	0.12 - 0.16	Suppliers quotations	Same as the PV module case, these values represent the lowest and highest quotation found.
BOS	$C_{BOS,ref}$ [USD/$W_{p,DC}$]	1.5	(86)	On page 85 the specific cost of the BOS for some locations is showed.
Tracking	$C_{tracking,ref}$ [USD/$W_{p,DC}$]	0.15 – 0.48	(87)(Pg.91), (88), (89),	0.5 in 2012 according to (90) (Pg. 39) and an average of 0.4 on the next year edition (89) (Pg. 42)

Indirect CAPEX

$$C_{indirect,PV} = C_{E\&D} + C_{Land} + C_{TAX}$$

$$C_{Land,PV} = F_{size,ref} \times C_{Land,ref} \times IC_{DC}$$

Table 24 – Technical reference values used in the indirect PV CAPEX cost functions

Cost	Ref Unit	South Africa	Reference	Comments
E&D	$X_{E\&D,\%}$ [%]	0.5 - 10	(91)	-
Land	$F_{Size,ref}$ [Ha/MW]	1.4 – 2	(26)	-
	$C_{land,ref}$ [USD/Ha]	6,987.1	(26)	-
Tax	$X_{tax,\%}$ [%]	28	(26)	TAX (VAT)
	$\delta_{tax,CAPEX}$	1	(26)	-

PV OPEX REFERENCE COSTS

$$OPEX_{PV} = C_{Labor,PV} + C_{Insurance,PV}$$

$$C_{Labor,PV} = C_{Labor,ref} \times IC_{DC}$$

$$C_{Insurance,PV} = CAPEX_{PV} \times \left(\frac{X_{Insurance,\%}}{100} \right)$$

Table 25 – Technical reference values used in the PV OPEX cost functions

Cost	Ref Unit	Value	Reference
Labour	$C_{Labor,ref}$ [USD/Wp]	0.015 – 0.02	(92)
Insurance	$X_{insurance,\%}$	0.25-0.5% of CAPEX	(93) (87)

Table 26 – Technical specifications for the PV modules implemented in the model

	PV mdule	Standard Test Conditions (STC)			Normal Operating Cell Temperature [NOCT] Conditions			Peak Power	Eff	V_{mpp}	I_{mpp}	V_{OC}	I_{SC}	$V_{max,Sys}$	Cell Number	Power Coeff.	V_{oc} Coeff.	I_{sc} Coeff.	Manfctr. Tol	Price
		G [W/m²]	AM [-]	T_{cell} [C]	G [W/m²]	T_{cell} [C]	$T_{cell,ref}$ [C]	[Wp]	[%]	[V]	[A]	[V]	[A]	[V]		[%]	[mV]	[mA]	[%]	[USD/W]
	SOUTH AFRICA																			
1	**ReneSola 310W**	1000	1,5	25	20	45	800	310	0,160	37,0	8,38	45,0	8,80	1000	72	0,40	-135,00	3,52	5	0,55
2	**ReneSola 265W**	1000	1,5	25	20	45	800	265	0,163	30,6	8,66	37,9	9,19	1000	60	0,43	-117,49	2,76	5	0,54
3	**BYD P6C-36 310W**	1000	1,5	25	20	45	800	310	0,160	36,4	8,52	45,8	8,99	1000	72	0,43	-119,00	5,15	2	0,54

Table 27 – Technical specifications for the inverters implemented in the model

Inverter	$V_{DC,MAX}$ [V]	$V_{mpp,MAX}$ [V]	$V_{mpp,MIN}$ [V]	$I_{DC,MAX}$ [A]	EFF [%]	$Power_{rated}$ [kW]	Price [USD/W]	Comment
SOUTH AFRICA								
SMA SUNNY CENTRAL 800 CP XT	1000	850	641	1400	0,984	800	0,130	*Preliminary quotation*
INGECON SUN POWER MAX	1000	820	578	1800	0,989	1000	0,130	*Preliminary quotation*
ABB PVS8001-57	1100	850	600	1710	0.988	1000	0.124	*Preliminary quotation*

```
function [o,result] = Select_op_hrs(o)

%%Dispatch strategy for intermediate/peak load PV-CSP operation (South
Africa)

%%Define operating and peak hours

priceFile                                                              =
(['C:\DYESOPT\marketData\priceData\',o.model.priceFile,'.txt']);
priceData       = dlmread(priceFile, ',', 1, 0);

%                                  loadFile                            =
(['C:\DYESOPT\marketData\priceData\','Yearly_load_points_constant','.txt'])
;
% loadData = dlmread(loadFile,'',1,0);
%
% avg_load = mean(loadData);
% limit = 0.95; %percentage limit at which we have peak load

 yprice          = max(0, priceData(:,2)');
 if length(yprice) > 8761
    oldprice = yprice;
    yprice = 0;
     for i = 1:8761
         yprice(i) = oldprice(i);
     end
 end

weatherFile     = (['C:\DYESOPT\climateData\data\',o.model.wFile,'.txt']);
wData       = dlmread(weatherFile, ',', 4, 0);
y_G          = max(0, wData(:,5)');

L = 8760;



count = 1;

%% First n_tar is calculated
% n_tar is a vector that determines the 'number of tariff changes' each day
% length(n_tar) = number of days in the year

for j = 1:24:L
    n_tar(count) = 0;
    for i=j:j+23;
        if yprice(i+1) == yprice(i)
            i = i;
        else
            n_tar(count)        = n_tar(count) + 1; %Vector with number of
tariff changes each day
            hour_tar(n_tar(count),count)  =  i;  %Hour  at  which  the  rariff
changes (rows) each day(columns)
        end
    end
    count = count + 1;
end
```

```
%% Then the daily tariff matrix is calculated
% tariff_matrix is a 3D matrix that contains a [24 x 3] 2D matrix per day
% with the following structure: [hour price 0].
% In priority_matrix, the rows are ordered from highest price to lowest -
% every day.

contar = 1;
for i = 1:length(n_tar) %i = days

    for k = 1:(length(hour_tar(:,i))) %k = hours
        if hour_tar(k,i) > 0
            tariff_matrix(k,:,i) = [hour_tar(k,i) yprice(hour_tar(k,i)) 0];
%assign hour of tariff change in the first column and corresponding price
in the second column
        elseif hour_tar(k,i) == 0 %If there is a tariff change in the first
hour of the file...
            tariff_matrix(k,:,i) = [hour_tar(k,i) yprice(i*24) 0]; %boh
            % to check if this works
        end
    end
    priority_matrix(:,:,i)  =  sortrows(tariff_matrix(:,:,i),2);  %sort  in
order of price
    %end
end

%Loop that assigns a 'priority number' to each tariff of the day. 1 is the
%highest, 2 the second highest etc.

for i=1:length(priority_matrix(1,1,:)) %365 days
    priority_matrix(length(priority_matrix(:,1,i)),3,i) = 1; %assign 1 to
the highest price (located in the last row of each day from line 69)
    for j = (length(priority_matrix(:,1,i))-1):-1:1      %from second-last
row to first..
        if priority_matrix(j,2,i) == priority_matrix(j+1,2,i) %if price of
current row is the same as row below...
            priority_matrix(j,3,i) = priority_matrix(j+1,3,i); %assign same
priority number
        else
            priority_matrix(j,3,i)  =  priority_matrix(j+1,3,i)+1;  %else,
increase the priority number (lower priority)
        end
    end

    real_n_tariff(i) = priority_matrix(1,3,i);% Real number of tariffs each
day

    tariff_matrix(:,:,i)  =  sortrows(priority_matrix(:,:,i),1);  %sort  in
order of time
end

%%  Then an 'annual matrix' is calculated to convert from 3D to a 2D matrix
% annual_matrix has the following structure [hour price order/day]
% annual_matrix has 8761 rows (hours in the year - from 0 to 8760)

annual_tariff_matrix = tariff_matrix(:,:,1);
for k = 2:length(tariff_matrix(1,1,:))
    annual_tariff_matrix = [annual_tariff_matrix; tariff_matrix(:,:,k)];
end
```

```
annual_tariff_matrix = sortrows(annual_tariff_matrix,-1);

for i = 1:length(annual_tariff_matrix(:,1))
    if annual_tariff_matrix(i,1) > 0
        corrected(i,:) = annual_tariff_matrix(i,:);
    end
end

annual_tariff_matrix = sortrows(corrected,1);

k = 1; annual_matrix(L,3) = 0;
for j = 1:L
    annual_matrix(j,1) = j;
    if annual_matrix(j,1) <= annual_tariff_matrix(k,1)
        annual_matrix(j,2) = annual_tariff_matrix(k,2);
        annual_matrix(j,3) = annual_tariff_matrix(k,3);
    else
        if k < length(annual_tariff_matrix(:,1))
            k = k + 1;
            annual_matrix(j,2) = annual_tariff_matrix(k,2);
            annual_matrix(j,3) = annual_tariff_matrix(k,3);
        else
            annual_matrix(j,2) = annual_tariff_matrix(1,2);
            annual_matrix(j,3) = annual_tariff_matrix(1,3);
        end
    end
end

%% Define yprice, price vector.
% yprice is a 8761x2 matrix with structure: [price order/day], meaning that
% is equal to the last two columns of annual_matrix

yprice = yprice';
for i = 1:length(yprice)
    if i > length(annual_matrix(:,1))
        yprice(i,2) = annual_matrix(i-1,3);
    else
        yprice(i,2) = annual_matrix(i,3);
    end
end

%% Define operating hours based on price

for i = 1:length(yprice)

    if yprice(i,1) == 0

        yprice(i,3) = 0;
    else
        yprice(i,3) = 1;
    end
end
result.PDS.yprice = yprice;
result.PDS.op_hours = yprice(:,3);
result.PDS.peak_hours = zeros(length(yprice(:,2)),1);

% Determine peak hours
for i = 1:length(yprice(:,2))
```

```
if yprice(i,2) == 1 %If it is the hour with the highest price... (put a
range in case of more compex price pattern)

    result.PDS.peak_hours(i,1) = 1;
end
end

if o.design.PDS == 1

    yprice2 = yprice;
    yprice2(:,3) = yprice(:,1);
    prfilename                                                          =
(['C:\DYESOPT\plantLayouts\',o.model.plant,'\input\prfile.txt']);

dlmwrite(prfilename, yprice2);

end


lat = dlmread(weatherFile,',',[1 0 1 0]);
day_of_year = 0;
```

```
function [result, o] = CSP_setpoint(o, result)

result.PV_CSP.ICnominal = zeros(length(result.PDS.yprice(:,2)),1);

% Determine the nominal electrical power output from the PV-CSP plant
if o.design.load == 1 %Fixed output


result.PV_CSP.ICnominal(:,1) = o.PC.W_el/1e3; % [MWe]

elseif o.design.load == 2%Variable output

    for i = 1:length(result.PDS.yprice(:,2))

        if result.PDS.yprice(i,2) ==  1 %if it is a peak hour run at
nominal output

            result.PV_CSP.ICnominal(i) = o.PC.W_el/1e3; % [MWe]

        else
            if i <= 1896 || i >= 6384 %Summer + Spring (South Africa)
            result.PV_CSP.ICnominal(i) =
o.design.load_factor_summer*o.PC.W_el/1e3; % [MWe]
            else         %Winter + Autumn (South Africa)
                result.PV_CSP.ICnominal(i) =
o.design.load_factor_winter*o.PC.W_el/1e3; % [MWe]
            end
        end

if o.model.mode == 1  && o.model.mode1 ~= 3
     if result.PVO.P_AC_Farm(i) >= (result.PV_CSP.ICnominal(i)/o.PC.Gen_Eff
- 0.30*(o.PC.Wgross/1000)) %0.70*(o.PC.Wgross/1000)

       result.PVO.P_AC_Farm_net(i)    =
max(0,(result.PV_CSP.ICnominal(i)/o.PC.Gen_Eff - 0.30*(o.PC.Wgross/1000)));
%(o.PC.W_load - 0.30*(o.PC.Wgross/1000))

       result.PVO.P_AC_Farm_crtld(i)  = result.PVO.P_AC_Farm(i) -
result.PVO.P_AC_Farm_net(i);



    else

       result.PVO.P_AC_Farm_crtld(i)  = 0 ;

       result.PVO.P_AC_Farm_net(i)    = result.PVO.P_AC_Farm(i) ;
     end


end
if o.model.mode1 == 3

    result.PVO.P_AC_Farm_crtld(i)  = 0 ;

    result.PVO.P_AC_Farm_net(i)    = result.PVO.P_AC_Farm(i) ;
```

```
end
    end
end

if o.model.mode == 1
% Define required CSP load at every hour based on PV output
for j = 2:length(result.PVO.P_AC_Farm)-1

     if result.PDS.op_hours(j) == 0 %|| (o.model.op_hours(j-1) == 0 &&
o.model.op_hours(j+1) == 0)  %Avoid starting up the CSP for only one hour

    result.PV_CSP.CSPload_desired(j) = 0;

     else

      result.PV_CSP.CSPload_desired(j) = result.PV_CSP.ICnominal(j) -
result.PVO.P_AC_Farm_net(j);% [MWe]

     end

    result.PV_CSP.PV_over(j) = result.PVO.P_AC_Farm(j) -
result.PVO.P_AC_Farm_net(j);
    result.PV_CSP.f_loadCSP(j)  =
result.PV_CSP.CSPload_desired(j)/result.PV_CSP.ICnominal(j);% factor [-]

end

else

    result.PVO.P_AC_Farm_net = zeros(1,8761);
    result.PVO.P_AC_Farm_crtld = zeros(1,8761);
    result.PVO.DC_P_Curt = zeros(1,8761);
    result.PVO.Global_rad = zeros(1,8761);

    for j = 2:length(result.PV_CSP.ICnominal)-1
    if result.PDS.op_hours(j) == 0
        result.PV_CSP.CSPload_desired(j) = 0;

        else

      result.PV_CSP.CSPload_desired(j) = result.PV_CSP.ICnominal(j);

    end
    result.PV_CSP.PV_over(j) = 0;
    result.PV_CSP.f_loadCSP(j)  =
result.PV_CSP.CSPload_desired(j)/result.PV_CSP.ICnominal(j);% factor [-]

    end



end

end
```

```
function o = dispatch_2(o,yprice,result)


weatherFile     = (['C:\DYESOPT\climateData\data\',o.model.wFile,'.txt']);
wData       = dlmread(weatherFile, ',', 4, 0);
y_G          = max(0, wData(:,5)');



%% Estimate hourly irradiance and hourly power from field based on field
design and weather data
% in this loop yprice is expanded (two added columns)
% column 3 is  shows the hourly PB thermal demand  (W/m2), based on teh CSP
% setpoint
% column 4 is the expected field power at that hour (W/m2), an approx value
% based on annual weather data, field design and a safe factor.
L = 8760;

lat = dlmread(weatherFile,',',[1 0 1 0]);
day_of_year = 0;

az_step = 360/(o.field.nAz-1);
az_vector = -180:az_step:180;
el_step = 90/(o.field.nEl-1);
el_vector = 0:el_step:90;

for i = 1:L
    time_of_day = mod(i,24);
    if time_of_day == 1
        day_of_year = day_of_year + 1;
    else
        day_of_year = day_of_year;
    end
    [az(i),   el(i)]   =   getSolarPosition(time_of_day,   day_of_year,   lat,
'degree');
    if el(i) <= 0
        el(i) = 0.01;
    elseif el(i) >= 90
        el(i) = 89.99;
    end
    if az(i) <= -180
        az(i) = -179.99;
    elseif az(i) >= 180
        az(i) = 179.99;
    end
    efffield(i)                                                              =
interp2(el_vector,az_vector,o.field.effMatrix,el(i),az(i));

    %yprice(i,3) = ((o.rec.Qnom*1000/o.rec.EFF)/o.field.Aaper);
    yprice(i,3)                                                              =
((o.rec.Qnom*1000*(result.PV_CSP.CSPload_desired(i)/(o.PC.W_el/1e3)))/o.fie
ld.Aaper)/o.rec.EFF;%Assuming  linear  relationship  between  thermal  and
electrical powers
    y_Ghour(i)                =                mean(y_G(((i-1)*((length(y_G)-
1)/8760)+1):(i*((length(y_G)-1)/8760)))); %SAME EXACT VECTOR AS y_G -.-
    yprice(i,4) = y_Ghour(i)*efffield(i)*o.STO.dispatch_f; %W/m^2 or Wh/m^2
(it is equivaent since the timestep is one hour)
end
```

```
%% Daymatrix definition
% daymatrix(:,:,:) is a 3D matrix composed of n-days 2D matrices.
% daymatrix(:,:,n) is a 2D matrix that expands yprice matrix to incorporate
% 2 additional columns: [price priority/day Qf_nom Qf control hour/day]

% First, h_day is calcualted to estimate how many hours should the plant
% operate per day, based on Qf_nom at SM=1 and hourly Qf:
h_day = zeros(1,365);
count = 1;
for j = 1:24:(length(yprice(:,1))-1)
    h_day(count) = 0;
    for i=j:j+23;
        if result.PDS.op_hours(i) == 1
        h_day(count) = 0 + yprice((i),4)/yprice((i),3) + h_day(count);
        end
    end;
    count = count+1;
end
h_day = ceil(h_day);


% Then daymatrix is created, a 3D matrix originated from yprice (2D matrix)
count = 1;
for j = 1:24:(length(yprice(:,1))-1)
    for i=j:j+23
        daymatrix(:,:,count) = yprice((j:j+23),:);
    end
    count = count +1;
end

% daymatrix(:,:,j) is expanded to have other two columns:
% column 5 is a parameter used to control when to (1) or not to operate (0)
% column 6 is just the actual hour of the year.

for i=1:length(daymatrix(1,1,:))
    count_hday = 0; count_STO = 0;
    for j = 1:24
        daymatrix(j,6,i) = j-1;
    end
    ordered_daymatrix(:,:,i)  =  sortrows(daymatrix(:,:,i),[2  -6]);  % rows
are ordered from highest price to lowest
    for j = 1:24
        if count_hday < h_day(i)  && ordered_daymatrix(j,1,i) > 0
            if ordered_daymatrix(j,4,i) < ordered_daymatrix(j,3,i) % if Qf
is less than PB demand...
                if     (o.STO.time     -     count_STO)     >     (1     -
(ordered_daymatrix(j,4,i)/ordered_daymatrix(j,3,i))) %if I have enough TES
to run for an hour
                    ordered_daymatrix(j,5,i)= 1; % Then this hour is to be
operated
                    count_hday  = count_hday + 1; % hour counter increases
                    count_STO              =     count_STO     +     (1     -
ordered_daymatrix(j,4,i)/ordered_daymatrix(j,3,i));    %    remaining    TES
decreases
                else %If I do not have enough TES to run for an hour but
perhaps there is some incoming power then...
```

```
                    count_STO                       =       count_STO       -
ordered_daymatrix(j,4,i)/ordered_daymatrix(j,3,i);   %   my   TES   counter
decreases - it gets charged.
                end
            else % if Qf is greater than nominal...
                ordered_daymatrix(j,5,i)= 1; % Then sure this is hour is to
be operated
                count_hday  = count_hday + 1; % hour counter increases

            end
        end
    end
    daymatrix(:,:,i) = sortrows(ordered_daymatrix(:,:,i),6);% I reorder as
a function of time...

end

%% Annual matrix and final matrix
annual_matrix = daymatrix(:,:,1);
for i = 2:length(daymatrix(1,1,:))
    annual_matrix = [annual_matrix;daymatrix(:,:,i)];
end

matrix(length(annual_matrix(:,1)),4) = 0;
for i = 1:length(annual_matrix(:,1))
    matrix(i,1) = i-1;
end
matrix(:,2) = annual_matrix(:,4);
matrix(:,3) = annual_matrix(:,1);
matrix(:,4) = annual_matrix(:,5);

for i = 1:(length(matrix(:,4)) - (24+2)*60/o.model.dt)

    if  abs(matrix(i,4))  <  abs(matrix(i+1,4))  &&  abs(matrix(i+1,4))  >
abs(matrix(i+2,4))
        matrix(i+1,4) = abs(matrix(i,4));
        for j = 1:(24*60/o.model.dt)
            if abs(matrix(i+j,4)) == 0 && abs(matrix(i+j+1,4)) > 0
                matrix(i+j,4) = 1;
            end
        end

    end
end

o.model.dispatch_matrix = matrix;

prfilename                                                                  =
(['C:\DYESOPT\plantLayouts\',o.model.plant,'\input\prfile.txt']);

dlmwrite(prfilename, matrix);


end
```

```
 function [result,o] = write_CSPloadfile(o,result)

if o.design.PDS == 2
result.PDS.corrected_op_hours = o.model.dispatch_matrix(:,4);
else
    result.PDS.corrected_op_hours = result.PDS.op_hours;
end

for j = 2:length(result.PV_CSP.ICnominal)-1

     if result.PDS.corrected_op_hours(j) == 0 %|| (o.model.op_hours(j-1) ==
0 && o.model.op_hours(j+1) == 0)  %Avoid starting up the CSP for only one
hour

    result.PV_CSP.CSPload_desired(j) = 0;

if o.model.mode == 1
    result.PVO.P_AC_Farm_net(j)     =     result.PVO.P_AC_Farm_net(j)     +
result.PVO.P_AC_Farm_crtld(j); %Correct PV curtailment based on corrected
op_hours
    result.PVO.P_AC_Farm_crtld(j) = 0;
else

    result.PVO.P_AC_Farm_net(j) = 0;
    result.PVO.P_AC_Farm_crtld(j) = 0;
    result.PVO.DC_P_Curt(j) = 0;
    result.PVO.Global_rad(j) = 0;
end
     end


if o.model.mode1 == 3

    matrix_loadfile(j,1) = j-1;% time [h] ----> will it work if I change to
minutes?
    matrix_loadfile(j,2) = result.PDS.corrected_op_hours(j);
    matrix_loadfile(j,3) = 0;
    matrix_loadfile(j,4) = result.PVO.P_AC_Farm_net(j);
    matrix_loadfile(j,5) = 0; %Divide by gen. efficiency to send mechanical
power to trnsys
    matrix_loadfile(j,6) = result.PDS.peak_hours(j);
    matrix_loadfile(j,7) = result.PVO.P_AC_Farm_crtld(j); % just to check
the other method
    matrix_loadfile(j,8) = result.PVO.DC_P_Curt(j);
    matrix_loadfile(j,9) = result.PVO.Global_rad(j); % just to check
    matrix_loadfile(j,10) = result.PDS.op_hours(j);
else
    matrix_loadfile(j,1) = j-1;% time [h] ----> will it work if I change to
minutes?
    matrix_loadfile(j,2) = result.PDS.corrected_op_hours(j);
    matrix_loadfile(j,3) = result.PV_CSP.f_loadCSP(j);
    matrix_loadfile(j,4) = result.PVO.P_AC_Farm_net(j);
    matrix_loadfile(j,5)  =  result.PV_CSP.CSPload_desired(j)/o.PC.Gen_Eff;
%Divide by gen. efficiency to send mechanical power to trnsys
    matrix_loadfile(j,6) = result.PDS.peak_hours(j);
    matrix_loadfile(j,7) = result.PVO.P_AC_Farm_crtld(j); % just to check
the other method
    matrix_loadfile(j,8) = result.PVO.DC_P_Curt(j);
    matrix_loadfile(j,9) = result.PVO.Global_rad(j); % just to check
```

```
    matrix_loadfile(j,10) = result.PDS.op_hours(j);

end
     end

%Calculate planned yearly energy production based on PDS

result.plant.PV_CSP_Etot_planned=  (sum((result.PVO.P_AC_Farm_net(1,1:8760))
+ (result.PV_CSP.CSPload_desired)))/1e3; %[GWh]


loadCSPfilename                                                          =
(['C:\DYESOPT\plantLayouts\',o.model.plant,'\input\loadCSPfile.txt']);

dlmwrite(loadCSPfilename, matrix_loadfile)

end
```

```
function result = calculateComponentPower(o, result)

%calculate generator output%
result.plant.EpGen                                                    =
result.plant.EpNet.*generatorEfficiency(result.plant.EpNet/(o.PC.W/1e3),
sqrt(o.PC.Gen_Eff), sqrt(o.PC.Gen_Eff));
result.plant.EpParas                                                  =
result.plant.Eparas.*generatorEfficiency(result.plant.Eparas/(o.PC.Wparas/1
e3),  sqrt(o.PC.Gen_Eff), sqrt(o.PC.Gen_Eff));


%determine when CSP power plant is online%
for j = 1:length(result.plant.EpGen)
    if result.plant.EpGen(j) == 0;
        result.plant.fLoad(j) = 0;
    else
        result.plant.fLoad(j) = 1;
    end
end

%determine when PV power plant is online%

%determine when PV-CSP power plant is online%
for j = 1:length(result.plant.PV_CSP_Power)
    if o.model.mode1 == 3
        o.PC.W = o.F.Cap*1e3;
    end
%                   if        result.econ.signal_price(j)    ==    0    %&&
result.plant.PV_CSP_Power(j)<=  0.30*o.PC.W/1e3      %Power  plant  is  not
online:  neglect TRNSYS oscillations when plant shuts down
%         result.plant.PV_CSP_fLoad(j) = 0;
%         result.plant.EpGen(j) = 0;
%         result.plant.EpParas(j) = 0;
%         result.plant.PV_CSP_Power(j) = 0;
    if   result.plant.PV_CSP_Power(j)  >=  0.90*o.PC.W/1e3   %Power  plant  is
online and at nominal output
       result.plant.PV_CSP_fLoad_nom(j) = 1;
       result.plant.PV_CSP_fLoad(j) =1;

    elseif        result.plant.PV_CSP_Power(j)    <    0.90*o.PC.W/1e3    &&
result.plant.PV_CSP_Power(j)>= 0.20*o.PC.W/1e3
       result.plant.PV_CSP_fLoad_nom(j) = 0;
       result.plant.PV_CSP_fLoad(j) =1;                              %Plant is
online but not at nominal output
    else
        result.plant.PV_CSP_fLoad_nom(j) = 0;
       result.plant.PV_CSP_fLoad(j) =0;
    end

end

result.plant.EpGross = result.plant.EpGen + result.plant.EpParas;

result.plant.Etot = sum(result.plant.EpGen)*(o.model.dt/3600);% [MWh]
result.plant.Epar_tot = sum(result.plant.EpParas)*(o.model.dt/3600);% [MWh]
result.plant.Egross_tot    =    sum(result.plant.EpGross)*(o.model.dt/3600);%
[MWh]

result.plant.Epar.P1    = sum(result.plant.Wparas.WP1)*(o.model.dt/3600);
```

```
result.plant.Epar.P2    = sum(result.plant.Wparas.WP2)*(o.model.dt/3600);
result.plant.Epar.Psalt                                                    =
sum(result.plant.Wparas.WPsalt)*(o.model.dt/3600);
result.plant.Epar.COND  = sum(result.plant.Wparas.COND)*(o.model.dt/3600);

% checkdispatch vector is a 1-0 vector that is 1 if the time of production
% corresponded/matched to that which was predefined in the PDS (predifined
dispatch strategy)

%Determine  the operation hours that  match with the PDS
for j = 1:length(result.plant.fLoad)
    %if    result.plant.fLoad(j)    ==    abs(result.econ.signal(j))    &&
abs(result.econ.signal(j)) == 1;
    if    result.plant.fLoad(j)    ==    ceil(result.econ.signal(j))    &&
ceil(result.econ.signal(j)) == 1;
    result.plant.checkdispatch(j) = 1;
    else
        result.plant.checkdispatch(j) = 0;
    end
end

%Determine the operation hours that match with base hours
for j = 1:length(result.plant.PV_CSP_fLoad)

    if result.plant.PV_CSP_fLoad(j) == ceil(result.econ.signal_base(j)) &&
ceil(result.econ.signal_base(j)) == 1;
    result.plant.checkdispatch_base(j) = 1;
    else
        result.plant.checkdispatch_base(j) = 0;
    end
end
%Determine the operation hours that match with peak hours
for j = 1:length(result.plant.PV_CSP_fLoad)

    if result.plant.PV_CSP_fLoad(j) == ceil(result.econ.signal_peak(j)) &&
ceil(result.econ.signal_peak(j)) == 1;
    result.plant.checkdispatch_peak(j) = 1;
    else
        result.plant.checkdispatch_peak(j) = 0;
    end
end

%Determine the operation hours that match with peak hours AT NOMINAL OUTPUT

for j = 1:length(result.plant.PV_CSP_fLoad)

    if result.plant.PV_CSP_fLoad(j) == ceil(result.econ.signal_peak(j)) &&
ceil(result.econ.signal_peak(j))  ==  1  &&  result.plant.PV_CSP_Power(j)  >=
0.90*o.PC.W/1e3
    result.plant.checkdispatch_peak1(j) = 1;
    else
        result.plant.checkdispatch_peak1(j) = 0;
    end
end

for j = 1:length(result.plant.Qfield)
    if result.plant.Qfield(j) == 0;
        result.plant.sfLoad(j) = 0;
    else
```

```
        result.plant.sfLoad(j) = 1;
    end
end

result.plant.EpGen_base = zeros(1, length(result.plant.EpGen));
result.plant.EpGen_peak = zeros(1, length(result.plant.EpGen));


for i = 1 : length(result.econ.signal_price)
if result.econ.signal_base(i) == 1
result.plant.EpGen_base(i) = result.plant.EpGen(i);
else
result.plant.EpGen_base(i) = 0;
end

if result.econ.signal_peak(i) == 1
    result.plant.EpGen_peak(i) = result.plant.EpGen(i);
else
    result.plant.EpGen_peak(i) = 0;
end
end

% Predefined dispatch strategy check factors
result.plant.checkPDS0                                                  =
sum(result.plant.PV_CSP_fLoad)/sum(ceil(result.econ.signal_price));
%ratio between dynamic operation hours and price hours.
result.plant.checkPDS                                                   =
sum(result.plant.PV_CSP_fLoad_nom)/sum(ceil(result.econ.signal_price));
%ratio between dynamic operation hours AT NOMINAL OUTPUT and price hours.
%result.plant.checkPDS1                                                 =
sum(result.plant.checkdispatch)/sum(result.plant.PV_CSP_fLoad);       %ratio
between matched with PDS and dynamic operating hours
result.plant.checkPDS2                                                  =
sum(result.plant.checkdispatch)/sum(ceil(result.econ.signal));        %ratio
between matched with PDS and PDS hours
result.plant.checkPDS3                                                  =
sum(ceil(result.econ.signal))/sum(ceil(result.econ.signal_price));
%ratio between PDS hours and price hours
result.plant.checkPDS1                                                  =
sum(result.plant.checkdispatch_base)/sum(ceil(result.econ.signal_base));
%ratio between base dynamic operation hours and price base hours
result.plant.checkPDS4                                                  =
sum(result.plant.checkdispatch_peak)/sum(ceil(result.econ.signal_peak));
%ratio between peak dynamic operation hours and price peak hours
result.plant.checkPDS5                                                  =
sum(result.plant.checkdispatch_peak1)/sum(ceil(result.econ.signal_peak));
%ratio between peak dynamic operation hours and price peak hours at nominal
output
if o.model.mode ==2
result.plant.checkPDS7                                                  =
sum(result.plant.EpGen_base)/(o.PC.Wset*((o.design.load_factor_summer      +
o.design.load_factor_winter)/2)*sum(result.econ.signal_base));
result.plant.checkPDS8                                                  =
sum(result.plant.EpGen_peak)/(o.PC.Wset*sum(result.econ.signal_peak));
%Capacity factor during peak hours
end

% Annual efficiency values %
```

```
result.plant.EFFth_avg                                                    =
sum(result.plant.EFFth)/sum(result.plant.fLoad > 0);
result.plant.EFFsf_avg                                                    =
sum(result.plant.EFFsf)/sum(result.plant.sfLoad > 0);
result.plant.EFFs2el_avg                    =    result.plant.EFFth_avg    *
result.plant.EFFsf_avg * o.rec.EFF * o.PC.Gen_Eff;

%calculate total operation hours%
result.plant.NOH = sum(result.plant.fLoad > 0) * (o.model.dt/3600); %CSP
only
result.plant.PV_CSP_NOH    =    sum(result.plant.PV_CSP_fLoad    >    0)    *
(o.model.dt/3600); %PV_CSP
result.plant.PV_CSP_NOH_diff      =      abs(result.plant.PV_CSP_NOH      -
sum(result.PDS.op_hours)); %Difference between NOH and planned operation
hours

% CSP net THERMAL capacity (or gross electrical capacity): before generator

result.CSP_cap_final = o.PC.W; % To use it on final result display

% Calculate PV solar park electricity yield..............................%
if o.model.mode == 1
result.PV_plant.Etot_net      = sum(result.PVO.P_AC_Farm_net)/1e3;  %[GWh]
result.PV_plant.Etot          = result.PVO.P_AC_Farm_El_year/1e3;  %[GWh]

result.PV_plant.Etot_Life    =    sum(result.PVO.P_AC_Farm_El_degraded/1e3);
%[GWh]

result.PV_plant.PV_farm_AC_cap_final  =  o.PVSZ2.PV_farm_AC_cap_final;  %  To
use it on final result display

result.PV_plant.PV_farm_cap_final = o.PVSZ2.PV_farm_cap_final; % To use it
on final result display

% PV_CSP total production.................................................%
result.plant.PV_CSP_EpGen                   =      result.plant.EpGen      +
result.plant.Net_PV_Power;
result.plant.PV_CSP_Etot          =          result.plant.Etot/1e3          +
result.PV_plant.Etot_net; %[GWh]
%result.plant.PV_CSP_Etot2                                                =
sum(result.plant.PV_CSP_Power)*(o.model.dt/3600)/1e3*o.PC.Gen_Eff;   %before
generator

result.plant.PV_CSP_EpGen_base = zeros(1, length(result.plant.EpGen));
result.plant.PV_CSP_EpGen_peak = zeros(1, length(result.plant.EpGen));

for i = 1 : length(result.econ.signal_price)
if result.econ.signal_base(i) == 1
result.plant.PV_CSP_EpGen_base(i)       =       result.plant.EpGen(i)       +
result.plant.Net_PV_Power(i);
else
result.plant.PV_CSP_EpGen_base(i) = 0;
end

if result.econ.signal_peak(i) == 1
    result.plant.PV_CSP_EpGen_peak(i)     =     result.plant.EpGen(i)     +
result.plant.Net_PV_Power(i);
else
```

```
    result.plant.PV_CSP_EpGen_peak(i) = 0;
end
end

if o.model.mode1 == 3
result.plant.checkPDS7                                                  =
sum(result.plant.PV_CSP_EpGen_base)/(o.F.Cap*(sum(result.econ.signal_base))
);
result.plant.checkPDS8                                                  =
sum(result.plant.PV_CSP_EpGen_peak)/(o.F.Cap*sum(result.econ.signal_peak));
%Capacity factor during peak hours
result.plant.checkPDS6                                                  =
result.plant.PV_CSP_Etot/result.plant.PV_CSP_Etot_planned; % Ratio between
PV_CSP real production and predefined production
else
result.plant.checkPDS6                                                  =
result.plant.PV_CSP_Etot/result.plant.PV_CSP_Etot_planned; % Ratio between
PV_CSP real production and predefined production

end
result.plant.checkPDS7                                                  =
sum(result.plant.PV_CSP_EpGen_base)/(o.PC.Wset*((o.design.load_factor_summe
r + o.design.load_factor_winter)/2)*sum(result.econ.signal_base));
result.plant.checkPDS8                                                  =
sum(result.plant.PV_CSP_EpGen_peak)/(o.PC.Wset*sum(result.econ.signal_peak)
); %Capacity factor during peak hours
end

end
```